

**INSTITUTO NACIONAL DE PROPRIEDADE INDUSTRIAL**  
 PROTOCOLO CERN  
 08/05/2014 14:47 DEMG  
  
 BR 10 2014 011120 4

< Uso exclusivo do INPI >

Espaço reservado para o protocolo

Espaço reservado para a etiqueta

Espaço reservado para o código QR



**INSTITUTO NACIONAL DA PROPRIEDADE INDUSTRIAL**

**Sistema de Gestão da Qualidade**  
**Diretoria de Patentes**

<b>DIRPA</b>	Tipo de Documento:  Formulário	DIRPA	Página:  1/3
Título do Documento:		Código: <b>FQ001</b>	Versão: <b>2</b>
<b>Depósito de Pedido de Patente</b>			Procedimento: <b>DIRPA-PQ006</b>

**Ao Instituto Nacional da Propriedade Industrial:**

O requerente solicita a concessão de um privilégio na natureza e nas condições abaixo indicadas:

**1. Depositante (71):**

- 1.1 Nome: Universidade Federal de Minas Gerais
- 1.2 Qualificação: Instit. de Ensino e Pesquisa
- 1.3 CNPJ/CPF: 17217985000104
- 1.4 Endereço Completo: Av. Antonio Carlos, 6627 - Pampulha, Belo Horizonte - MG, Brasil
- 1.5 CEP: 31270-901
- 1.6 Telefone: (31) 3409-4774
- 1.7 Fax: (31) 3409-6430
- 1.8 E-mail: patentes@ctit.ufmg.br

continua em folha anexa

**2. Natureza:**  Invenção  Modelo de Utilidade  Certificado de Adição

**3. Título da Invenção ou Modelo de Utilidade (54):**

DERIVADOS ALQUILTRIAZÓLICOS COM ATIVIDADE ANTITUMORAL, PROCESSO DE OBTENÇÃO E USO

continua em folha anexa

**4. Pedido de Divisão:** do pedido Nº  **Data de Depósito:**

**5. Prioridade:**  Interna (66)  Unionista (30)

O depositante reivindica a(s) seguinte(s):

País ou Organização do depósito	Número do depósito (se disponível)	Data de depósito

continua em folha anexa

INSTITUTO NACIONAL DA PROPRIEDADE INDUSTRIAL  
 PROTOCOLO CERN  
 08/05/2014 14:47 DEMG  
  
 014140000782  
 52400.110705/2014-39



<b>DIRPA</b>	Tipo de Documento:  <b>Formulário</b>	<b>DIRPA</b>	Página:  <b>2/3</b>
Título do Documento:  <b>Depósito de Pedido de Patente</b>		Código:  <b>FQ001</b>	Versão:  <b>2</b>

**6. Inventor (72):**

Assinale aqui se o(s) mesmo(s) requer(em) a não divulgação de seus nome(s), neste caso não preencher os campos abaixo.

6.1 Nome: ROSSIMIRIAM PEREIRA DE FREITAS

6.2 Qualificação: PROFESSORA

6.3 CPF: 761.212.086-00

6.4 Endereço Completo: RUA CAPRI, 110, BAIRRO BANDEIRANTES, BELO HORIZONTE, MG

6.5 CEP: 31.340-440

6.6 Telefone: 31 - 3409-4774

6.7 FAX: 31 - 3409-4774

6.8 E-mail: patentes@ctit.ufmg.br

 continua em folha anexa**7. Declaração de divulgação anterior não prejudicial.**

Artigo 12 da LPI – período de graça.

Informe no item 11.13 os documentos anexados, se houver.

**8. Declaração na forma do item 3.2 da Instrução Normativa PR nº 17/2013:**

Declaro que os dados fornecidos no presente formulário são idênticos ao da certidão de depósito ou documento equivalente do pedido cuja prioridade está sendo reivindicada.

**9. Procurador (74):**

9.1 Nome:

9.2 CNPJ/CPF:

9.3 API/OAB:

9.4 Endereço Completo:

9.5 CEP:

9.6 Telefone:

9.7 FAX:

9.8 E-mail:

 continua em folha anexa**10. Listagem de sequências biológicas.**

Informe nos itens 11.9 ao 11.12 os documentos anexados, se houver.



<b>DIRPA</b>	Tipo de Documento:  <b>Formulário</b>	<b>DIRPA</b>	Página:  <b>3/3</b>
Título do Documento:		Código: <b>FQ001</b>	Versão: <b>2</b>
<b>Depósito de Pedido de Patente</b>			Procedimento: <b>DIRPA-PQ006</b>

**11. Documentos Anexados:**

(Assinale e indique também o número de folhas):

(Deverá ser indicado o número total de somente uma das vias de cada documento).

	<b>Documentos Anexados</b>	<b>folhas</b>
<input checked="" type="checkbox"/> 11.1	Guia de Recolhimento da União (GRU).	02
<input checked="" type="checkbox"/> 11.2	Procuração.	01
<input type="checkbox"/> 11.3	Documentos de Prioridade.	—
<input type="checkbox"/> 11.4	Documento de contrato de trabalho.	—
<input checked="" type="checkbox"/> 11.5	Relatório descritivo.	21
<input checked="" type="checkbox"/> 11.6	Reivindicações.	04
<input checked="" type="checkbox"/> 11.7	Desenho(s) (se houver). Sugestão de figura a ser publicada com o resumo: nº, _____ por melhor representar a invenção (sujeito à avaliação do INPI).	12
<input checked="" type="checkbox"/> 11.8	Resumo.	01
<input type="checkbox"/> 11.9	Listagem de sequências em arquivo eletrônico: _____ nº de CDs ou DVDs (original e cópia).	—
<input type="checkbox"/> 11.10	Código de controle alfanumérico no formato de código de barras referente às listagem de sequências.	—
<input type="checkbox"/> 11.11	Listagem de sequências em formato impresso.	—
<input type="checkbox"/> 11.12	Declaração relativa à Listagem de sequências.	—
<input checked="" type="checkbox"/> 11.13	Outros (especificar) Portarias, Anexo de Inventores, Anexo de Depositantes, DOE.	05

**12. Total de folhas anexadas: 46 fls.**

**13. Declaro, sob as penas da Lei que todas as informações acima prestadas são completas e verdadeiras.**

Belo Horizonte, 08/05/14

Local e Data

Assinatura e Carimbo

Profa. Adelina Martha dos Reis

Pró-Reitora de Pesquisa/ UFMG

Portaria nº 1.536/2014

**ANEXO DE DEPOSITANTES**

**Título: DERIVADOS ALQUILTRIAZÓLICOS COM ATIVIDADE ANTITUMORAL,  
PROCESSO DE OBTENÇÃO E USO**

Página 1

Nome: Fundação de Amparo à Pesquisa do Estado de Minas Gerais - FAPEMIG

Qualificação: Fundação

CNPJ / CPF / Número INPI: 21949888000183

Endereço Completo: Rua Raul Pompéia, 101, 11º andar - São Pedro, Belo Horizonte - MG, Brasil

CEP: 30.330-080

Telefone: (31) 3409-4774

FAX: (31)3409-6430

E-mail: patentes@ctit.ufmg.br

**ANEXO DE INVENTORES**

**Título: DERIVADOS ALQUILTRIAZÓLICOS COM ATIVIDADE ANTITUMORAL,  
PROCESSO DE OBTENÇÃO E USO**

**Página 1**

Nome: VANESSA SILVA ARAÚJO

Qualificação: QUIMICA

CPF: 052.077.576-79

Endereço Completo: RUA FLOR DE ÍNDIO, 70, APTO. 306, BAIRRO LIBERDADE, BELO HORIZONTE, MG

CEP: 31.270-215

Telefone: 31 - 3409-4774

FAX: 31 - 3409-6430

E-mail: patentes@ctit.ufmg.br

---

Nome: ROSEMEIRE BRONDI ALVES

Qualificação: QUÍMICA

CPF: 493.928.246-53

Endereço Completo: RUA CÂNDIDO FERNANDES, 20, BAIRRO UNIÃO, BELO HORIZONTE, MG

CEP: 31.170-410

Telefone: 31 - 3409-4774

FAX: 31 - 3409-6430

E-mail: patentes@ctit.ufmg.br

---



001-9

## RECEIPO DO SACADO

Local de Pagamento

Pagável em qualquer Banco

Cedente

INPI - Instituto Nacional da Propriedade Industrial

Data do Documento	Nº. documento	Especie doc.	Acéite	Data Proces.	Vencimento
31/10/2013	1307893117	RC	N	31/10/2013	Contra-apresentação
Usu Banco	Cartera	Especie	Quantidade	Valor	Agência/Código Cedente 2234-9/333.028-1

Número: NN Complementar: Peticionamento: Papel

Natureza: 10 - Patente de Cod Serviço

200 - Depósito de pedido nacional de invenção (PI), Depósito de pedido nacional de modelo de utilidade (MU), Depósito de pedido nacional de certificado de adição de invenção (C) e Entrada na fase nacional do PCT

Petição Vinculada RPI Valor

R\$ 95,00

Governo Federal - Guia de Recolhimento da União. GRU - Cobrança

Sacado

Universidade Federal de Minas Gerais

Av. Antônio Carlos, 6627 - Unidade Administrativa II - 2º andar- sala 2008, Belo Horizonte, BR/MG, 31270-901

Sacador/Avalista

Corte na linha pontilhada

Autenticação mecânica - Controle Cedente



SIAFI2013-DOCUMENTO-CONSULTA-CONGRU (CONSULTA GUIA DE RECOLHIMENTO DA UNIAO

11/11/13 11:04

USUARIO : FILIPPE

DATA EMISSAO : 08Nov13 TIPO : 1 - PAGAMENTO NUMERO : 2013GR800735

UG/GESTAO EMITENTE : 153273 / 15229 - PRO-REITORIA DE PESQUISA/UFMG

UG/GESTAO FAVORECIDA : 183038 / 18801 - INSTITUTO NACIONAL DA PROPRIEDADE INDU

RECOLHEDOR : 153273 GESTAO : 15229

CODIGO RECOLHIMENTO : 72200 - 6 COMPETENCIA: NOV13 VENCIMENTO: 06Nov13

DOC. ORIGEM: 153273 / 15229 / 2013RP000887 PROCESSO :

RECURSO : 3

(=) VALOR DOCUMENTO : 95,00

(-) DESCONTO/ABATIMENTO:

(-) OUTRAS DEDUÇOES :

(+ ) MORA/MULTA :

(+ ) JUROS/ENCARGOS :

(+ ) OUTROS ACRESCIMOS :

(=) VALOR TOTAL : 95,00

NOSSO NUMERO/NUMERO REFERENCIA : 00000000221307893117

CODIGO DE BARRAS : 89620000000 9 95000001010 4 95523127220 9 00360640000 4

OBSERVACAO

Natureza 10 - patente de Cod 200 - Depósito de pedido nacional de invenção (PI), Depósito de pedido nacional de modelo de utilidade (MU), Depósito de pedido

LANCADO POR : 09102350661 - FILIPPE UG : 153273 08Nov2013 13:58

PF1=AJUDA PF3=SAI PF2=DADOS ORC/FIN PF4=ESPELHO PF12=RETORNA

<b>BANCO DO BRASIL</b>	001-9	<b>RECIBO DO SACADO</b>			
<i>Local de Pagamento</i> <b>Pagável em qualquer Banco</b>					<i>Vencimento</i> <b>Contra-apresentação</b>
<i>Cedente</i> <b>INPI - Instituto Nacional da Propriedade Industrial</b>					<i>Agência/Código Cedente</i> <b>2234-9/333.028-1</b>
<i>Data do Documento</i> 13/03/2014	<i>Nº. documento</i> 1401703990	<i>Especie doc.</i> RC	<i>Acente</i> N	<i>Data Proces.</i> 13/03/2014	<i>Nosso Número</i> <b>00.000.2.8.14.0170399.0</b>
<i>Uso Banco</i>	<i>Carteira</i> 18/086	<i>Espécie</i> R\$	<i>Quantidade</i>	<i>Valor</i> <b>R\$ 9,00</b>	<i>(-) Valor Documento</i> <b>R\$ 9,00</b>
<i>Número:</i> NN Complementar: 0000221307893117 <i>Peticionamento: Papel</i>					<i>(-) Desconto/Abatimento</i>
<i>Cod</i> 800 - <i>Serviço</i> Complementação de retribuição					<i>(-) Outras deduções</i>
					<i>(+) Mora/Multa</i>
					<i>(+) Outros Acréscimos</i>
					<i>(=) Valor Cobrado</i> <b>R\$ 9,00</b>
<i>Governo Federal - Guia de Recolhimento da União. GRU - Cobrança</i>					
<i>Sacado</i> <b>Universidade Federal de Minas Gerais</b> Av. Antônio Carlos, 6627 - Unidade Administrativa II - 2º andar- sala 2008, Belo Horizonte, BR/MG, 31270-901					<i>Autenticação mecânica - Controle Cedente</i>
<i>Sacador/Avalista</i>					
<i>Corte na linha pontilhada</i>					

— SIAFI2014-DOCUMENTO-CONSULTA-CONGRU (CONSULTA GUIA DE RECOLHIMENTO DA UNIAO  
22/04/14 11:28

USUARIO : FILIPPE  
DATA EMISSAO : 15Abr14 TIPO : 1 - PAGAMENTO NUMERO : 2014GR800209  
UG/GESTAO EMITENTE : 153273 / 15229 - PRO-REITORIA DE PESQUISA/UFG  
UG/GESTAO FAVORECIDA : 183038 / 18801 - INSTITUTO NACIONAL DA PROPRIEDADE INDU  
RECOLHEDOR : 153273 GESTAO : 15229  
CODIGO RECOLHIMENTO : 72200 - 6 COMPETENCIA: VENCIMENTO: 11Abr14  
DOC. ORIGEM: 153273 / 15229 / 2014RP000275 PROCESSO :

RECURSO : 3

(=) VALOR DOCUMENTO : 9,00

(-) DESCONTO/ABATIMENTO:

(-) OUTRAS DEDUÇOES :

(+) MORA/MULTA :

(+) JUROS/ENCARGOS :

(+) OUTROS ACRESCIMOS :

(=) VALOR TOTAL : 9,00

NOSSO NUMERO/NUMERO REFERENCIA : 00000000281401703990

CODIGO DE BARRAS : 89670000000 4 09000001010 9 95523127220 9 00360640000 4

OBSERVACAO

NN Complementar 0000221307893117 Cod 800 - Complementação de retribuição - Referente GRU/2014/020

LANCADO POR : 56099762604 - DELIANE UG : 153273 15Abr2014 13:49  
PF1=AJUDA PF3=SAI PF2=DADOS ORC/FIN PF4=ESPELHO PF12=RETORNA



UNIVERSIDADE FEDERAL DE MINAS GERAIS  
GABINETE DO REITOR

**PORTARIA N° 064, DE 25 DE MARÇO DE 2014**

O REITOR DA UNIVERSIDADE FEDERAL DE MINAS GERAIS, no uso de suas atribuições e, de acordo com o disposto nos artigos 11 e 12 do Decreto-Lei nº 200, de 25 de fevereiro de 1967,

**RESOLVE:**

Delegar competência à **PRÓ-REITORA DE PESQUISA**, professora **ADELINA MARTHA DOS REIS**, e ao seu substituto eventual, para, no âmbito da Pró-Reitoria de Pesquisa:

- a) autorizar a realização de despesas dentro dos limites orçamentários da Unidade 153273;
- b) autorizar a concessão de suprimento de fundos a servidores da Unidade, bem como determinar a baixa de responsabilidade;
- c) requisitar passagens e transportes em geral, por quaisquer vias, nos limites da dotação orçamentária da Unidade Gestora 153273;
- d) autorizar viagens de servidores, a serviço da Unidade, arbitrando-lhes as respectivas diárias, obedecidas as disposições legais pertinentes;
- e) assinar termos de outorga, convênios de cooperação e contratos com a Fundação de Amparo à Pesquisa de Minas Gerais – FAPEMIG; Federação das Indústrias e suas filiadas; Secretaria de Estado de Ciência e Tecnologia; Conselho Nacional de Desenvolvimento Tecnológico – CNPq; Financiadora de Estudos e Projeto – Finep; Coordenação de Aperfeiçoamento de Pessoal de Nível Superior – CAPES; e Ministério da Ciência e Tecnologia;
- f) assinar contratos, decorrentes de licitação, de sua dispensa ou inexigibilidade, no âmbito da Pró-Reitoria de Pesquisa;
- g) assinar todo e qualquer documento necessário para depósito, processamento, adição, retificação, substituição, modificação, ampliação e resposta de relatórios referentes a objeto de proteção de Propriedade Intelectual junto aos órgãos competentes, em âmbito nacional e internacional.

Belo Horizonte, 25 de março de 2014.

Prof. Jaime Arturo Ramírez  
Reitor

SCG/vsf

Avenida Antônio Carlos, 6627 - 31270-901 - Belo Horizonte - Minas Gerais  
Tel: (31) 3409-4127 - Fax: (31) 3409-4130 - [sadm@gabinete.ufmg.br](mailto:sadm@gabinete.ufmg.br) - Home page: [www.ufmg.br](http://www.ufmg.br)

L:\Document\Portaria\p14-064

## PROCURAÇÃO

A FUNDAÇÃO DE AMPARO À PESQUISA DO ESTADO DE MINAS GERAIS - FAPEMIG, pessoa jurídica de direito público, com sede na Rua Raul Pompéia, nº 101, Bairro São Pedro, na cidade de Belo Horizonte, Minas Gerais, inscrita no CNPJ sob o nº 21.949.888/0001-83, neste ato representada pela Procuradora do Estado de Minas Gerais e Procuradora-Chefe da FAPEMIG, Catarina Barreto Linhares, brasileira, OAB/MG 67.181, MASP 598.208-7, de acordo com a Portaria PRE Nº004/2012, confere poderes especiais à UNIVERSIDADE FEDERAL DE MINAS GERAIS - UFMG, inscrita no CNPJ/MF sob o nº 17.217.985/0001-04, na pessoa de seu representante legal ou procurador devidamente constituído, para representá-la junto ao Instituto Nacional da Propriedade Industrial – INPI, nos processos de proteção intelectual da UFMG em que a FAPEMIG figure como cotitular, conforme Deliberação 34/2008 da FAPEMIG, podendo efetuar os seguintes procedimentos e seus desdobramentos: depósitos de patente, registros de programas de computador e registros de desenhos industriais, conforme os atos previstos em lei, agindo em conjunto ou separadamente, para o bom e fiel cumprimento do presente mandado.



Belo Horizonte, 16 de 05 de 2013

Selo de fiscalização  
AUTENTICAÇÃO  
BZ0 08785



Catarina Barreto Linhares  
Procuradora do Estado de Minas Gerais  
Procuradora Chefe da FAPEMIG

CATARINA BARRETO LINHARES  
Procuradora do Estado  
OAB/MG 67.181 - MASP: 598.208-7

# MINAS GERAIS

ÓRGÃO OFICIAL DOS PODERES DO ESTADO

DIÁRIO DO EXECUTIVO, LEGISLATIVO E PUBLICAÇÕES DE TERCEIROS

## Atos do Governador

ATOS ASSINADOS PELO SENHOR GOVERNADOR DO  
ESTADO, EM DATA DE ONTEM:

Pela Fundação de Amparo à Pesquisa do Estado de Minas Gerais

designa, nos termos do art. 14, II, da Lei nº 869, de 5 de julho de 1952 e tendo em vista a Lei Delegada nº 182, de 21 de janeiro de 2011 e o Decreto nº 45.537, de 27 de janeiro de 2011; MARIO NETO BORGES, MASP 1099717-9, para o cargo de provimento em comissão de PRESIDENTE, código PR-AP01, de recrutamento amplo, da Fundação de Amparo à Pesquisa do Estado de Minas Gerais.

# FAPEMIG

## Fundação de Amparo à Pesquisa do Estado de Minas Gerais

### PORTARIA PRE Nº 004/2012

Altera à Portaria PRE 051/2009 incluindo novas competências  
O Presidente da Fundação de Amparo à Pesquisa do Estado de Minas Gerais – FAPEMIG, no uso das atribuições que lhe conferem o art. 15, inciso VIII, da Lei nº Estadual 11.552, de 03 de agosto de 1994, Resolve: Art. 1º - Delega novas competências à Procuradora-Chefe, Catarina Barreto Linhares e ao Assessor da Presidência, Ildeu Viana da Silva, para a prática, em nome da Fundação de Amparo à Pesquisa do Estado de Minas Gerais - FAPEMIG, dos atos a seguir relacionados, perante o Instituto Nacional de Propriedade Intelectual – INPI, órgão do Ministério do Desenvolvimento, Indústria e Comércio, perante o Ministério da Agricultura, Pecuária e Abastecimento, por meio do Serviço Nacional de Proteção de Cultivares (SNPC) e do Registro Nacional de Cultivares – RNC e perante a Fundação Biblioteca Nacional, podendo agir em conjunto ou separadamente, com poderes para requerer e obter proteção de propriedade industrial, registros, receber notificações administrativas, apresentar impugnações, recursos administrativos, promover contra a autoridade competente prova ou contraprova pertinentes à titularidade de direitos de propriedade intelectual, efetuar pagamentos de quaisquer taxas de manutenção, impugnar recursos administrativos, requerer a anotação de alteração de nomes e titularidade, e tudo o mais que for necessário e de direito. Art. 2º - Esta Portaria entrará em vigor na data de sua publicação e revogam-se as disposições em contrário. Belo Horizonte, 28 de fevereiro de 2012. Ass) Prof. Mario Nelo Borges, PhD - Presidente da FAPEMIG

29 268557 - 1

## **DERIVADOS ALQUILTRIAZÓLICOS COM ATIVIDADE ANTITUMORAL, PROCESSO DE OBTENÇÃO E USO**

[001] A presente invenção descreve derivados 1,2,3-alquiltriazólicos com atividade antitumoral e o processo de obtenção dos mesmos. Os compostos foram obtidos através de reações rápidas, de fácil realização, reproduzíveis, e todas com bons rendimentos. Além disso, esses derivados apresentaram atividade antitumoral em concentrações micromolares. Portanto, a presente invenção trata, também, do uso desses derivados como antitumoral.

[002] Alquifosfolipídios sintéticos de cadeia simples (AFLs) são uma classe relativamente nova de agentes antitumorais que, ao contrário dos fármacos quimioterapêuticos convencionais, atuam sobre as membranas das células tumorais para induzir apoptose, e não sobre o DNA. AFLs acumulam nas células e interferem de forma dependente nas vias de sinalização de sobrevivência dos lipídios, nomeadamente PI3K-AkT e Raf-Erk1/2, e na biossíntese dos mesmos. Alquillisofosfolipídios (ALFs) e alquifosfocolinas (AFCs) são éteres lipídicos que representam esta classe de AFLs como potenciais agentes anticâncer. Os fármacos miltefosina (hexadecilfosfocolina), perifosina (octadecil-(1,1-dimetil-4-piperidinio)fosfato), erucilfosfocolina (*cis*-13-docosenilfosfocolina), ilmofosina (1-hexadeciltio-2-metoximetil-*rac*-glicero-3-fosfocolina) e erufosina (erucilfosfo-N,N,N,-trimetilpropilamônio) pertencem à classe dos AFCs que são derivados de ALFs pela remoção do grupo glicerol de lisofosfatidilcolina (LysoPC). Já no fármaco edelfosina (1-O-octadecil-2-O-metil-*rac*-glicero-3-fosfocolina), a subunidade glicerol é mantida. A miltefosina é um dos AFCs mais estudados e exerce atividade antiproliferativa contra várias linhagens celulares tumorais, apresentando também potente atividade leishmanicida, como consequência da interferência nas vias metabólicas dos parasitas e indução de apoptose. Os fármacos miltefosina e perifosina já são comercializados em vários países (MCGWIRE, B. S.; SATOSKAR A. R. Leishmaniasis: clinical syndromes and treatment. *Q. J. Med.*, 2014, 107, 7-14) para o tratamento de tumores e, no caso da miltefosina, para o tratamento de leishmaniose humana e canina (ALAM, MD. M. et al. Synthesis,

characterization and Akt phosphorylation inhibitory activity of cyclopentanecarboxylate-substituted alkylphosphocholines. *Bioorg. Med. Chem. Lett.*, 2013, 21, 2018-2024; WOERLY, V. et al. Clinical efficacy and tolerance of miltefosine in the treatment of canine leishmaniosis. *Parasitol. Res.*, 2009, 105, 272-275).

[003] Estudos de relação estrutura-atividade de alquilfosfolipídios revelam que a cadeia alquílica longa e um grupo polar são essenciais para a atividade antitumoral. Nos últimos anos, um número grande de trabalhos tem relatado a síntese e a atividade biológica de vários AFCs (PINCHUK, A. N. et al. Synthesis and structure-activity relationship effects on the tumor activity of radioiodinated phospholipid ether analogues. *J. Med. Chem.*, 2006, 49, 2155-2165; CALOGEROPOULOU, T. et al. Design and synthesis of potent antileishmanial cycloalkylidene-substituted ether phospholipid derivatives. *J. Med. Chemistry.*, 2008, 51, 897-908; AVLONITIS, N. et al. Antileishmanial ring-substituted ether phospholipids. *J. Med. Chem.*, 2003, 46, 755-767; LUKAC, M. et al. Synthesis and biological activity of dialkylphosphocholines. *Bioorg. Med. Chem. Lett.*, 2009, 19, 6346-6349; COGHI, P. et al. Parallel synthesis and antileishmanial activity of ether-linked phospholipids. *Bioorg. Med. Chem. Lett.*, 2008, 18, 4658-4660; HORNILLOS, V. et al. Synthesis of 16-mercaptophexadecylphosphocholine, a miltefosine analog with leishmanicidal activity. *Bioorg. Med. Chem. Lett.*, 2006, 16, 5190-5193; SAUGAR, J. M. et al. Synthesis and biological evaluation of fluorescent leishmanicidal analogues of hexadecylphosphocholine (Miltefosine) as probes of antiparasite mechanisms. *J. Med. Chem.*, 2007, 50, 5994-6003; HORNILLOS, V. et al. Synthesis of BODIPY-labeled alkylphosphocholines with leishmanicidal activity, as fluorescent analogues of miltefosine. *Bioorg. Med. Chem. Lett.*, 2008, 18, 6336-6339). Embora estruturalmente simples, a purificação destes compostos é muito difícil, demorada, cara e os rendimentos da síntese são frequentemente muito baixos. As dificuldades advêm, em parte, da alta polaridade destes compostos, o que dificulta a purificação.

[004] Já os compostos contendo núcleos heterocíclicos sintéticos do tipo 1,2,3-triazóis tem recebido grande atenção nos últimos anos por causa de sua ampla gama de propriedades farmacológicas. Por exemplo, vários trabalhos

apresentam o uso de 1,2,3-triazóis como substâncias com atividade anti-HIV (ALVAREZ, R. et al. 1,2,3-Triazole-[2',5'-bis-O-(tert-butyldimethylsilyl)-beta-D-ribofuranosyl]-3'-spiro-5''-(4''-amino-1'',2''-oxathiole 2'',2''-dioxide) (TSAO) analogues: Synthesis and anti-HIV-1 activity. *J. Med. Chem.*, 1994, 37, 4185-4194; VELAZQUES, S. et al. Regiospecific synthesis and anti-human immunodeficiency virus activity of novel 5-substituted N-alkylcarbamoyl and N,N-dialkylcarbamoyl 1,2,3-triazole-TSAO analogues. *Antiviral Chem. Chemother.*, 1998, 9, 481-489; BRIK, A. et al. Rapid diversity-oriented synthesis in microtiter plates for *in situ* screening of HIV protease inhibitors. *Chem. Bio. Chem.*, 2003, 4, 1246-1248; WHITING, M. et al. Inhibitors of HIV-1 protease by using *in situ* click chemistry. *Angew. Chem. Int. Ed.*, 2006, 45, 1435-1439; MONTAGU, A. et al. Synthesis of new C5-(1-substituted-1,2,3-triazol-4 or 5-yl)-20-deoxyuridines and their antiviral evaluation. *Eur. J. Med. Chem.*, 2011, 46, 778-786).

[005] Montagu e colaboradores (2011), por exemplo, relatam a importância e atividade de 1,2,3-triazóis dissubstituídos contra vírus da herpes simples tipo 1 (HSV-1), herpes simples tipo 2 (HSV-2), varicela-zoster (VZV TK<sup>+</sup> e TK<sup>-</sup>) e citomegalovírus (AD-169 e cepas Davis).

[006] Outra atividade descrita para essa classe de compostos é a antimicrobiana (GENIN, M. J. et al. Substituent effects on the antibacterial activity of nitrogen-carbon-linked (azolylphenyl)oxazolidinones with expanded activity against the fastidious gram-negative organisms *Haemophilus influenzae* and *Moraxella catarrhalis*. *J. Med. Chem.*, 2000, 43, 953-970; GONZAGA, D. T. G. et al. Recent advances in the synthesis of new antimycobacterial agents based on the 1H-1,2,3-triazoles. *Curr. Topics in Med. Chem.*, 2013, 13, 2850-2865).

[007] Já Gonzaga e colaboradores (2013) em sua revisão citam, por exemplo, a importância desta classe de compostos bioativos como potenciais agentes antituberculose.

[008] Outra aplicação é o uso de 1,2,3-triazóis com atividade inibidora de enzimas (OLESEN, P. H. et al. Synthesis and *in vitro* characterization of 1-(4-aminofurazan-3-yl)-5-dialkylaminomethyl-1H-[1,2,3]triazole-4-carboxylic acid

derivatives. A new class of selective GSK-3 inhibitors. *J. Med. Chem.*, 2003, 46, 3333-3341; PANDE, V. et al. Structural basis for the GSK-3beta binding affinity and selectivity against CDK-2 of 1-(4-aminofuran-3yl)-5-dialkylaminomethyl-1*H*-[1,2,3]triazole-4-carboxylic acid derivatives. *Bioorg. Med. Chem. Lett.*, 2005, 15, 5129-5135; KLEIN, M. et al. Synthesis of chiral 1,4-disubstituted-1,2,3-triazole derivatives from amino Acids. *Molecules*, 2009, 14, 5124-5143; BENERJEE, D. R. et al. Design, synthesis and characterization of novel inhibitors against mycobacterial  $\beta$ -ketoacyl CoA reductase FabG4. *Org. Biomol. Chem.*, 2014, 12, 73-85). Benerjee e colaboradores (2014) relataram recentemente o potencial de inibição da enzima FabG4 (Rv0242c) de *Mycobacterium tuberculosis* por 1,2,3-triazóis polifenólicos.

[009] É importante ressaltar também a atividade anticancerígena intensamente relatada para 1,2,3-triazóis (PRAVEENA, K. S. S. et al. Synthesis of 2,2,4-trimethyl-1,2-dihydroquinolinyl substituted 1,2,3-triazol derivatives: Their evaluation as potential PDE 4B inhibitors possessing cytotoxic properties against cancer cells. *Bioorg. Chem.*, 2014, 53, 8-14; KURUMURTHY, C. et al. Synthesis of novel 1,2,3-triazole tagged pyrazolo[3,4-b]pyridine derivatives and their cytotoxic activity. *Bioorg. Med. Chem. Lett.*, 2014, 24, 746-749). No trabalho de Kurumurthy e colaboradores, é relatada a síntese de novos 1,2,3-triazóis derivados de pirazolo[3,4-b]piridina, que apresentaram atividade contra células tumorais humanas U937, THP-1, células HL60 e B16-F10. Todos esses estudos corroboram o fato destes compostos estarem entre os sistemas heterocíclicos mais pesquisados nas últimas décadas, principalmente devido à sua fácil acessibilidade sintética por reações de cicloadição do tipo “click”.

[010] Considerando a potencial atividade antitumoral das alquilfosfocolinas e a especulação de que sua atividade antitumoral esteja associada à presença de uma subunidade hidrofóbica ligada a um grupo polar hidrofilico e também o relato da atividade antitumoral para compostos 1,2,3-triazólicos, a presente invenção focaliza a síntese de potenciais protótipos antitumorais simples contendo um anel 1,2,3-triazólico e cadeias alquílicas com diferentes tamanhos e funcionalizações, na tentativa de correlacionar a

atividade antitumoral desta nova classe de compostos, alquiltriazóis, com a classe dos AFCs.

[011] Os pedidos de patente encontrados no estado da técnica que tratam de compostos 1,2,3-triazólicos abordam processos de obtenção deste tipo de composto. Uma busca recente em bancos de dados de patentes mostrou que nos últimos cinco anos um grande número de trabalhos (cerca de 140) foi depositado sobre triazóis, incluindo pedidos de patente relacionadas ao uso de 1,2,3-triazóis como potencial antibacteriano, como por exemplo, WO2012137099, "IMIDAZOLE, PYRAZOLE, AND TRIAZOLE DERIVATIVES USEFUL AS ANTIBACTERIAL AGENTS", no qual são descritas as sínteses de 26 compostos derivados do ácido hidroxâmico; como antitumoral WO2012111025, "1,2,3-TRIAZOLE CONTAINING ARTEMISININ COMPOUNDS AND PROCESS FOR PREPARATION THEREOF", no qual são relatadas a síntese de 10 moléculas derivadas da artemisinina; e de inibição enzimática WO2012138877, "INHIBITEURS DES SÉRINE HYDROLASES DE TYPE N1- ET N2-CARBAMOYL-1,2,3-TRIAZOLE ET MÉTHODES ASSOCIÉES" que descreve a síntese de 15 moléculas derivadas da ureia.

[012] Considerando os artigos e patentes encontrados e os exemplos citados acima sobre compostos triazólicos com atividade biológica, verifica-se que em nenhum caso foram descritas moléculas contendo longas cadeias alquílicas ligadas ao núcleo 1,2,3-triazólico separando grupos funcionais diversos, o que diferencia a tecnologia ora em foco, das já existentes, tanto pela estrutura das moléculas quanto pela facilidade para sua obtenção.

[013] A vantagem principal dessa tecnologia foi a obtenção rápida, de diversas novas substâncias químicas, aqui chamadas alquiltriazóis, estruturalmente mais simples que as alquilfosfocolinas, e com atividade antitumoral em escala micromolar, o que é bastante promissor como nova classe de compostos farmacologicamente ativos.

#### **BREVE DESCRIÇÃO DAS FIGURAS**

[014] A Figura 1 mostra o esquema de síntese para a obtenção das azidas usadas como materiais de partida, os reagentes, bem como os

respectivos rendimentos obtidos. As condições reacionais empregadas foram: (i) HBr (48%), tolueno, 110°C, 24 h, 65-87%; (ii) NaN<sub>3</sub>, DMSO, t.a, 24 h, 48-80%; (iii) diclorometano, cloreto de mesila, trietilamina, t.a, 24 h, 37-90%; (iv) KF/18-crown-6, DMSO, 110°C, 24 h, 47-49%. As azidas 4a, 5a e 5b são descritas pela primeira vez.

[015] A Figura 2 mostra o esquema de síntese dos triazóis 10a a 10j, os reagentes e as proporções empregadas destes, bem como os respectivos rendimentos. As condições reacionais empregadas foram: (i) ascorbato de sódio (20 mol%), CuSO<sub>4</sub>.5H<sub>2</sub>O (8 mol%), CH<sub>2</sub>Cl<sub>2</sub>:H<sub>2</sub>O (1:1), t.a, 24 h. R= Diferentes tipos de substituição de acordo com o alcino comercial utilizado.

[016] A Figura 3 mostra o esquema de síntese para a obtenção dos derivados triazólicos contendo iodo 11a a 11d, os reagentes, bem como os respectivos rendimentos. As condições reacionais foram: (i) NaI, acetona, refluxo, 24 h. R= Diferentes tipos de substituição de acordo com o alcino comercial utilizado.

[017] A Figura 4 mostra apoptose em células de carcinoma de cólon humano (RKO). As células foram incubadas (48 horas) com o composto 10e (B. 1µM, C. 10 µM e D. 100 µM), 11a (F. 1µM, G. 10 µM e H. 100 µM) e etoposídeo (E. 1 µM). A Figura 4A mostra o controle de vida (sem adição de qualquer composto). A seta indica a morte celular por apoptose (verde). As células viáveis são coradas em vermelho. Escala: 20µm.

[018] A Figura 5 mostra o espectro de absorção na região do infravermelho (ATR) do composto 10a.

[019] A Figura 6 mostra o espectro de RMN de <sup>1</sup>H do composto 10a (200 MHz, CDCl<sub>3</sub>).

[020] A Figura 7 mostra o espectro de RMN de <sup>13</sup>C do composto 10a (50 MHz, CDCl<sub>3</sub>).

[021] A Figura 8 mostra o espectro de Massas de 10a (ESI-MS).

[022] A Figura 9 mostra o espectro de absorção na região do infravermelho (ATR) do composto 10c.

[023] A Figura 10 mostra o espectro de RMN de  $^1\text{H}$  do composto 10c (200 MHz,  $\text{CDCl}_3$ ).

[024] A Figura 11 mostra o espectro de RMN de  $^{13}\text{C}$  do composto 10c (50 MHz,  $\text{CDCl}_3$ ).

[025] A Figura 12 mostra o espectro de Massas de 10c (ESI-MS).

[026] A Figura 13 mostra o espectro de absorção na região do infravermelho (ATR) do composto 10e.

[027] A Figura 14 mostra o espectro de RMN de  $^1\text{H}$  do composto 10e (200 MHz,  $\text{CDCl}_3$ ).

[028] A Figura 15 mostra o espectro de RMN de  $^{13}\text{C}$  do composto 10e (50 MHz,  $\text{CDCl}_3$ ).

[029] A Figura 16 mostra o espectro de Massas de 10e (ESI-MS).

[030] A Figura 17 mostra o espectro de absorção na região do infravermelho (ATR) do composto 10i.

[031] A Figura 18 mostra o espectro de RMN de  $^1\text{H}$  do composto 10i (200 MHz,  $\text{CDCl}_3$ ).

[032] A Figura 19 mostra o espectro de RMN de  $^{13}\text{C}$  do composto 10i (50 MHz,  $\text{CDCl}_3$ ).

[033] A Figura 20 mostra o espectro de Massas de 10i (ESI-MS).

[034] A Figura 21 mostra o espectro de absorção na região do infravermelho (ATR) do composto 11a.

[035] A Figura 22 mostra o espectro de RMN de  $^1\text{H}$  do composto 11a (200 MHz,  $\text{CDCl}_3$ ).

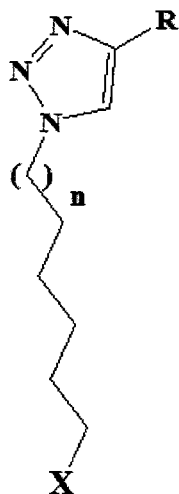
[036] A Figura 23 mostra o espectro de RMN de  $^{13}\text{C}$  do composto 11a (50 MHz,  $\text{CDCl}_3$ ).

[037] A Figura 24 mostra o espectro de Massas de 11a (ESI-MS).

## **DESCRIÇÃO DETALHADA DA INVENÇÃO**

[038] A presente invenção consiste no processo de preparação de 14 moléculas contendo o núcleo 1,2,3-triazólico, cadeias alquílicas longas e variados grupos funcionais nas terminações das cadeias das moléculas.

[039] Os compostos preparados apresentam as seguintes estruturas químicas:



Onde:

$X = -O_3SCH_3, -I$  ou  $-F$ ;

$n = 1, 4$  ou  $7$ ;

$R = -CH_2OH, -(CH_2)_3OH, -(CH_2)_2COOH$  ou  $-COOCH_2CH_3$ .

[040] O processo geral de síntese dos compostos supracitados consistiu nas seguintes etapas:

- Preparação de álcoois monobromados  $HOCH_2(CH_2)_nCH_2Br$ , onde  $n = 4, 7$  ou  $10$ , a partir dos dióis 1,6-hexanodiol, 1,9-nonadiol ou 1,12-dodecanodiol, respectivamente;
- Transformação dos monobrometos obtidos  $HOCH_2(CH_2)_nCH_2Br$  na etapa “a” nos azido alcoóis correspondentes  $HOCH_2(CH_2)_nCH_2N_3$ , onde  $n = 4, 7$  ou  $10$ ;

- c) Obtenção de compostos mesilados,  $\text{MsOCH}_2(\text{CH}_2)_n\text{CH}_2\text{N}_3$ , a partir dos azido alcoóis obtidos,  $\text{HOCH}_2(\text{CH}_2)_n\text{CH}_2\text{N}_3$ , onde  $n= 4, 7$  ou  $10$ , na etapa “**b**”;
- d) Obtenção de compostos fluorados,  $\text{FCH}_2(\text{CH}_2)_n\text{CH}_2\text{N}_3$ , a partir dos compostos mesilados obtidos,  $\text{MsOCH}_2(\text{CH}_2)_n\text{CH}_2\text{N}_3$ , onde  $n= 4, 7$  ou  $10$ , na etapa “**c**”;
- e) Reação “click” entre os precursores azido mesilados ou fluorados obtidos nas etapas “**c**” e “**d**” com os alcinos 4-pentin-1-ol, álcool propargílico, propiolato de etila ou ácido 4-pentinóico;
- f) Reação de substituição nucleofílica ou não dos compostos azido mesilados com iodeto de sódio, seguido de purificação dos sólidos obtidos.

[041] A proposta sintética revelou-se simples e limpa, em comparação com as já existentes para a preparação de alquilfosfocolinas, por exemplo, uma vez que não foram requeridos meios sofisticados de purificação, uma das desvantagens encontradas no estado da técnica. Empregaram-se somente colunas cromatográficas filtrantes.

[042] A metodologia consistiu primeiramente na obtenção de compostos monobromados utilizando os dióis 1,6-hexanodiol, 1,9-nonadiol ou 1,12-dodecanodiol como materiais de partida. Uma segunda etapa foi a obtenção das azidas orgânicas correspondentes por uma reação de  $\text{SN}_2$  do grupo brometo pela azida. A terceira etapa foi a síntese dos mesilatos de alquilazidas também por uma reação de  $\text{SN}_2$ . A quarta etapa consistiu na obtenção de cadeias fluoradas por reação de substituição de mesilatos com fluoreto. A quinta etapa do trabalho consistiu na obtenção dos derivados 1,2,3-triazólicos, via reação “click” entre os “blocos de construção” obtidos anteriormente e contendo uma função azida e alcinos terminais como o 4-pentin-1-ol, o álcool propargílico, o propiolato de etila e o ácido 4-pentinóico. A metodologia empregada utilizou como fonte de cobre (I) o sulfato de cobre pentahidratado na presença do agente redutor ascorbato de sódio. Para a obtenção de triazóis contendo iodo, partiu-se de triazóis mesilados e procedeu-se uma reação de

substituição nucleofílica com iodeto de sódio. Todos os produtos obtidos foram purificados por simples filtração em coluna de sílica gel.

[043] Os ensaios antitumorais *in vitro* com os alquiltriazóis foram conduzidos com duas linhagens celulares tumorais: HeLa (ATCC CCL2, carcinoma cervical) e RKO-AS45-1 (ATCC CRL-2579, carcinoma colorretal) e uma linhagem de células normais WI-26VA-4 (ATCC CCL-95.1, fibroblastos de pulmão).

[044] O processo de síntese dos derivados 1,2,3-triazólicos, suas caracterizações e o estudo biológico dos mesmos podem ser melhor compreendidos através dos seguintes exemplos, não limitantes.

**Exemplo 1: Procedimento geral para a síntese dos compostos azido funcionalizados 4a, 4b, 4c, 5a e 5b e caracterização dos mesmos**

[045] Os compostos azido funcionalizados 4a, 4b, 5a e 5b, obtidos através dos procedimentos abaixo descritos (ver esquema de síntese na Figura 1), foram usados como materiais de partida para a reação “click”.

**A) Procedimento de obtenção de 4a, 4b e 4c**

[046] A uma solução de 1,6-hexanodiol (1a) (1,00 a 2,00 equiv.) em tolueno (30 a 40 mL) adicionou-se ácido bromídrico 48% (1,00 a 2,00 equiv.). A mistura foi mantida sob agitação a 110°C por 24 horas em um sistema contendo um extrator de água (Dean Starck). Após este tempo, o tolueno foi removido e o sólido obtido foi cromatografado em coluna de sílica usando misturas (v/v) de hexano/acetato como eluente (100/0, 90/10, 80/20, 0/100), o que forneceu o composto 2a com 93% de rendimento. O produto 2a (1,00 a 2,00 equiv.) foi dissolvido em dimetilsulfóxido (DMSO) (20 a 30 mL) e a esta mistura adicionou-se uma solução 0,5 mol/L de azida de sódio em DMSO (1,00 a 2,00 equiv.). A solução resultante foi mantida sob agitação, a temperatura ambiente, por 23 horas. Após este tempo acrescentaram-se 30 mL de água destilada matendo-se a agitação por 10 minutos adicionais. A mistura foi extraída com éter etílico e a fase etérea foi lavada com água destilada. A fase orgânica foi seca com sulfato de sódio anidro, filtrada e o solvente removido. O sólido obtido foi cromatografado em coluna de sílica usando misturas (v/v) de

hexano/acetato de etila como eluente (100/0, 90/10, 80/20, 50/50), o que forneceu o composto 3a com 48% de rendimento. O produto 3a (1,00 a 2,00 equiv.) foi dissolvido em diclorometano (20 a 30 mL) e a solução foi mantida em banho de gelo, acrescentando-se lentamente a ela cloreto de mesila (2,00 a 4,00 equiv.) e trietilamina (2,00 a 4,00 equiv.). Deixou-se a mistura sob agitação magnética à temperatura ambiente por 24 horas. Após este tempo a mistura foi vertida sobre gelo picado contido em um funil de separação e procedeu-se a extração empregando diclorometano. A fase orgânica foi secada com sulfato de sódio anidro, filtrada e em seguida o solvente foi removido. O resíduo obtido foi cromatografado em coluna de sílica usando misturas (v/v) de hexano/acetato de etila como eluente (100/0, 90/10, 50/50, 70/30), o que forneceu o composto 4a com 37% de rendimento.

[047] O procedimento descrito acima foi utilizado também para a obtenção de 4b, trocando o diol de partida, em vez de 1,6-hexanodiol foi utilizado o 1,9-nonadiol comercial (1b), com 90% de rendimento, e 4c onde o diol de partida foi o 1,12-dodecanodiol comercial (1c); 4c foi obtido com 80% de rendimento. O composto 4b já foi descrito na literatura (GOUNDRY, W.R.F.; BALDIWIN, J.E.; LEE, V. Total synthesis of cytotoxic sponge alkaloids hachijodines F and G. *Tetrahedron*, 2003, 59, 1719-1729; GRUBE, A.; TIMM, C.; KÖCK, M. Synthesis and mass spectrometric analysis of cyclostelletamines H, I, K and L. *European Journal of Medicinal Chemistry*, 2006, 5, 1285-1295). Também o composto 4c já foi descrito na literatura (SHOREY, B. J.; LEE, V.; BALDWIN, J. E. Synthesis of the Arctic sponge alkaloid viscosaline and the marine sponge alkaloid theonelladin C. *Tetrahedron*, 2007, 63, 5587-5592).

### Procedimento de obtenção de 5a e de 5b

[048] A uma solução de metanossulfonato de 9-azidonononila (4b) (1,00 a 2,00 equiv.) em dimetilsulfóxido seco (4 a 8 mL) adicionou-se fluoreto de potássio (1,00 a 2,00 equiv.) e éter de coroa 18-crow-6 (2,00 a 4,00 equiv.). A mistura foi mantida sob agitação magnética por 24 horas a 110°C. Após este período foram adicionados 5 mL de água destilada e a mistura foi extraída com diclorometano. A fase orgânica foi secada com sulfato de sódio anidro, filtrada

e em seguida o solvente foi removido. O sólido obtido foi cromatografado em coluna de sílica gel usando misturas (v/v) de hexano/acetato de etila como eluente (100/0, 90/10) fornecendo o composto 5a com 47% de rendimento.

[049] O mesmo procedimento foi utilizado para a obtenção de 5b. Para isso foi utilizada uma solução de metanossulfonato de 12-azidodecanila, como material de partida; o composto 5b foi obtido com 49% de rendimento.

### B) Caracterização dos compostos

[050] Os compostos foram caracterizados por espectroscopia no Infravermelho, além de análise dos espectros de Ressonância Magnética Nuclear de  $^1\text{H}$  e de  $^{13}\text{C}$ .

[051] Tabela 1- Dados de RMN de  $^1\text{H}$ , RMN de  $^{13}\text{C}$  e de IV dos compostos 5a e 5b.

Composto	RMN de $^1\text{H}$ (200 MHz, $\text{CDCl}_3$ ) $\delta$ (ppm)	RMN de $^{13}\text{C}$ (50 MHz, $\text{CDCl}_3$ ) $\delta$ (ppm)	IV ( $v_{\text{máx}}$ , $\text{cm}^{-1}$ )
5a	1,20-1,49 (m, 12H), 1,52-1,81 (m, 2H), 3,26 (t, $J = 6,0$ Hz, 2H), 4,43 (td, $J = 6,0$ Hz, $J = 48,0$ , 2H)	25,3; 26,8; 29,0; 29,2; 29,3; 29,5; 30,6 (d, $J = 19,0$ ); 84,3 (d, $J = 163,0$ )	2929, 2857, 2091, 1350, 1171
5b	1,19-1,44 (m, 18H). 1,52-1,80 (m, 2H), 3,26 (t, $J = 6,0$ Hz, 2H), 4,44 (t, $J = 6,0$ Hz, 2H)	25,25; 26,85; 29,00; 29,22; 29,29; 29,52; 30,56 (d, $J = 19,0$ ); 84,34 (d, $J = 163,0$ )	2929, 2857, 2091, 1350, 1171

### Exemplo 2: Procedimento geral para a síntese de alquiltriazóis (10a a 10j) e caracterização dos mesmos

#### A) Procedimento de obtenção

[052] O derivado 4a, 4c, 5a ou 5b (1,00 a 2,00 equiv.) contendo o grupo azido (compostos que se apresentam como óleos viscosos), foi adicionado a um balão contendo 1 mL de diclorometano, 1 mL de água, CuSO<sub>4</sub>.5H<sub>2</sub>O (0,08 a 1,60 equiv.), ascorbato de sódio (0,20 a 0,40 equiv.) e o alcino desejado (pent-4-in-1-ol (6) ou propiolato de etila (7) ou ácido 4-pentinóico (8) ou álcool propargílico (9) (1,00 a 2,00 equiv.). A mistura reagente foi vigorosamente agitada à temperatura ambiente durante 24 horas. Após a conclusão da reação, 5 mL de água foram adicionados, seguido por extração com diclorometano. A fase orgânica resultante foi lavada com uma solução a 25% de EDTA tamponada com NH<sub>4</sub>Cl a pH 9,5; foi seca com Na<sub>2</sub>SO<sub>4</sub> e, em seguida, o solvente foi removido. O produto bruto obtido em cada reação foi purificado por cromatografia em coluna sobre sílica gel com diclorometano puro, seguido de misturas (v/v) de diclorometano/ EtOAc (80:20, 50:50, 20:80) como eluentes para a obtenção dos compostos puros correspondentes 10a a 10j. A Figura 2 mostra o esquema de síntese empregado.

### B) Caracterização dos produtos

[053] Os produtos foram caracterizados por espectroscopia no Infravermelho, análise dos espectros de Ressonância Magnética Nuclear de <sup>1</sup>H e de <sup>13</sup>C, além de espectrometria de massas (ver Figuras 5 a 20).

[054] Tabela 2- Dados de RMN de <sup>1</sup>H, RMN de <sup>13</sup>C e de IV dos compostos 10a a 10j.

Composto	RMN de <sup>1</sup> H (200 MHz, CDCl <sub>3</sub> ) $\delta$ (ppm)	RMN de <sup>13</sup> C (50 MHz, CDCl <sub>3</sub> ) $\delta$ (ppm)	IV ( $\nu_{\text{máx}}$ , cm <sup>-1</sup> )
10a	1,24-1,50 (m, 4H), 1,65-1,96 (m, 6H), 2,79 (t, $J$ = 6,0, 2H), 2,98 (s, 3H), 3,66 (t, $J$ = 6,0 Hz, 2H), 4,18 (t, $J$ = 6,0 Hz,	21,50; 24,45; 25,43; 28,44; 29,62; 31,76; 36,86; 49,64; 60,77; 69,96; 121,14; 147,22	3276, 2916, 2850, 1331, 1162, 1052- 848

	2H), 4,30 (t, $J = 6,0$ Hz, 2H), 7,33 (s, 1H)		
10b	1,30-1,38 (m, 6H), 1,68 (qn, $J = 6,0$ Hz, 2H), 1,90 (qn, $J = 6,0$ Hz, 2H), 2,95 (s, 3H), 4,15 (t, $J = 6,0$ Hz, 2H), 4,42-4,26 (m, 4H), 8,08 (s, 1H)	14,18; 24,68; 25,59; 28,70; 29,79; 37,21; 50,29; 61,12; 69,67; 127,33; 140,13; 160,65	2945, 2915, 2869, 1728, 1344, 1197, 1097-957, 1166, 1156, 1097, 915
10c	1,02-1,45 (m, 10H), 1,57-1,71 (m, 2H), 1,70-1,99 (m, 4H), 2,76 (t, $J = 6,0$ Hz, 2H), 2,94 (s, 3H), 3,63 (t, $J = 6,0$ Hz, 2H), 4,15 (t, $J = 6,0$ Hz, 2H), 4,24 (t, $J = 6,0$ Hz, 2H), 7,24 (s, 1H)	21,85; 24,92; 25,86; 28,53; 28,93; 29,80; 31,93; 36,91; 49,50; 61,39; 70,11; 120,73; 147,38	3276, 2919, 2851, 1332, 1164, 1059- 848
10d	1,14-1,33 (m, 10H), 1,39 (t, $J = 6,0$ Hz, 2H), 1,71 (qn, $J = 6,0$ , 2H), 1,81-1,99 (m, 2H), 2,90 (s, 3H), 4,19 (t, $J = 6,0$ Hz, 2H), 4,30-4,50 (m, 4H), 8,08 (s, 1H)	14,37; 25,35; 26,28; 28,79; 29,10; 30,14; 37,40; 50,68; 60,99; 70,08; 127,33; 140,19; 160,64	2936, 2912, 2852, 1713, 1352, 1215, 1168, 1051- 979
10e	1,25-1,44 (m, 16H), 1,75 (qn, $J = 6,0$ Hz,	21,89; 25,21; 26,30; 28,80; 28,92; 29,21;	3389, 2916, 2850, 1332,

	2H), 1,84-1,99 (m, 4H), 2,84 (t, $J = 6,0$ Hz, 2H), 3,01 (s, 3H), 3,71 (t, $J = 6,0$ Hz, 2H), 4,22 (t, $J = 6,0$ Hz, 2H), 4,31 (t, $J = 6,0$ Hz, 2H), 7,34 (s, 1H)	30,12; 31,96; 37,14; 50,09; 61,29; 70,24; 121,89; 147,43	1163, 1045-956
10f	1,18-1,26 (m, 16H), 1,50-1,69 (m, 4H), 2,19-2,50 (m, 4H), 2,94 (s, 3H), 3,19 (t, $J = 6,0$ Hz, 2H), 4,15 (t, $J = 6,0$ Hz, 2H), 7,98 (s, 1H)	33,18; 37,14; 51,01; 70,31; 115,56; 136,35; 178,87	2916, 2850, 1729, 1331, 1163, 1052-952, 850
10g	1,20-1,30 (m, 16H), 1,41 (t, $J = 6,0$ Hz, 2H), 1,74 (qn, $J = 6,0$ Hz, 2H), 1,87-1,98 (m, 2H), 2,97 (s, 3H), 4,18 (t, $J = 6,0$ Hz, 2H), 4,39-4,45 (m, 4H), 8,05 (s, 1H)	14,16; 25,20; 26,13; 28,78; 28,92; 29,17; 29,50; 29,97; 37,11; 50,49; 60,99; 69,99; 127,18; 140,09; 160,66	2916, 2850, 1717, 1341, 1226, 1207, 1168, 1046-943, 848
10h	1,16-1,38 (m, 16H), 1,62-1,88 (m, 4H), 2,95 (s, 3H), 4,16 (t, $J = 6,0$ Hz, 2H), 4,27 (t, $J = 6,0$ Hz, 2H), 4,70 (s, 2H), 7,54 (s, 1H)	25,44; 26,31; 28,84; 28,95; 29,25; 30,12; 31,17; 50,26; 55,88; 121,78; 147,77	3117, 3023, 2916, 2850, 1331, 1162, 1120, 1052-951

10i	1,29-1,40 (m, 10H), 1,68 (qnd, $J = 2,0$ Hz, $J = 24,0$ Hz, 2H), 1,83-1,98 (m, 4H), 2,83 (t, $J = 8,0$ Hz, 2H), 3,66-3,74 (m, 2H), 4,31 (t, $J =$ 8,0 Hz, 2H), 4,43 (td, $J = 8,0$ Hz, $J =$ 48,0 Hz, 2H), 7,54 (s, 1H)	21,85; 24,87; 26,26; 28,69; 28,88; 29,04; 30,09; 30,22 (d, $J =$ 13,5 Hz); 31,96; 50,05; 61,25; 84,00 (d, $J = 163,0$ Hz); 120,78; 147,24	3312, 2913, 2848, 1050
10j	1,21-1,44 (m, 16H), 1,56-2,05 (m, 6H), 2,86 (t, $J = 6,0$ Hz, 2H), 3,70 (t, $J = 6,0$ Hz, 2H), 4,32 (t, $J =$ 6,0 Hz, 2H), 4,55 (td, $J = 6,0$ Hz, $J =$ 46,0 Hz, 2H), 7,34 (s, 1H)	21,68; 25,21; 26,61; 29,58; 30,42; 30,52 (d, $J = 19,0$ Hz); 32,17; 49,84; 61,71; 84,21 (d, $J = 179,5$ Hz); 121,01; 147,35	3321, 2917, 2846, 1006

**Exemplo 3: Procedimento geral para a síntese de 11a a 11d e caracterização dos compostos obtidos**

#### A) Procedimento de obtenção

[055] A uma solução dos compostos 10c, 10d, 10e ou 10g (1,00 a 2,00 equiv.) separadamente em acetona (5 mL), foi adicionado iodeto de sódio (2,00 a 4,00 equiv.), e a mistura foi aquecida sob refluxo por 24 horas. Cada mistura foi diluída com água e extraída com diclorometano. As fases orgânicas foram combinadas e secadas com  $\text{Na}_2\text{SO}_4$  anidro, e o solvente foi removido. O resíduo obtido foi cromatografado em sílica gel utilizando EtOAc/MeOH (v/v) (100:0; 80:20 e 0:100) como eluentes para obtenção dos compostos puros 11a a 11d. A Figura 3 mostra o esquema de síntese empregado.

### B) Caracterização dos produtos

[056] Os produtos foram caracterizados por espectroscopia no Infravermelho, análise dos espectros de Ressonância Magnética Nuclear de  $^1\text{H}$  e de  $^{13}\text{C}$ , além de espectrometria de massas (ver Figuras 21 a 24).

[057] Tabela 3 - Dados de RMN de  $^1\text{H}$ , RMN de  $^{13}\text{C}$  e de IV dos compostos 11a a 11d.

Composto	RMN de $^1\text{H}$ (200 MHz, $\text{CDCl}_3$ ) $\delta$ (ppm)	RMN de $^{13}\text{C}$ (50 MHz, $\text{CDCl}_3$ ) $\delta$ (ppm)	IV ( $\nu_{\text{máx}}$ , $\text{cm}^{-1}$ )
11a	1,24-1,34 (m, 10H), 1,74-1,94 (m, 6H), 2,80 (t, $J = 6,0$ Hz, 2H), 3,17 (t, $J = 6,0$ Hz, 2H), 3,67 (t, $J = 6,0$ Hz, 2H), 4,29 (t, $J = 6,0$ Hz, 2H), 7,31 (s, 1H)	7,51; 22,03; 26,56; 28,49; 29,00; 29,27; 30,39; 32,20; 33,56; 50,70; 61,64; 121,05; 147,62	3350, 2924, 2851
11b	1,15-1,39 (m, 16H), 1,61-2,3 (m, 6H), 2,83 (t, $J = 6,0$ Hz, 2H), 3,18 (t, $J = 6,0$ Hz, 2H), 3,70 (t, $J = 6,0$ Hz, 2H), 4,30 (m, 4H), 8,06 (s, 1H)	7,34; 21,91; 26,35; 28,36; 28,85; 29,22; 29,29; 30,16; 30,33; 31,97; 33,99; 49,98; 61,35; 120,79; 147,36	3308, 2917, 2848
11c	1,22-1,28 (m, 10H), 1,41 (t, $J = 6,0$ Hz, 3H), 1,71-1,85 (m, 2H), 1,86-1,96 (m, 2H), 3,18 (t, $J = 6,0$ Hz, 2H), 4,30-4,51 (m, 4H), 8,07 (s, 1H)	7,37; 14,50; 26,50; 28,67; 29,08; 29,56; 30,33; 30,64; 33,34; 50,64; 61,81; 127,36; 140,53; 160,80	2919, 2848, 1723, 1216, 1197, 1164

11d	1,15-1,39 (m, 16H), 1,41 (t, $J = 6,0$ Hz, 2H), 1,81 (t, $J = 6,0$ Hz, 2H), 1,95 (qn, $J = 6,0$ Hz, 2H), 3,18 (t, $J = 6,0$ Hz, 2H), 4,33-4,47 (m, 4H), 8,06 (s, 1H)	6,89; 14,29; 26,30; 28,33; 28,79; 29,09; 30,14; 30,36; 33,42; 50,87; 61,06; 127,17; 140,09; 160,81	2919, 2848, 1723, 1224, 1207, 1164, 777
-----	--	---	--

#### Exemplo 4: Ensaios Biológicos

##### A) Ensaio de Viabilidade Celular

[058] Foram utilizadas linhagens celulares humanas para análise de citotoxicidade dos produtos obtidos. As linhagens utilizadas foram WI-26VA-4 (fibroblasto de pulmão ATCC CCL-95.1, células normais), HeLa (carcinoma cervical ATCC CCL2) e RKO-AS45-1 (carcinoma colorretal ATCC CRL-2579).

[059] A citotoxicidade dos compostos nessas linhagens celulares foi avaliada pelo ensaio da redução do MTT (3-(4,5-dimetiltiazol-2-il)-2,5-difeniltetrazólico). O MTT é um sal tetrazólico que reage com as mitocôndrias de células viáveis formando um cristal de cor violeta (formazan). Para o ensaio de viabilidade celular as células foram transferidas para uma placa de 96 poços na concentração de  $1 \times 10^5$  células/poço. As placas foram inicialmente incubadas por 24 horas em estufa a  $37^\circ\text{C}$  em atmosfera úmida de  $\text{CO}_2$  a 5%. Após esse período as células foram lavadas com solução salina tamponada (PBS). As moléculas a serem testadas foram diluídas nas concentrações que variaram de 2 a  $1000 \mu\text{mol/L}$  em meio de cultivo RPMI, suplementado com 1% de soro fetal bovino. Após a diluição os compostos foram adicionados à placa. Em paralelo, como controle positivo, foi testado o etoposídeo, indutor de apoptose em linhagens tumorais humanas. Após 48 horas de incubação, os poços foram lavados com PBS novamente, e adicionou-se  $100 \mu\text{L}$ /poço do sal tetrazólico MTT na concentração de  $5 \text{mg/mL}$ . Incubou-se por mais 3 horas. As placas foram centrifugadas por 5 minutos a  $320\text{g}$ , retirou-se o sobrenadante e aplicou-se  $50 \mu\text{L}$  de DMSO em cada poço para solubilizar os cristais de formazan. A leitura foi realizada em leitor de microplacas a  $550\text{nm}$ . Os ensaios

de citotoxicidade foram realizados em triplicatas. Os resultados podem ser observados na Tabela 4.

[060] Tabela 4 – Resultados da atividade citotóxica *in vitro* dos alquiltriazóis contra células humanas de carcinoma de cólon (RKO), células de carcinoma uterino (HeLa) e células de fibroblasto de pulmão (WI-26VA4, células normais) e índice de seletividade (IS).

<b>Composto</b>	<b>IC<sub>50</sub> (µM) ± DP<sup>a</sup></b>			<b>IS<sup>b</sup> (WI/HeLa)</b>	
	<b>HeLa</b>	<b>RKO</b>	<b>WI</b>	<b>WI/RKO</b>	
10a	210,10 ± 5,18	397,90 ± 6,54	489,15 ± 4,02	2,33	1,23
10b	202,18 ± 0,31	198,23 ± 18,02	339,34 ± 27,86	1,67	1,71
10c	24,48 ± 5,20	182,03 ± 28,4	ND	ND	ND
10d	37,10 ± 3,90	20,49 ± 5,80	ND	ND	ND
10e	11,05 ± 3,70*	16,70 ± 3,40*	ND	ND	ND
10f	35,95 ± 7,38 *	99,94 ± 0,89	39,45 ± 10,42	1,09	0,39
10g	208,17 ± 25,12	180,16 ± 5,92	490,41 ± 4,03	2,35	2,72
10h	21,87 ± 0,78 *	19,87 ± 4,22 *	36,54 ± 3,21	1,67	1,84
10i	84,25 ± 9,92	307,21 ± 8,77	184,43 ± 1,51	2,19	0,60
10j	25,82 ± 9,19 *	90,82 ± 0,83	80,48 ± 12,66	3,11	1,13
11a	12,77 ± 1,16 *	14,57 ± 2,18 *	21,40 ± 3,36	1,67	1,47
11b	145,33 ± 13,22	138,16 ± 10,10	27,68 ± 4,08	0,19	0,20
11c	52,22 ± 12,74	199,01 ± 26,30	253,82 ± 59,95	4,87	2,27
11d	26,61 ± 2,20 *	62,23 ± 2,55	71,84 ± 14,10	2,70	1,15
Etoposideo *	11,35 ± 2,73	10,66 ± 2,23	4,30 ± 1,34	0,39	0,40

<sup>a</sup>Valores das médias ± desvio padrão.

<sup>b</sup>IS = LC<sub>50</sub> WI/IC<sub>50</sub> HeLa e <sup>b</sup>IS = LC<sub>50</sub> WI/IC<sub>50</sub>RKO

\*Estatisticamente diferente ( $p < 0,05$ ).

ND = não determinado

[061] Pelos resultados pode-se observar que os compostos 10c e 11a foram mais ativos contra as linhagens tumorais HeLa e os compostos 10e e 11a contra as linhagens tumorais RKO, apresentando valores de IC<sub>50</sub> que variaram de 11,05 a 16,70 µmol/L. A mesma faixa de ação foi observada pelo fármaco etoposídeo, cujo IC<sub>50</sub> variou 10,66 a 11,35 µmol/L. A Tabela 4 apresenta os resultados obtidos.

[062] Todos os compostos sintetizados possuem estruturas químicas inovadoras e diferentes dos principais antitumorais atualmente disponíveis para

uso clínico tais como o próprio etoposídeo, cisplatina e 5-fluorouracila. São sintetizados em poucas etapas (no máximo 5 etapas) e não apresentam estereocentros em suas estruturas. A ausência de estereocentros torna não só a síntese desses compostos metodologicamente mais simples como também facilita a sua purificação devido à ausência de isômeros.

[063] A dose que inibe em 50% o crescimento das células ( $IC_{50}$ ) na presença dos compostos testes foi determinada em comparação com células cultivadas sem a presença de compostos (considerada 100% de viabilidade). A inibição de cada composto foi quantificada através de uma curva dose-resposta. Foi utilizado o programa OriginPro versão 8.0 para confecção das curvas de  $IC_{50}$ .

#### **B) Detecção de apoptose por meio do ensaio de TUNEL e imunofluorescência**

[064] A análise de morte celular por apoptose foi realizada utilizando o kit APO-BrdU TUNEL. O efeito dos compostos 10c, 10e e do etoposídeo, indutor de apoptose já descrito pela literatura e usado como controle positivo neste teste, foram avaliados sobre a fragmentação de DNA utilizando células RKO AS-45-1. As células foram incubadas com os compostos durante 48 horas e fixadas utilizando uma solução de etanol 70% a 4°C. Foram então adicionado às células, 5-bromo-2'-desoxiuridina-5'-trifosfato (BrdUTP) que, na presença da desoxinucleotidil Terminal Transferase (TdT), incorpora-se à extremidades do DNA fragmentado. O BrdUTP incorporado ao DNA fragmentado foi reconhecido pelo anticorpo monoclonal anti-BrdU conjugado com Alexa Fluor 488. As células foram visualizadas por microscopia de fluorescência usando um microscópio Axiovert Zeiss 200.

[065] A citotoxicidade destes compostos está associada com a indução de apoptose nas linhagens celulares, conforme demonstrado na Figura 4. A adição dos compostos 10c e 10e em diferentes concentrações (1-100 $\mu$ mol/L) aumentou a quantidade de células em apoptose em comparação ao controle de vida, que não recebeu a adição de nenhum composto (Figura 4A). O mesmo

padrão de indução de apoptose foi observado com o etoposídeo, utilizado como padrão no experimento (Figura 4E).

[066] A indução da apoptose em linhagens tumorais é uma estratégia promissora para o desenvolvimento de fármacos antitumorais com ação terapêutica mais segura, uma vez que a apoptose não dispara a sinalização do sistema imune local. Tal condição evita, por exemplo, a formação de um processo inflamatório, diminuindo os efeitos colaterais no paciente e, consequentemente, aumentando sua adesão ao tratamento.

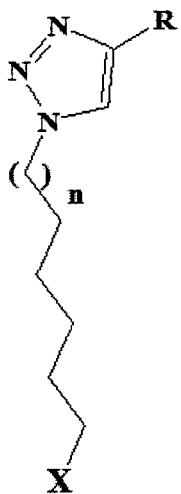
[067] Dentre todos os alquiltriazóis submetidos ao ensaio, dois deles apresentaram atividade antitumoral superior ao do fármaco utilizado em clínica médica, o etoposídeo, que foi utilizado como controle positivo neste ensaio. Supõe-se pelos resultados encontrados, que estes alquiltriazóis são promissores fármacos antitumorais. Ensaio para detecção de apoptose pelo ensaio de TUNEL foi realizado com o composto mais ativo na linhagem RKO-AS45-1, carcinoma colorretal (ATCC CRL-2579) em diferentes concentrações, no qual foi possível verificar que este foi capaz de induzir apoptose a partir da concentração de 10 $\mu$ mol/L.

### C) Análise Estatística

[068] A média dos valores de IC<sub>50</sub> foi comparada pelo teste de Tukey. As diferenças entre os valores obtidos foram avaliados pelo programa Origin 6.0. Valor de p < 0,05 foi considerado estatisticamente significativo.

## REIVINDICAÇÕES

**1- Derivados alquiltriazólicos, caracterizados por apresentarem a fórmula estrutural (I):**



Onde:

X=  $-O_3SCH_3$ , -I ou  $-F$ ;

n= 1, 4 ou 7;

R=  $-CH_2OH$ ,  $-(CH_2)_3OH$ ,  $-(CH_2)_2COOH$  ou  $-COOCH_2CH_3$ .

**2- Processo para obtenção de derivados alquiltriazólicos, caracterizado pelos compostos derivados serem aqueles descritos na reivindicação 1 e por compreender as seguintes etapas:**

- Preparação de álcoois monobromados  $HOCH_2(CH_2)_nCH_2Br$ , onde n= 4, 7 ou 10, a partir dos dióis 1,6-hexanodiol, 1,9-nonadiol ou 1,12-dodecanodiol, respectivamente;
- Transformação dos monobrometos obtidos,  $HOCH_2(CH_2)_nCH_2Br$ , na etapa “a” nos azido alcoóis correspondentes,  $HOCH_2(CH_2)_nCH_2N_3$ , onde n= 4, 7 ou 10;
- Obtenção de compostos mesilados,  $MsOCH_2(CH_2)_nCH_2N_3$ , a partir dos azido alcoóis obtidos,  $HOCH_2(CH_2)_nCH_2N_3$ , onde n= 4, 7 ou 10, na etapa “b”;

- d) Obtenção de compostos fluorados,  $FCH_2(CH_2)_nCH_2N_3$ , a partir dos compostos mesilados obtidos,  $MsOCH_2(CH_2)_nCH_2N_3$ , onde  $n= 4, 7$  ou  $10$ , na etapa “c”;
- e) Reação “click” entre os precursores azido mesilados ou fluorados obtidos nas etapas “c” e “d” com os alcinos pent-4-in-1-ol, álcool propargílico, ácido 4-pentinoico ou priopiolato de etila;
- f) Reação de substituição nucleofílica ou não dos compostos azido mesilados com iodeto de sódio, seguido de purificação dos sólidos obtidos.

**3- Processo para obtenção de derivados alquiltriazólicos, de acordo com a reivindicação 2, etapa “a”, caracterizado pelos alcoóis monobromados,  $HOCH_2CH_2CH_2Br$ ,  $HOCH_2(CH_2)_4CH_2Br$ ,  $HOCH_2(CH_2)_7CH_2Br$  serem obtidos utilizando solução do diol correspondente (1,00 a 2,00 equiv.) em tolueno (30 a 40 mL), adição de ácido bromídrico 48% (1,00 a 2,00 equiv.); agitação a 110°C por 24 horas; remoção do tolueno e purificação.**

**4- Processo para obtenção de derivados alquiltriazólicos, de acordo com a reivindicação 2, etapa “b”, caracterizado pelos azido alcoóis, cada um separadamente, serem obtidos utilizando os alcoóis monobromados (1,00 a 2,00 equiv.),  $HOCH_2CH_2CH_2Br$ ,  $HOCH_2(CH_2)_4CH_2Br$ ,  $HOCH_2(CH_2)_7CH_2Br$  dissolvidos em 20 a 30mL de dimetilsulfóxido, adição de uma solução 0,5 mol/L de azida de sódio em dimetilsulfóxido (1,00 a 2,00 equiv.); agitação da mistura por 23 horas; adição de 30 mL de água destilada, agitação por 10 minutos adicionais; extração da mistura com éter etílico, a fase etérea lavada com água destilada, secada com sulfato de sódio anidro, filtrada e o solvente removido, e purificação do sólido obtido.**

**5- Processo para obtenção de derivados alquiltriazólicos, de acordo com a reivindicação 2, etapa “c”, caracterizado pelos compostos mesilados,  $MsOCH_2CH_2CH_2N_3$ ,  $MsOCH_2(CH_2)_4CH_2N_3$ , e  $MsOCH_2(CH_2)_7CH_2N_3$ , separadamente, serem obtidos a partir dos azido alcoóis (1,00 a 2,00 equiv.) correspondentes dissolvidos em 20 a 30 mL de diclorometano; a solução**

mantida em banho de gelo, acrescentando-se lentamente à ela cloreto de mesila (2,00 a 4,00 equiv.) e trietilamina (2,00 a 4,00 equiv.); agitação magnética a temperatura ambiente por 24 horas; a mistura vertida sobre gelo picado e extração com diclorometano; a fase orgânica secada com sulfato de sódio anidro, filtrada e o solvente removido e o sólido resultante purificado.

**6- Processo para obtenção de derivados alquiltriazólicos, de acordo com a reivindicação 2, etapa “d”, caracterizado pelos compostos fluorados,  $\text{FCH}_2\text{CH}_2\text{CH}_2\text{N}_3$ ,  $\text{FCH}_2(\text{CH}_2)_4\text{CH}_2\text{N}_3$ ,  $\text{FCH}_2(\text{CH}_2)_7\text{CH}_2\text{N}_3$ , separadamente, serem obtidos a partir dos compostos mesilados (1,00 a 2,00 equiv.) correspondentes dissolvidos em 4 a 8 mL de dimetilsulfóxido seco, adição de 1,00 a 2,00 equiv. de fluoreto de potássio e 2,00 a 4,00 equiv. de éter de coroa 18-crow-6; agitação magnética da mistura por 24 horas a 110°C; após este período adição de 5 mL de água destilada e extração com diclorometano; secagem com sulfato de sódio anidro, filtração, remoção do solvente e purificação do sólido obtido.**

**7- Processo para obtenção de derivados alquiltriazólicos, de acordo com as reivindicações 3, 4, 5 e 6, caracterizado pelas purificações serem através de coluna de sílica usando misturas (v/v) de hexano/acetato de etila nas proporções 100/0, 90/10, 80/20, 0/100; 100/0, 90/10, 80/20, 50/50; 100/0, 90/10, 50/50, 70/30 e 100/0, 90/10, respectivamente, como eluentes.**

**8- Processo para obtenção de derivados alquiltriazólicos, de acordo com a reivindicação 2, etapa “e”, caracterizado pelos alquitriazóis compreenderem os descritos na reivindicação 1 e pela obtenção ser através de reação “click” entre os precursores azido mesilados ou fluorados obtidos nas etapas “c” e “d” com os alcinos comerciais pent-4-in-1-ol ou álcool propargílico ou ácido 4-pentinoico ou propiolato de etila.**

**9- Processo para obtenção de derivados alquiltriazólicos, de acordo com as reivindicações 2, etapa “e” e 8, caracterizado pela reação “click” entre os precursores azido mesilados ou fluorados (1,00 a 2,00 equiv.) obtidos nas**

etapas “c” e “d” ser adicionado a um balão contendo 1 mL de diclorometano, 1 mL de água, CuSO<sub>4</sub>.5H<sub>2</sub>O (0,08 a 1,60 equiv.), ascorbato de sódio (0,20 a 0,40 equiv.) e o alcino desejado (pent-4-in-1-ol (6) ou propiolato de etila (7) ou ácido 4-pentinóico (8) ou álcool propargílico (9) (1,00 a 2,00 equiv.); a mistura reagente vigorosamente agitada à temperatura ambiente durante 24 horas; seguido de adição de 5 mL de água; extração com diclorometano e a fase orgânica resultante lavada com uma solução a 25% de EDTA tamponada com NH<sub>4</sub>Cl a pH 9,5; secagem com Na<sub>2</sub>SO<sub>4</sub> e, em seguida, o solvente removido; e purificação do sólido obtido em cada reação.

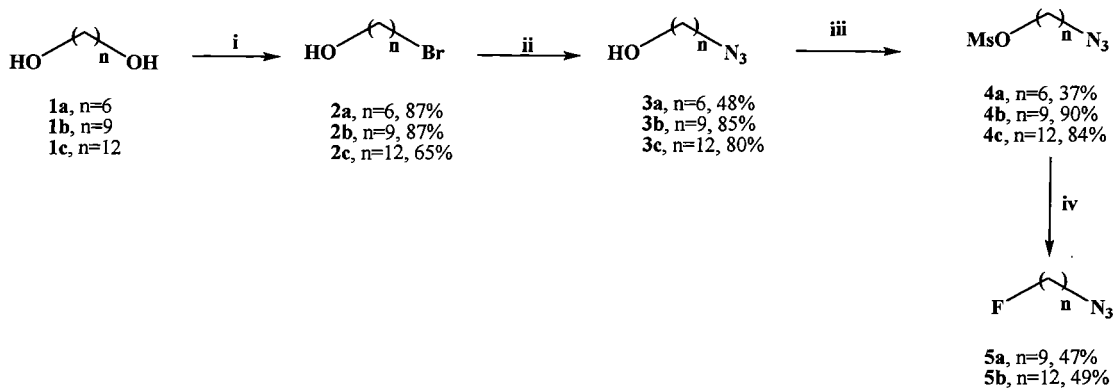
**10- Processo para obtenção de derivados alquiltriazólicos, de acordo com a reivindicação 9, caracterizado pela purificação dos sólidos ser através de coluna de sílica usando diclorometano puro, seguido de misturas (v/v) de diclorometano/acetato de etila (80/20, 50/50, 20/80) como eluente.**

**11- Processo para obtenção de derivados alquiltriazólicos, de acordo com a reivindicação 2, etapa “f”, caracterizado pela obtenção dos triazóis contendo iodo, serem a partir de triazóis mesilados através de uma reação de substituição nucleofílica com iodeto de sódio, seguido de purificação do sólido obtido.**

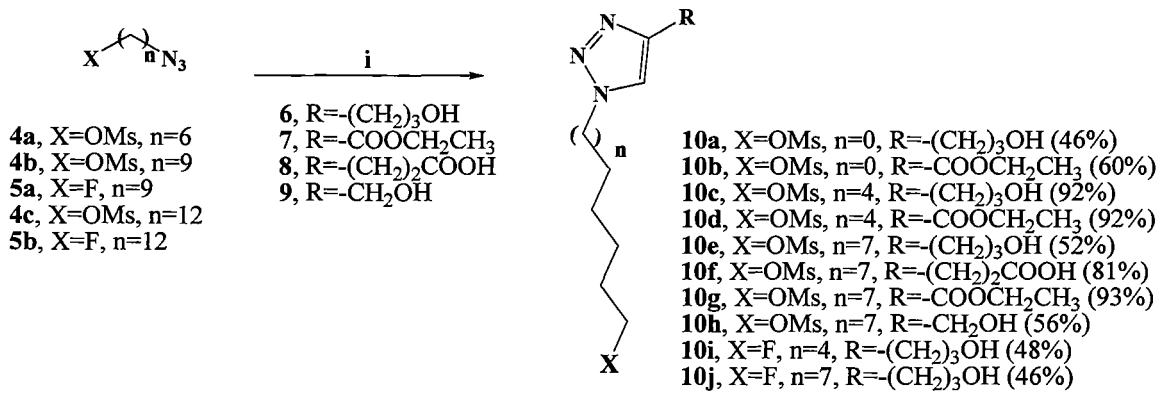
**12- Processo para obtenção de derivados alquiltriazólicos, de acordo com a reivindicação 11, caracterizado pela purificação dos sólidos ser através de coluna de sílica usando misturas (v/v) de acetato de etila/metanol (100/0; 80/20, 0/100) como eluente.**

**13- Uso dos derivados alquiltriazólicos, caracterizado por ser como antitumoral e os mesmos apresentarem fórmula estrutural (I) descrita na reivindicação 1.**

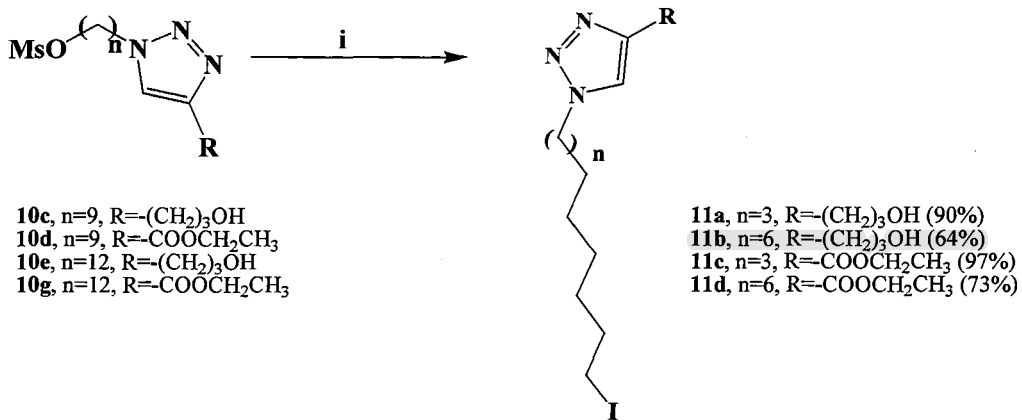
## FIGURAS



**Figura 1**

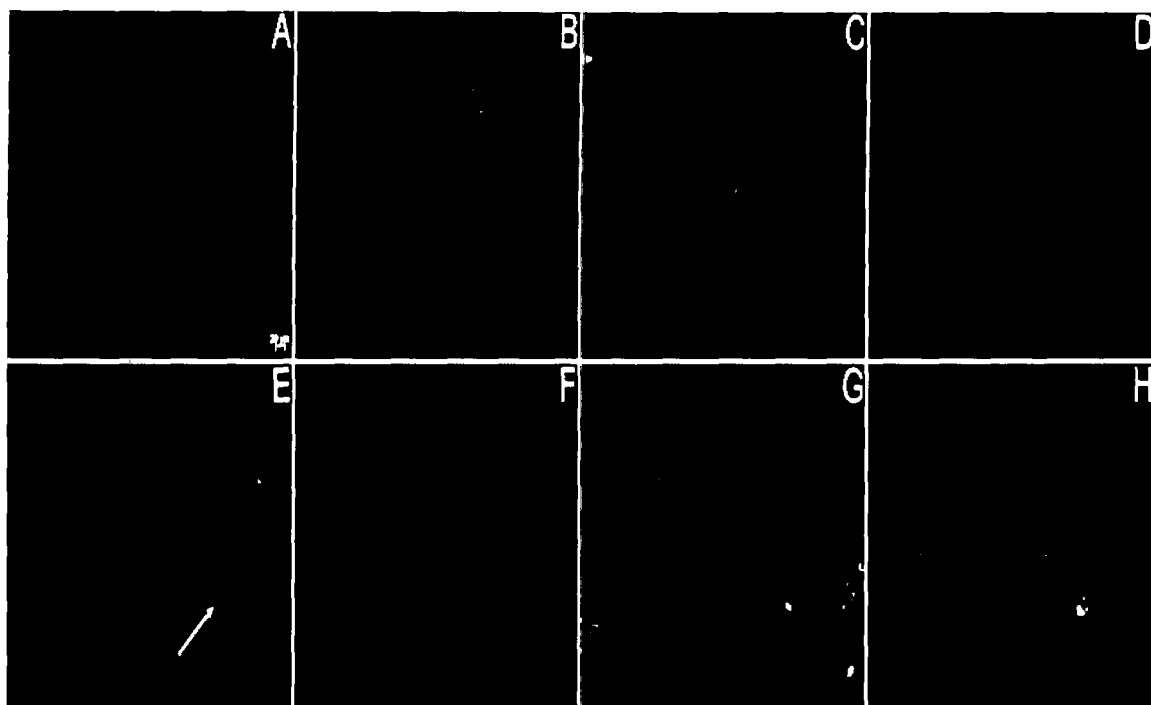
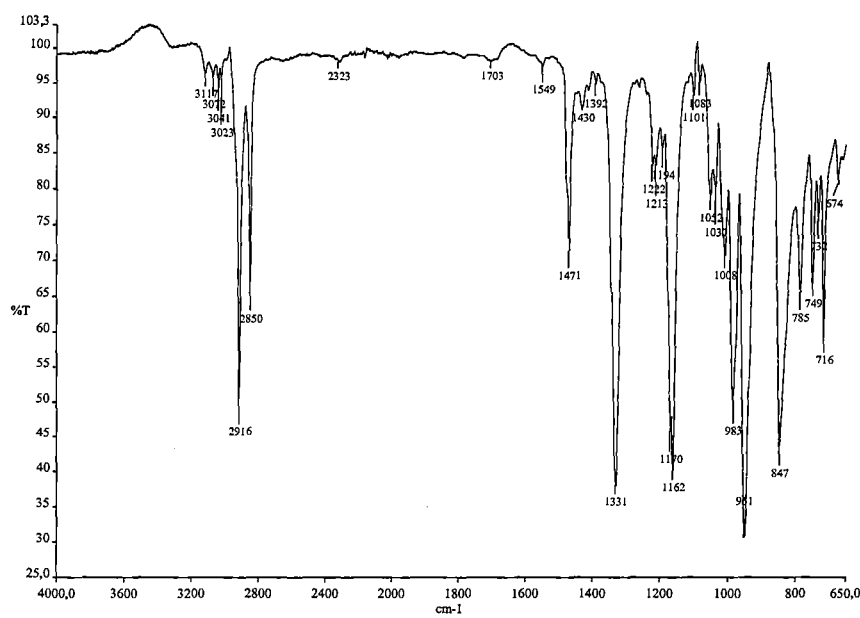


**Figura 2**



**Figura 3**

2/12

**Figura 4****Figura 5**

3/12

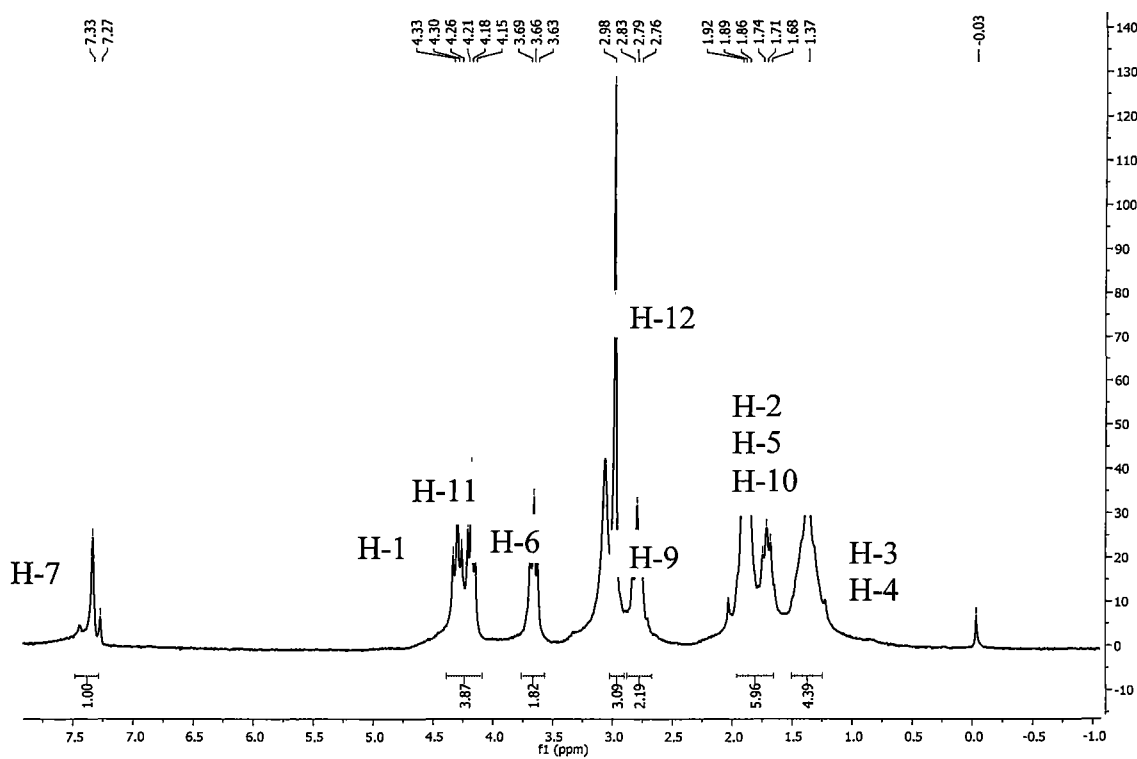


Figura 6

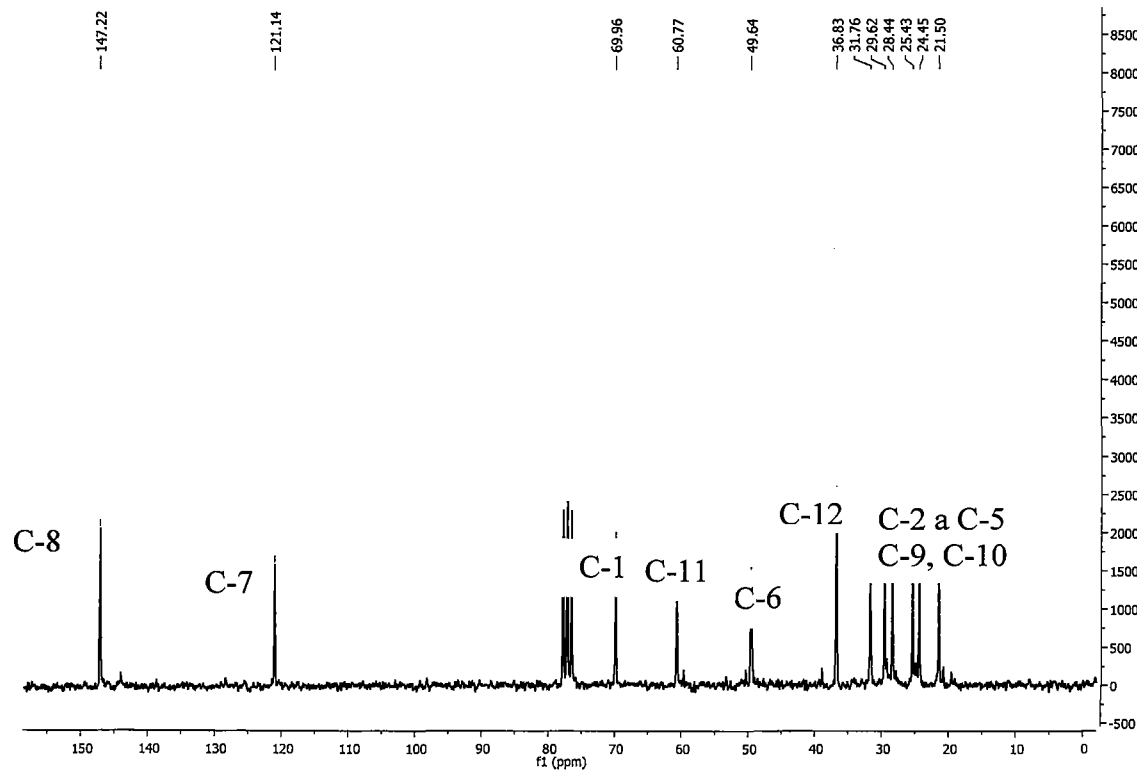
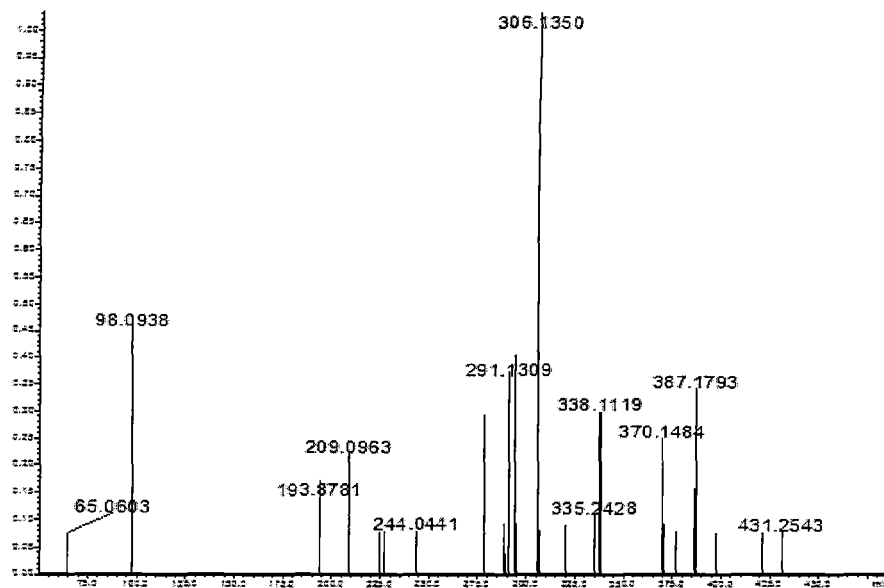
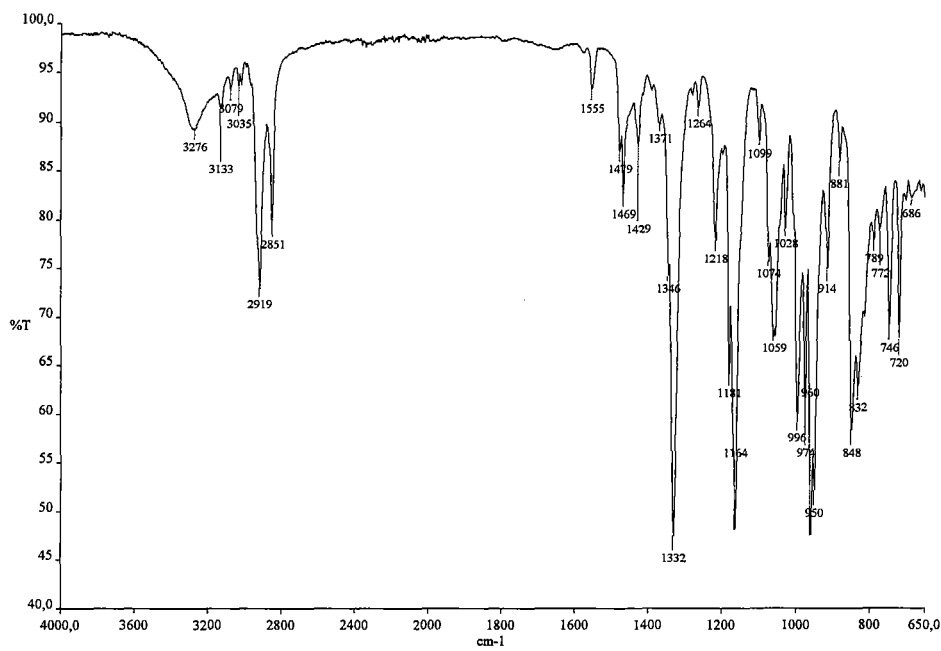


Figura 7

4/12

**Figura 8****Figura 9**

5/12

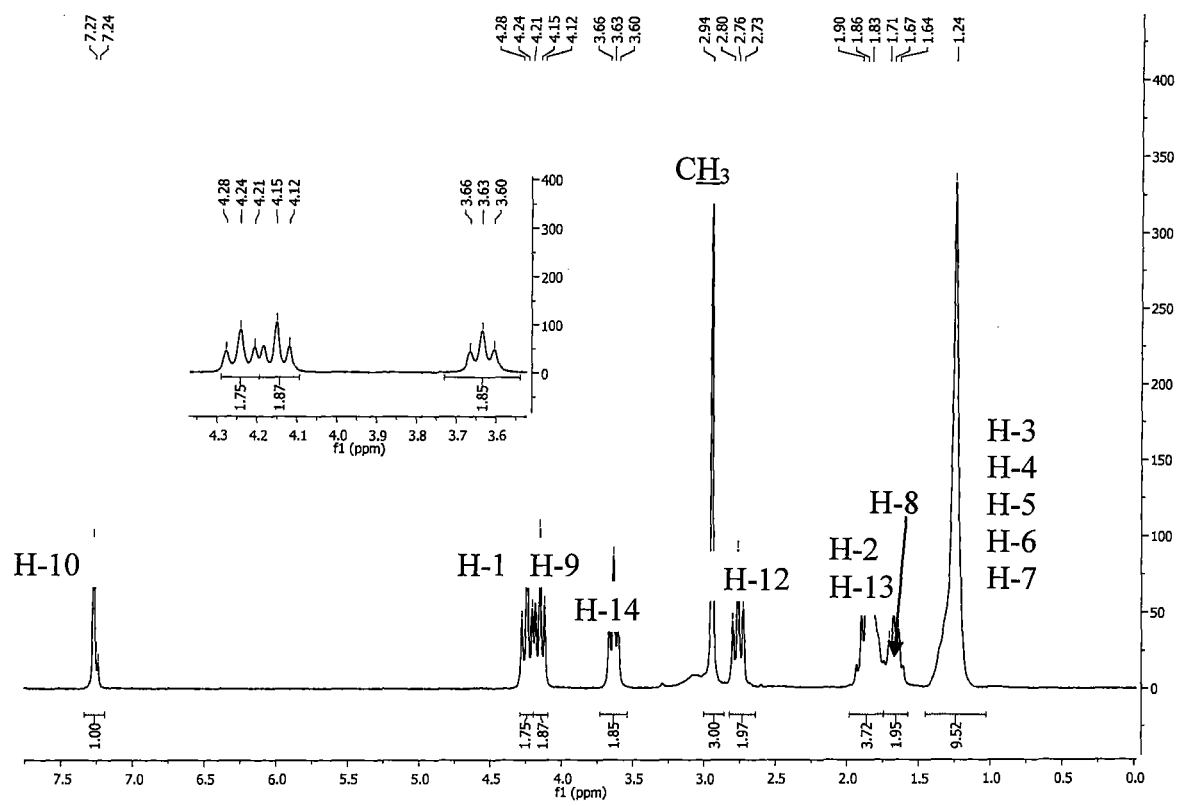


Figura 10

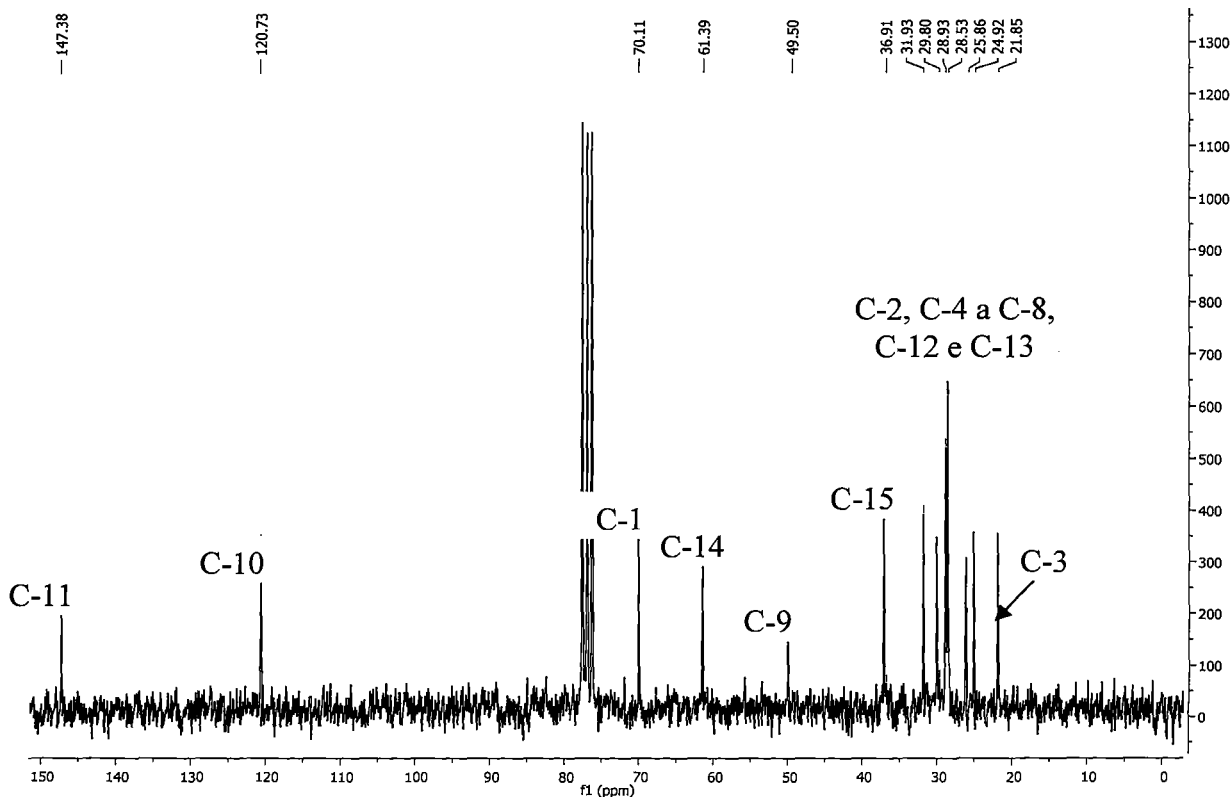
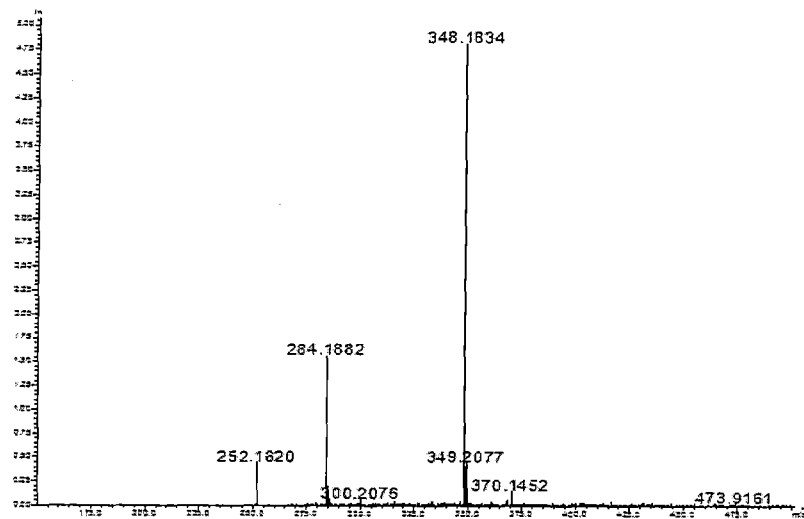
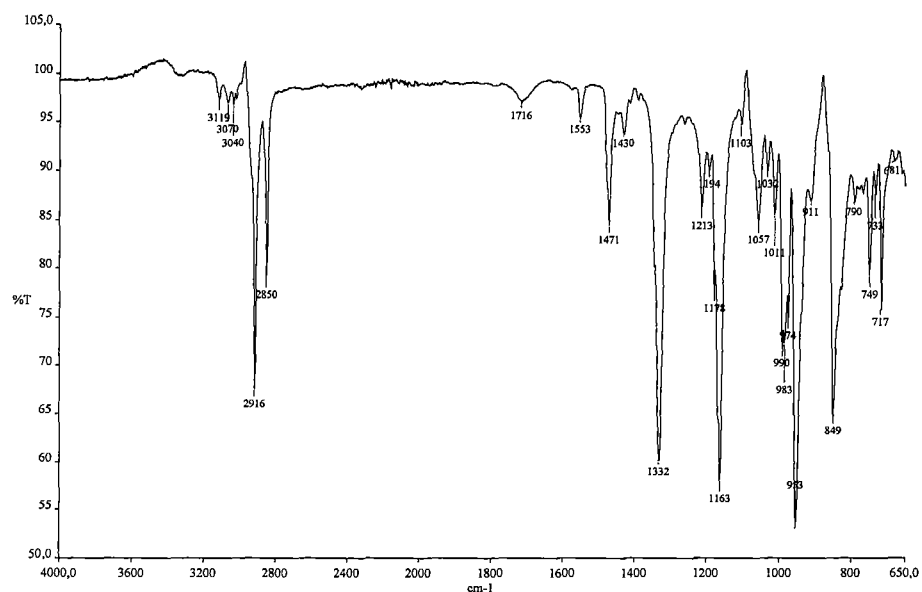
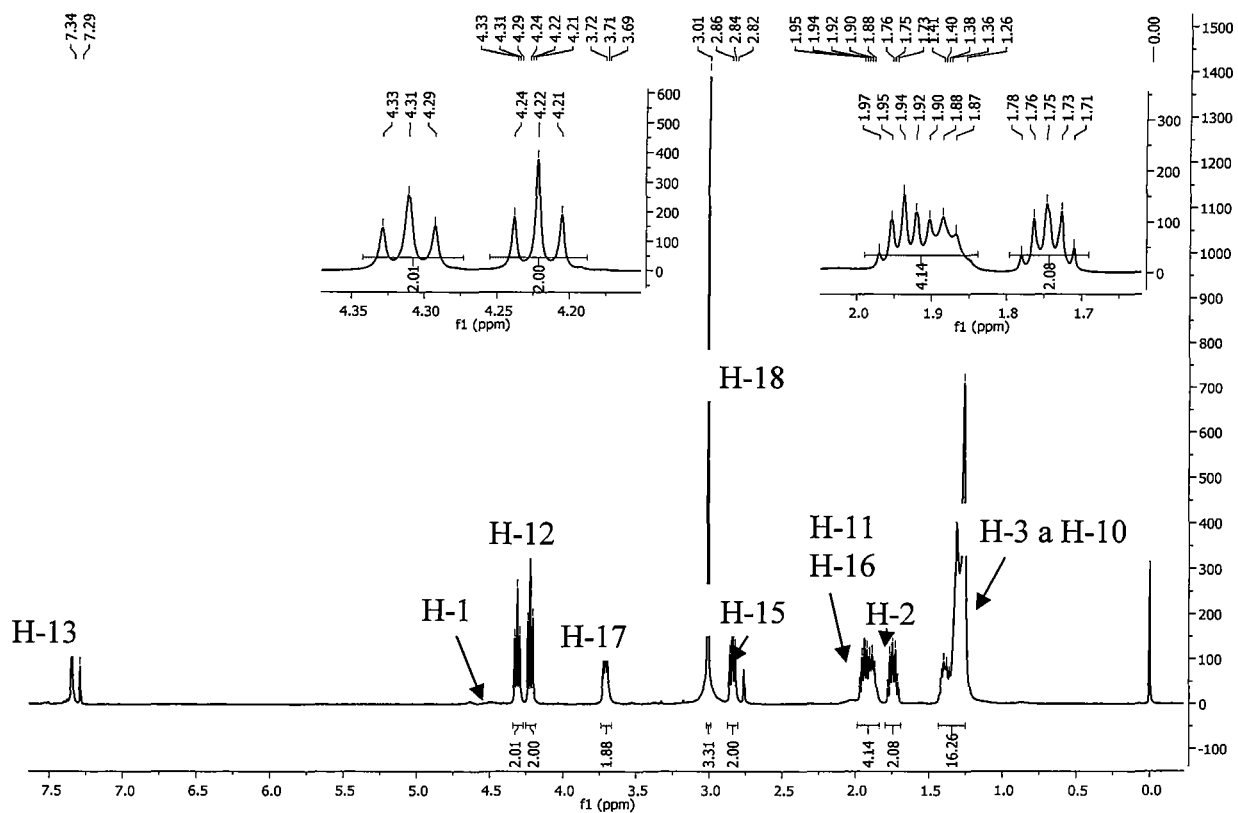


Figura 11

6/12

**Figura 12****Figura 13**

7/12



**Figura 14**

8/12

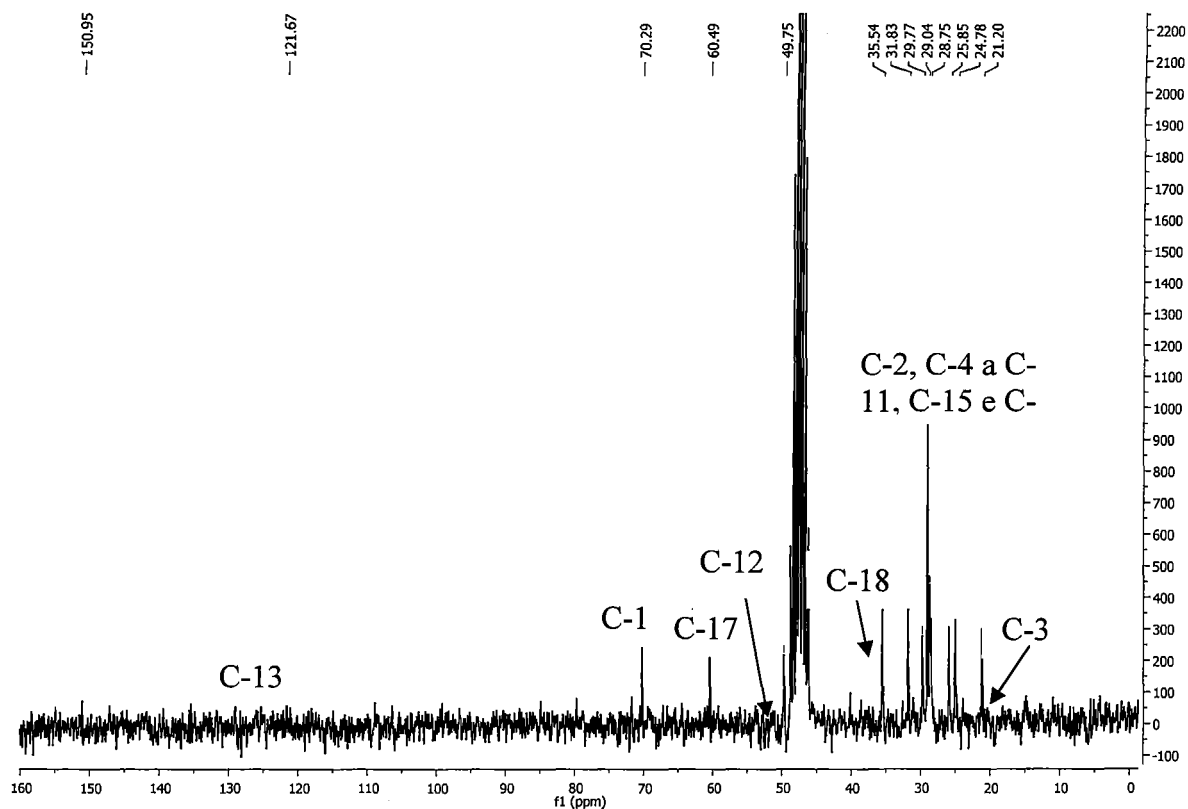


Figura 15

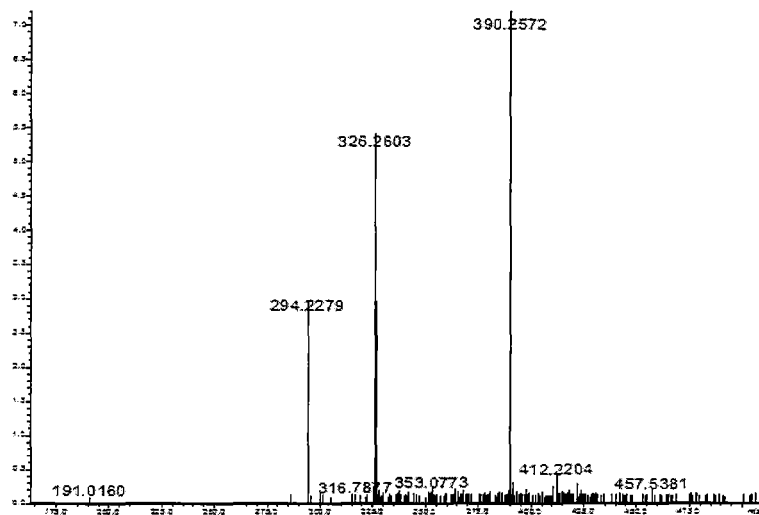
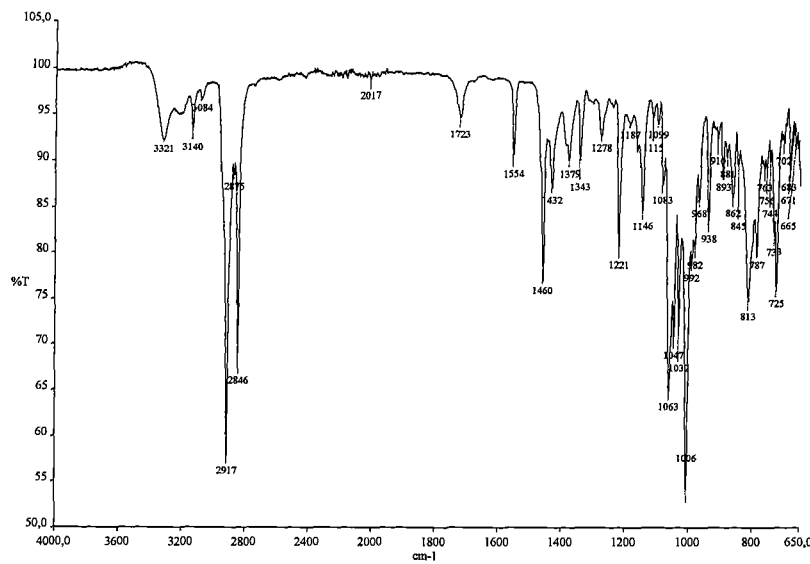
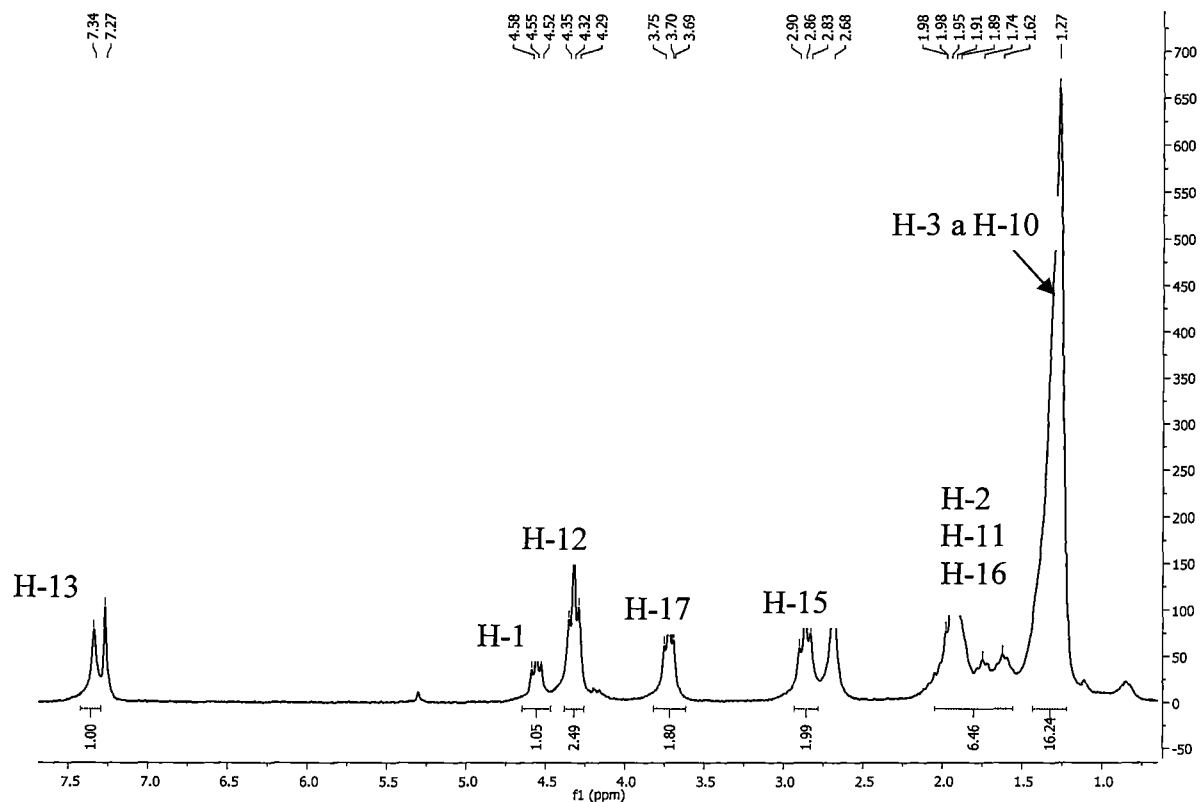


Figura 16

9/12

**Figura 17****Figura 18**

46

10/12

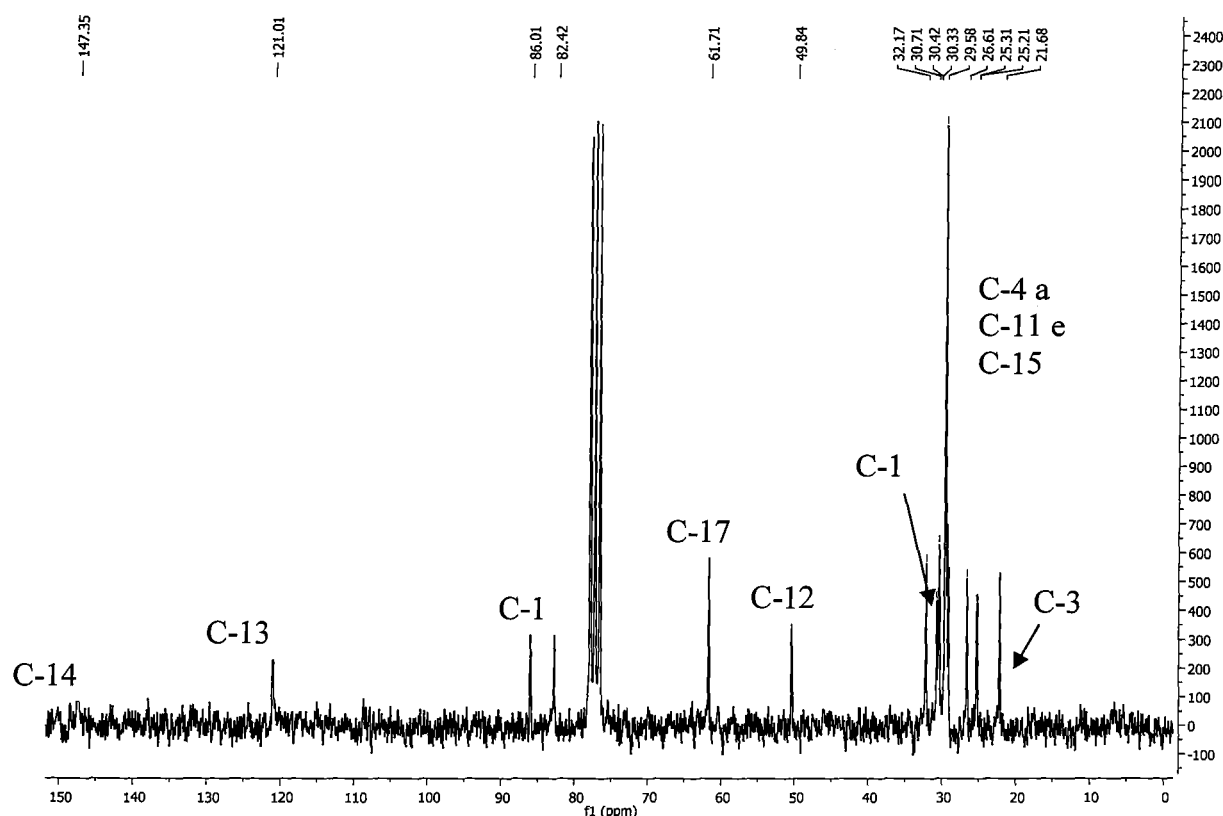


Figura 19

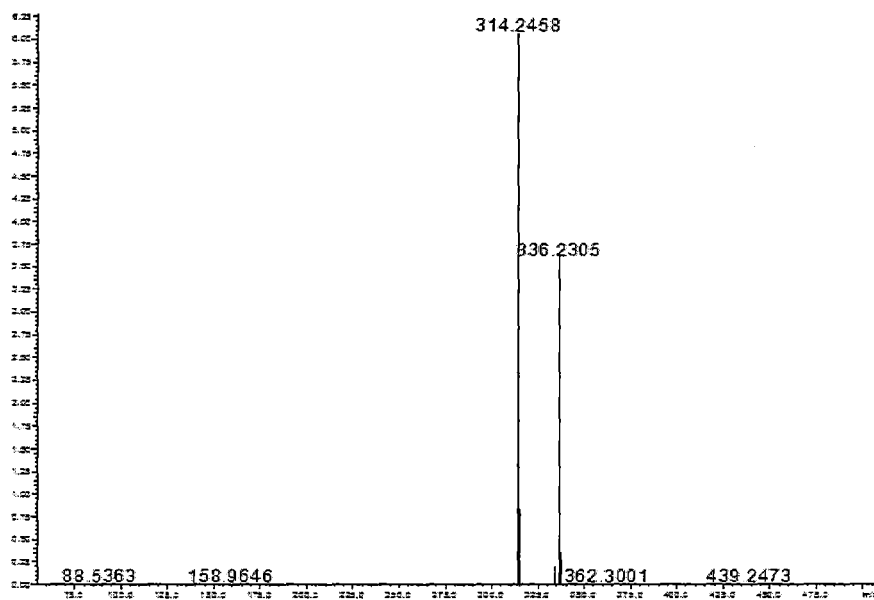
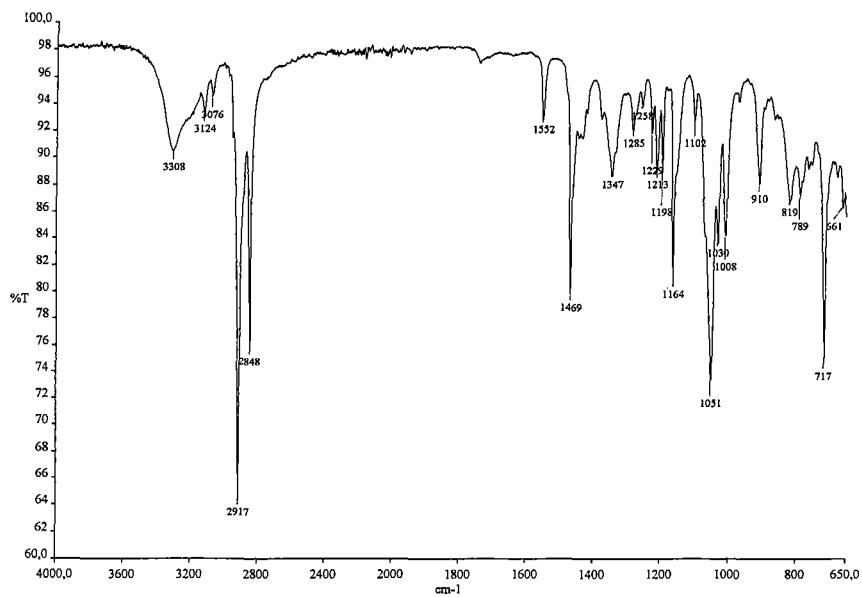
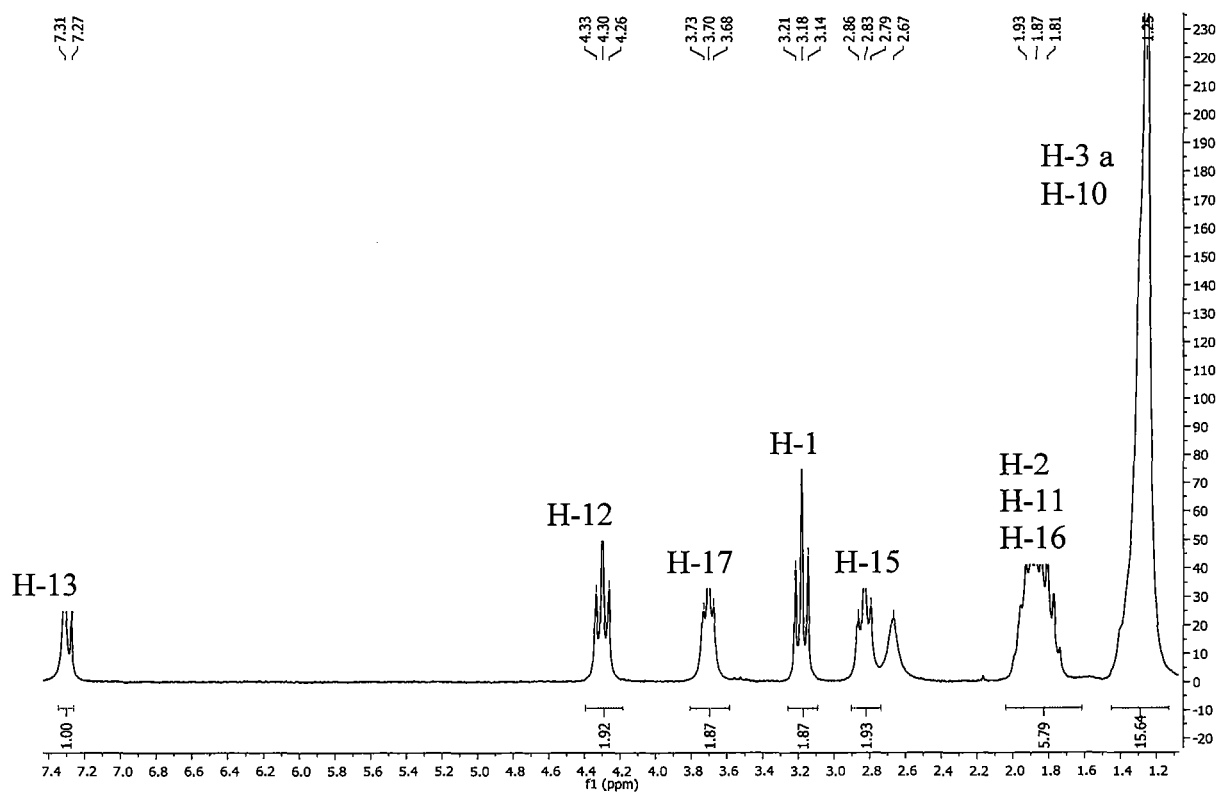


Figura 20

11/12

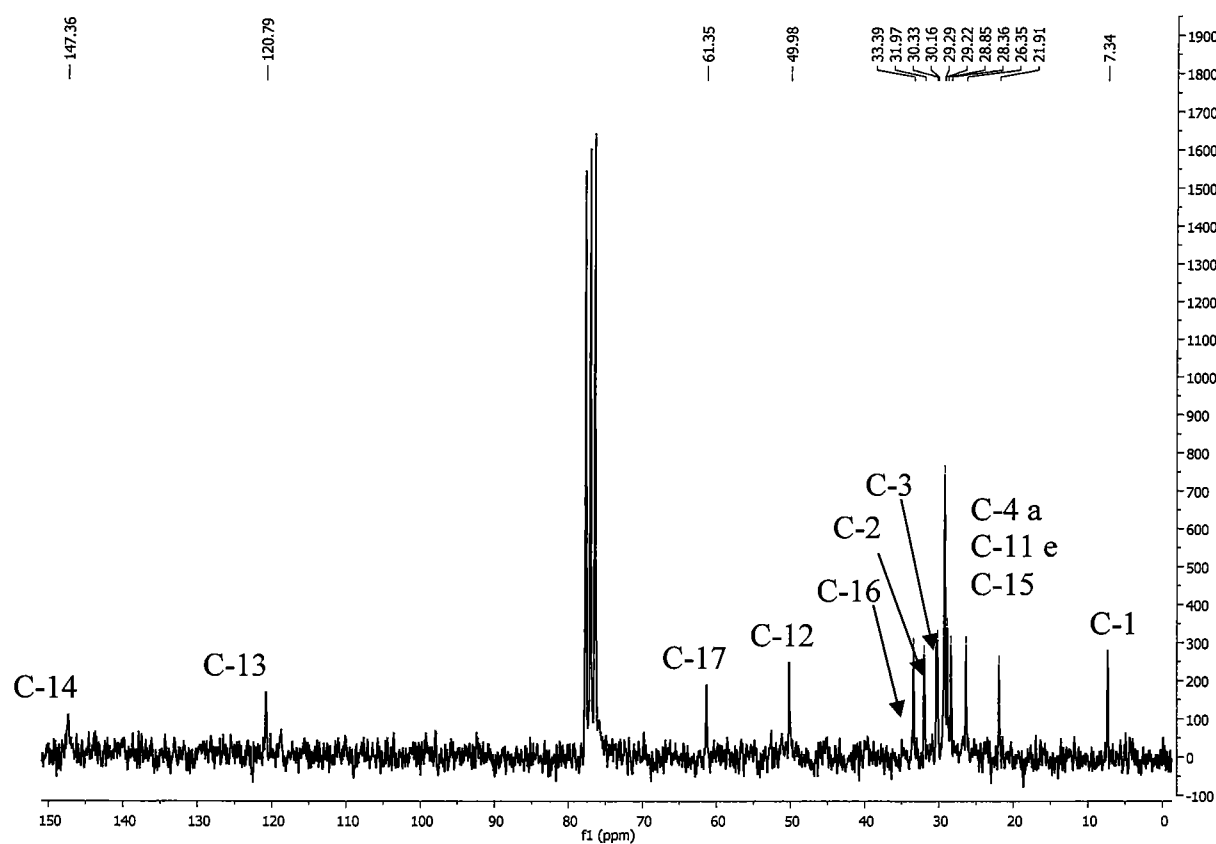
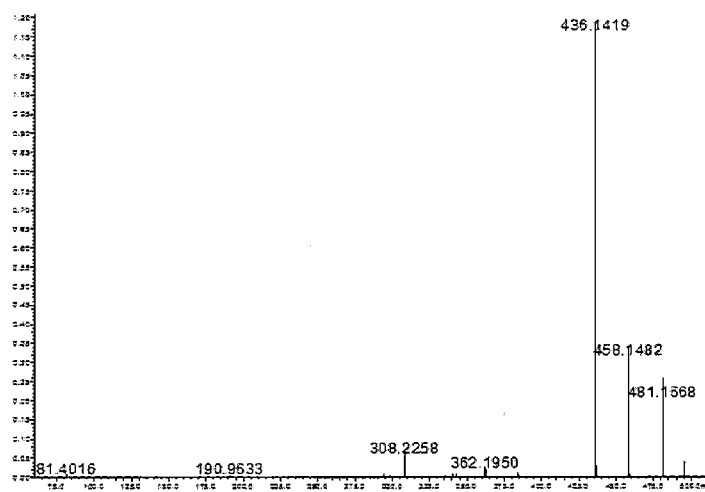


**Figura 21**



**Figura 22**

12/12

**Figura 23****Figura 24**

**RESUMO****DERIVADOS ALQUILTRIAZÓLICOS COM ATIVIDADE ANTITUMORAL,  
PROCESSO DE OBTENÇÃO E USO**

A presente invenção descreve derivados 1,2,3-alquiltriazólicos com atividade antitumoral e o processo de obtenção dos mesmos. Os compostos foram obtidos através de reações rápidas, de fácil realização, reproduzíveis, e todas com bons rendimentos. Além disso, esses derivados apresentaram atividade antitumoral em concentrações micromolares. Portanto, a presente invenção trata, também, do uso desses derivados como antitumoral.



## Research paper

## Leishmanicidal, antiproteolytic, and mutagenic evaluation of alkyltriazoles and alkylphosphocholines



Vanessa Silva Gontijo <sup>a</sup>, Patrícia Ferreira Espuri <sup>b</sup>, Rosemeire Brondi Alves <sup>a</sup>, Luiz Fernando de Camargos <sup>c</sup>, Fábio Vieira dos Santos <sup>c</sup>, Wagner Alves de Souza Judice <sup>d</sup>, Marcos José Marques <sup>b</sup>, Rossimiriam Pereira Freitas <sup>a,\*</sup>

<sup>a</sup> Departamento de Química, ICEX, UFMG, Av. Pres. Antônio Carlos, 6627, Pampulha, Belo Horizonte, MG 31270-901, Brazil

<sup>b</sup> Laboratório de Biologia Molecular de Microrganismos, Universidade Federal de Alfenas, 37130-000 Alfenas, MG, Brazil

<sup>c</sup> Núcleo de Química Biológica, Laboratório de Biologia Celular e Mutagênese (LaBCeM), Universidade Federal de São João del Rei (UFSJ), Divinópolis, MG 35501-296, Brazil

<sup>d</sup> Centro Interdisciplinar de Investigação Bioquímica, Universidade de Mogi das Cruzes, UMC, Mogi das Cruzes, SP, Brazil

## ARTICLE INFO

## Article history:

Received 9 March 2015

Received in revised form

22 May 2015

Accepted 2 June 2015

Available online 5 June 2015

## Keywords:

Alkyltriazoles

Antiproteolytic

Click chemistry

Heterocycle

## ABSTRACT

A series of 16 simple long-chain alkyltriazoles and two novel alkylphosphocholine derivatives containing an azide moiety were evaluated *in vitro* for their leishmanicidal activity against. Among the 18 compounds tested, the eight most active compounds against promastigote forms were selected for further evaluation against amastigote forms. These compounds were also evaluated for their cytotoxicity against murine macrophages and tested as inhibitors of cysteine protease rCPB2.8, an important target for development of antileishmanial drugs. The mutagenicity of some of these compounds was also evaluated in prokaryotic and eukaryotic cells to assess any genetic effects of the leishmanicidal candidates. The compound **4**, an alkylphosphocholine derivative, was found to be the most potent against amastigote forms with an IC<sub>50</sub> of 3.81 μM, comparable to that of pentamidine (IC<sub>50</sub> = 6.62 μM) and amphotericin B (IC<sub>50</sub> = 6.10 μM), two established leishmanicidal drugs. Compound **4** also exhibited the best selectivity index (SI) values of the series, demonstrating low toxicity against macrophages and a cLogP value higher than 5. Among the alkyltriazoles, compounds **13** and **14** were the most active against promastigote and amastigote forms. They were then evaluated for their mutagenicity *in vitro*; the mutagenicity index (MI) values were lower than 2, suggesting that these compounds are not mutagenic.

© 2015 Elsevier Masson SAS. All rights reserved.

## 1. Introduction

Leishmaniasis is a parasitic disease with more than 20 species of the protozoan genus *Leishmania* as the causative agents. It is endemic in 88 tropical and subtropical countries worldwide, with 350 million men, women, and children living at risk [1]. Leishmaniasis displays various clinical manifestations including visceral (VL), cutaneous (CL), and mucocutaneous (MCL) symptoms, depending on complex interactions between the parasite and host's immune response [2]. This disease is currently difficult to manage, mainly owing to a limited efficient treatments and the prevalence of drug resistance. The first line of drug treatment for all clinical manifestations of leishmaniasis consists of pentavalent antimonial

compounds such as sodium stibogluconate (Pentostam) or meglumine antimoniate (Glucantime). These drugs have been used in the treatment of leishmaniasis for over 50 years but have been found to cause several toxic effects, including myalgia, pancreatitis, cardiac arrhythmias, and hepatitis [3]. Second line drug treatments include amphotericin B and pentamidine; however, these drugs also present potentially serious adverse effects [4]. Though a liposomal formulation of amphotericin B (Amisome) has been developed to reduce the drug's toxicity, it is a more expensive option and thus can limit therapeutic use in developing countries [3]. Miltefosine, a newer compound of the alkylphospholipid class, is the first FDA-approved oral medicine to treat cutaneous and mucosal leishmaniasis. Efficient oral administration, moderate safety, and low toxicity favour the use of this drug, especially in certain cases such as for the treatment of children. However, its limitations include gastrointestinal toxicity and teratogenic action.

\* Corresponding author.

E-mail address: rossimiriam@pq.cnpq.br (R.P. Freitas).

The development of new, inexpensive, and safe drugs for the treatment of leishmaniasis remains a great challenge for researchers worldwide [5–8].

In recent years, 'click chemistry' or the 'click reaction,' a reaction chemically referred to as the copper-catalysed azide–alkyne cycloaddition or CuAAC, for the efficient synthesis of the 1,2,3-triazole nucleus, has attracted significant attention [9–12]. This heterocycle is easily obtained by the CuAAC reaction [13] and has occupied an important position in medicinal chemistry research [14]. The 1,2,3-triazole ring acts not only as a pharmacophore, but also as a linker between two or more substances through a molecular hybridization strategy. Furthermore, the triazole can act as a bioisostere of the amide group, presenting similar physicochemical properties. The triazole unit acts as a rigid linker, which accommodates the R<sup>1</sup> and R<sup>2</sup> groups (Fig. 1), at a distance of 5.0 Å (for comparison, the same distance on the amide groups is 3.8 Å). In contrast to amides, the triazole ring is stable, since it does not undergo hydrolysis, oxidation, or reduction. The 1,2,3-triazoles have a large dipole moment (5D) and nitrogen atoms on positions 2 and 3 act as weak hydrogen bond acceptors. In most recent years, compounds belonging to several chemical classes and containing 1,2,3-triazoles have been described as potential biological agents, including leishmanicidal drugs [15].

Recently we have synthesized a series of novel, structurally simple, long-chain alkyltriazoles and evaluated their activity against tumour cells [16]. A promising anticancer candidate was found in the series, with cytotoxicity comparable to that of etoposide, a known antitumour agent. In the current work, we have investigated the leishmanicidal activity of two new alkylphosphocholine analogues of miltefosine and 16 long-chain alkyltriazoles obtained via the click approach, which include 14 compounds previously described [16]. The compounds were tested against promastigote and amastigote forms of *Leishmania amazonensis*. Moreover, the cytotoxicity against murine peritoneal macrophages and the mutagenic effect of these compounds were also evaluated. We have also investigated the antiproteolytic activity of these compounds toward *Leishmania mexicana* cysteine protease, r-CPB2.8. Several papain-like cysteine proteases have been identified in different *Leishmania* spp and are thought to be crucial for the survival and infectivity of the parasite in its human host. These enzymes have been involved in successful invasion of host macrophages by promastigotes, subsequent transformation of parasitic forms, and evasion from the host immune system [17,18]. Because of the importance of cysteine proteases in the survival and life cycle of *Leishmania*, they have been targets for the development of antileishmanial drugs [19].

To complete the analyses performed in this study, the mutagenic effects of some compounds were evaluated. This has permitted the identification of potential mutagenic and carcinogenic effects and the study of the mechanisms by which these agents can cause damage and mutations in genetic material [20]. The monitoring of genotoxic effects of carcinogens in humans has been widely utilized for hazard identification or risk assessment purposes [21]. Mutagenic agents can cause severe genetic alterations and cancer at

doses much lower than those necessary to display acute toxicity. Therefore, specific exclusion of genotoxic effects is important in products used for human foods or drugs [22].

## 2. Methods and materials

### 2.1. General

Reagents and solvents were purchased as reagent grade PA and used without further purification. All melting points were measured on Fisher-Jonhs and are uncorrected. IR spectra were recorded on Perkin–Elmer Spectrum One SP-IR Spectrometer. <sup>1</sup>H and <sup>13</sup>C NMR spectra were recorded on a Bruker AVANCE DRX 200 MHz spectrometer using TMS as an internal standard. The results are presented as chemical shift δ in ppm, number of protons, multiplicity, J values in Hertz (Hz), proton position and carbon position. Multiplicities are abbreviated as follows: s (singlet), d (doublet), t (triplet), m (multiplet) and qn (quintet). High resolution mass spectra were recorded on ESI-MS Bruker Daltonics Micro TOF mass spectrometer with electrospray ionization coupled to time-of-flight (Solvent: MeOH). The progress of the reactions was monitored by TLC on Merck silica plates (GF254). Column chromatography was performed over silica gel 60, 70–230 mesh (Merck).

The enzyme r-CPB2.8 were generously gifted by Dr. Luiz Juliano (Department of Biophysics, Federal University of São Paulo, Brazil), E-64 (1-[[(Ltrans-epoxysuccinyl)-L-leucyl]amino]-4-guanidinobutane), and fluorogenic substrate Z-FR-AMC (carbobenzyloxy-Phe-Arg-(7-amino-4-methylcoumarin) were commercially obtained from Sigma–Aldrich Sigma (St. Louis, USA). Substrate hydrolyses were monitored in a spectrofluorometer F2500 Hitachi using the λ<sub>Ex</sub> = 380 nm and λ<sub>Em</sub> = 460 nm as wavelength, respectively, and the enzymatic molar concentrations were estimated by titration according to kinetic parameters [23].

### 2.2. Synthesis

#### 2.2.1. Synthesis of alkylphosphocholines 3 and 4

The calcium salt of phosphorylcholine **1** (1.0 equiv) was treated with an aqueous solution of oxalic acid (1.1 equiv). The precipitate calcium oxalate was removed by filtration, and the filtrate was titrated with tetra-n-butylammonium hydroxide until pH 9. The resulting solution was evaporated to dryness, and the residue was dissolved in 10 mL of toluene. After evaporating to dryness, the residue was re-dissolved in a further 10 mL toluene, evaporated again and the crude obtained was dried in a vacuum desiccator over P<sub>2</sub>O<sub>5</sub> to yield the choline phosphate tetra-n-butylammonium **2**. The compounds **3** and **4** were obtained by classic S<sub>N</sub>2 substitution between the compound **2** and methanesulfonate alkylazide compounds (**8a** or **8b**) in acetonitrile at room temperature for 24 h, followed by refluxing for 3 h. The crude product was purified by column chromatography over silica gel, eluting with methanol, to give pure compounds **3** and **4**.

**2.2.1.1. 9-azidenonylphosphocholine (3).** Colour less oil. Yield 19%. IR (ATR): 2928, 2855, 2094, 1223, 1082, 1059, 966, 816, 763, 722. <sup>1</sup>H NMR (200 MHz, CD<sub>3</sub>OD): 1.27–1.44 (m, 10H), 1.50–1.69 (m, 4H), 3.20 (s, 9H), 3.22–3.33 (m, 2H), 3.85 (qa; J<sub>H1–P</sub> = 6.0 and J<sub>H1–H2</sub> = 6.0, 2H), 3.73–3.94 (m, 2H), 4.12–4.32 (m, 2H). <sup>13</sup>C NMR (50 MHz, CD<sub>3</sub>OD): 25.38, 26.31, 28.40, 28.71, 28.84, 29.08, 29.19, 30.28, 30.42, 50.93, 53.25, 58.57, 63.48, 65.75. ESI-MS: m/z [M+Na]<sup>+</sup> calcd for C<sub>14</sub>H<sub>31</sub>N<sub>4</sub>O<sub>4</sub>P: 373.1981; found m/z [M+Na]<sup>+</sup>: 372.9000.

**2.2.1.2. 12-azidodecylphosphocholine (4).** Colour less oil. Yield 19%. IR (ATR): 2923, 2852, 2100, 1231, 1084, 1059, 968, 873, 796, 777.

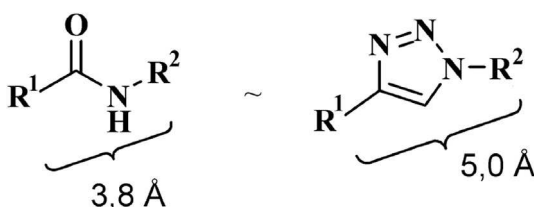


Fig. 1. 1,2,3-triazole: Bioisostere of amide.

<sup>1</sup>H NMR (200 MHz, CDCl<sub>3</sub>): 1.24–1.47 (m, 16H), 1.59–1.69 (m, 4H), 3.23 (s, 9H), 3.30–3.32 (m, 2H), 3.57–3.69 (m, 2H), 3.87 (qa; J<sub>H1-P</sub> = 6.0 eJ<sub>H1-H2</sub> = 6.0, 2H), 4.13–4.34 (m, 2H). <sup>13</sup>C NMR (50 MHz, CDCl<sub>3</sub>): 25.44, 26.33, 28.42, 28.78, 28.99, 29.18, 30.45, 50.93, 53.17, 58.59, 61.26, 65.38. ESI-MS: m/z [M+H]<sup>+</sup> calcd for C<sub>17</sub>H<sub>38</sub>N<sub>4</sub>O<sub>4</sub>P: 393.2631; found m/z [M+H]<sup>+</sup>: 393.2773.

### 2.2.2. Synthesis of 1,2,3-alkyltriazoles 10 and 11

To a stirred solution of the 1,12-dodecanediol (**5**) (1.00 equiv) in 30 mL of toluene HBr 48% (2.00 equiv) was added. The reaction was stirred at 110 °C for 24 h. The solvent was removed under reduced pressure, and the residue was purified by column chromatography over silica gel, eluting with hexane/EtOAc 9:1, to yield pure halo alcohol (**6**). This compound was transformed into their corresponding azidoalcohol (**7**) via classic S<sub>N</sub>2 substitution. A stock solution of 0.5 M NaN<sub>3</sub> in DMSO was prepared by stirring the solution for 24 h at room temperature. To a 100 mL round-bottom flask equipped with a magnetic stir bar was added a 0.5 M solution of NaN<sub>3</sub> in DMSO at room temperature. To this solution was added the bromo alcohol (**6**) (1.00 equiv) and the mixture was stirred for 24 h at room temperature. The reaction was quenched with H<sub>2</sub>O (50 mL) and stirred until it cooled to room temperature. The mixture was extracted with Et<sub>2</sub>O (3 × 30 mL), and the resultant extracts were washed with H<sub>2</sub>O (3 × 50 mL) and brine (50 mL). The organic layer was dried (Na<sub>2</sub>SO<sub>4</sub>) and filtered, and the residue obtained was purified by column chromatography over silica gel, eluting with hexane/EtOAc 9:1, to yield pure alkyl azidoalcohol (**7**). A solution of the azidoalcohol (**7**) (1.00 equiv) in CH<sub>2</sub>Cl<sub>2</sub> (50 mL) was cooled to 0 °C. Et<sub>3</sub>N (2.00 equiv) and methanesulfonyl chloride (2.00 equiv) were added. The reaction mixture was allowed to warm to room temperature and stirred for additional 24 h. The reaction mixture was poured into crushed ice (70 mL) and was then extracted with methylene chloride (3 × 30 mL). The organic layer was dried (Na<sub>2</sub>SO<sub>4</sub>), filtered and evaporated under reduced pressure. The residue obtained was purified by column chromatography over silica gel, eluting with hexane/EtOAc 9:1, to yield pure halo alcohol pure methanesulfonate alkylazide compound (**8**). The azide compound (**8**) (1.00 equiv) was added to a 10 mL round-bottom flask containing 1 mL of dichloromethane, 1 mL of water, CuSO<sub>4</sub>·5H<sub>2</sub>O (0.08 equiv), sodium ascorbate (0.20 equiv) and pent-4-yn-1-ol (1.00 equiv). The reaction mixture was vigorously stirred at room temperature for 24 h. After completion of the reaction, 5 mL of water were added, followed by extraction with dichloromethane (3 × 8 mL). The resulting organic layer was washed three times with a 25% EDTA solution buffered with NH<sub>4</sub>Cl at pH 9.5. The organic layer was dried with Na<sub>2</sub>SO<sub>4</sub> and the solvent was removed under reduced pressure. The crude product was purified by column chromatography over silica gel, eluting with dichloromethane: EtOAc (8:2 v/v; 5:5 v/v; 2:8 v/v), EtOAC and EtOAc/MeOH (8:2 v/v; 5:5 v/v; 2:8 v/v), to give pure compound **9**.

To a stirred solution of the compound **9** (1.00 equiv) in 5 mL of acetone was added 4-DMAP (0.40 equiv) and acetic anhydride (2.00 equiv). The reaction system was kept under magnetic stirring at room temperature for 24 h, poured into crushed ice (70 mL) and was then extracted with methylene chloride ( $3 \times 30$  mL). The organic layer was dried ( $\text{Na}_2\text{SO}_4$ ), filtered and evaporated under reduced pressure. The residue obtained was purified by column chromatography over silica gel, eluting with hexane/EtOAc 7:3, to yield pure compound **10**.

The compound **9** (1.00 equiv) was added to 10 mL of dichloromethane, the solution was cooled to 0 °C, Et<sub>3</sub>N (2.00 equiv) and methanesulfonyl chloride (2.00 equiv) were added. The reaction mixture was allowed to warm at room temperature and stirred for additional 24 h. The reaction mixture was poured into crushed ice (70 mL) and was then extracted with methylene chloride

( $3 \times 30$  mL). The organic layer was dried ( $\text{Na}_2\text{SO}_4$ ), filtered and evaporated under reduced pressure. The residue obtained was purified by column chromatography over silica gel, eluting with hexane/EtOAc 9:1, to yield pure compound **11**.

**2.2.2.1. 5-(4-(3-acetoxypropyl)-1*H*-1,2,3-triazol-1-yl)dodecyl methanesulfonate (**10**).** Yellow oil. Yield 73%. IR(ATR): 2918, 2852, 1730, 1345, 1328, 1163, 1036–951, 1244, 835.  $^1\text{H}$  NMR (200 MHz,  $\text{CDCl}_3$ ): 1.17–1.52 (m, 18H), 1.63–1.79 (m, 2H), 1.81–1.93 (m, 2H), 2.05 (s, 3H), (2.80, t,  $J_{15,16} = 6.0$ , 2H), 3.0 (s, 3H), 4.01–4.39 (m, 6H), 7.31 (s, 1H).  $^{13}\text{C}$  NMR (50 MHz,  $\text{CDCl}_3$ ): 20.84, 21.97, 25.26, 26.34, 28.21, 28.84, 28.96, 29.24, 30.19, 37.21, 49.92, 63.44, 70.14, 120.63, 146.65, 171.01. ESI-MS:  $m/z$  [M+H] $^+$  calcd for  $\text{C}_{20}\text{H}_{38}\text{N}_3\text{O}_5$ : 432.2532; found  $m/z$  [M+H] $^+$ : 432.2540.

**2.2.2.2. 5-(4-(3-methanesulfonatepropyl)-1H-1,2,3-triazol-1-yl)dodecyl methanesulfonate (**11**).** White solid. m.p. = 88–90 °C. Yield 56%. IR (ATR): 2916, 2850, 1331, 1165, 1057–953. <sup>1</sup>H NMR (200 MHz, CDCl<sub>3</sub>): 1.15–1.39 (m, 16H), 1.58–1.95 (m, 4H), 1.96–2.26 (m, 2H), 2.82 (t, J<sub>15,16</sub> = 6.0, 2H), 2.96 or 2.99 (s, 6H), 4.08–4.38 (m, 6H), 7.35 (s, 1H). <sup>13</sup>C NMR (50 MHz, CDCl<sub>3</sub>): 21.21, 25.24, 26.32, 28.56, 28.83, 28.95, 29.21, 29.24, 30.13, 37.20, 50.19, 69.03, 70.24, 121.16, 145.76. ESI-MS: *m/z* [M+H]<sup>+</sup> calcd for C<sub>19</sub>H<sub>38</sub>N<sub>3</sub>O<sub>6</sub>S<sub>2</sub>: 468.2202; found *m/z* [M+H]<sup>+</sup>: 468.1846.

### 2.3. Biological assays

### 2.3.1. In vitro leishmanicidal activity

**3.3.1.1. Leishmanicidal activity against promastigotes.** Promastigotes of *L. amazonensis* (MHOM/BR/71973/M2269) were grown on a 24-well plates in Schneider's Drosophila medium (Sigma, USA) supplemented with 10.0% (v/v) heat-inactivated fetal bovine serum and 1.0% penicillin (10000UI/mL)/streptomycin (10.0 mg/mL) (Sigma, USA). Cells were harvested in the log phase, resuspended in fresh medium, counted in Neubauer's chamber and adjusted to a concentration of  $1 \times 10^6$  cells/mL, using 24-wells plates. Compounds **10–25** (Fig. 2) were added to promastigote cultures ( $1 \times 10^6$  cells/mL) in the range of 0.10–40.00  $\mu\text{g}/\text{mL}$ , solubilized in dimethylsulfoxide (DMSO) (0.6%, v/v in all wells) and incubated at 25 °C. After 72 h of incubation, the surviving parasites were counted in a Neubauer's chamber and compared with controls, with just DMSO in concentration of 0.6% v/v, for the

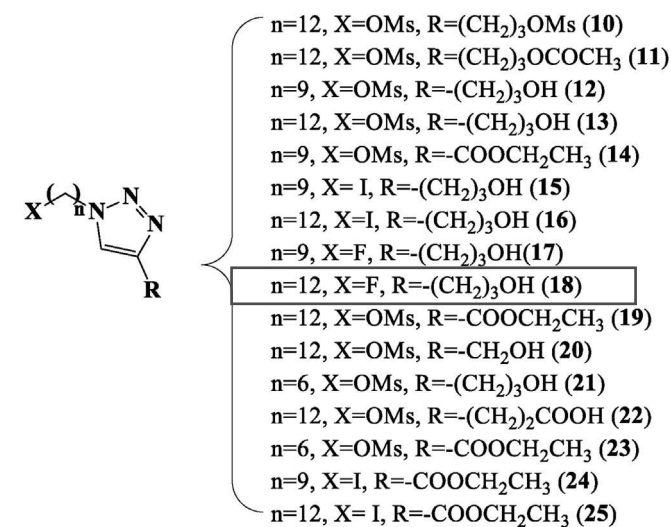


**Fig. 2.** Alkyltriazoles **12–25** obtained by Gontijo [16] and the new compounds **10** and **11**.

determination of 50.0% inhibitory growth concentration ( $IC_{50}$ ). All tests were performed in triplicate on three different times and amphotericin B (Sigma) was used as the reference drug. Animal procedures were performed with the approval of the Research Ethics Commission from Universidade Federal de Alfenas under number 600/2014 in agreement with the Guidelines for the Care and Use of Laboratory Animals.

**2.3.1.2. Leishmanicidal activity against amastigotes.** Murine peritoneal macrophages were maintained in RPMI 1640 medium (Sigma, USA) supplemented with 10.0% heat-inactivated fetal bovine serum at 37 °C in 5.0% CO<sub>2</sub> incubator. Cells were cultured in 24-well plates chamber on the glass slides of 13 mm (Nunc, USA) in a  $8 \times 10^5$  cells density per well and infected with late log-phase promastigotes at a ratio of 10:1 (parasite/macrophage) and incubated at 37 °C in 5.0% CO<sub>2</sub> incubator for 24 h. Non-phagocytosed promastigotes were removed by washing, and compounds **4**, **10**, **11**, **13**, **14**, **16**, **18** and **25** solubilized in DMSO (from 0.10 to 40.00 µg/mL) were administered at the concentration of 0.6% v/v. After 72 h, chamber slides were fixed in absolute methanol, stained with 10.0% Giemsa and examined on an Optical Light Microscope in oil immersion. The percentage of infected cells per well was calculated taking account at least 200 macrophages. The ratio of inhibition ( $IC_{50}$  value) was calculated in comparative to the control only with DMSO. All assays were performed in triplicate on three different times using pentamidine (Sigma) and amphotericin B (Sigma) as the reference drugs [16].

**2.3.1.3. Cytotoxicity evaluation.** A suspension of  $8 \times 10^5$  murine peritoneal macrophages, in RPMI 1640 medium, supplemented with 10.0% heat-inactivated fetal bovine serum and 1.0% penicillin (10000 UI/ml)/streptomycin (10 mg/mL) were added to each well in 24-well plates, on the glass slides of 13 mm. The plates were incubated in a 5.0% CO<sub>2</sub> air mixture at 37 °C to adhesion of the cells. After 24 h, the non-adherent cells were removed by washing with the RPMI 1640 medium. Then, several concentrations of compounds **4**, **10**, **11**, **13**, **14**, **16**, **18**, **25** and reference drugs ranging from 0.10 to 40.00 µg/mL in DMSO at the final concentration of 0.6% v/v) were added to the wells containing the cells and the plates were incubated for more 72 h. The non-adherent cells were removed by washing with the RPMI 1640 medium. Afterwards, the 3-(4,5-dimethylthiazol-2-yl)-2,5-diphenyltetrazoliumbromide (MTT) was solubilized in PBS (5.0 mg/mL) as solvent. Fifty microliter of this solution was added to RPMI 1640 medium in a final volume of 500.0 µL per well and incubated for 4 h [24]. Then, the medium was removed and 600.0 µL of DMSO was added to each well and homogenized for 15 min. Next, the absorbance of each individual well was calculated at 570 nm according to the following formula (OD represents optical density) using the Equation (1):

$$\% \text{ inhibition} = \left( \frac{\text{OD}_{\text{control}} - \text{OD}_{\text{compounds}}}{\text{OD}_{\text{control}}} \right) \times 100 \quad (1)$$

Each experiment was performed in triplicate on three different occasions, and the percentage of viable cells was calculated taking into account the cell culture control (medium + cells + DMSO 0.6% v/v). The 50.0% cytotoxicity concentrations ( $CC_{50}$ ) were determined and the selectivity factors (SF) established by the ratio between the values of  $CC_{50}$  and  $IC_{50}$  for amastigote forms.

### 2.3.2. Antiproteolytic activity

**2.3.2.1. Inhibitory activity against isoform r-CPB2.8.** The compounds **6**, **7**, **11**, **13**, **14**, **16**, **18** and **25** were tested for their potential inhibitory r-CPB2.8, inhibitory  $IC_{50}$ . The r-CPB2.8 was expressed, purified and activated as previously described [25,26]. The concentration of the

enzyme stock solution was determined by active-site titration with human cystatin C, which was a generous gift from M. Abrahamson (University of Lund, Sweden), using Z-Phe-Arg-MCA as substrate. Hydrolysis of the fluorogenic peptide substrate by enzyme was carried out in 0.1 M sodium acetate, pH 5.5 at 37 °C with previous activation of enzymes by 5 mM DTT for 10 min. The substrate hydrolysis was monitored by measuring the fluorescence at  $\lambda_{\text{em}} = 380$  nm with excitation at  $\lambda_{\text{ex}} = 460$  nm using a Hitachi F-2500 spectrofluorometer. The  $IC_{50}$  values were determined by non-linear regression using the GraFit 5.0 software (Eritacus Software Ltda) using the Equation (2).

$$y = \frac{\text{Range}}{1 + \left( \frac{x}{IC_{50}} \right)^s} \quad (2)$$

where Range is the fitted uninhibited value, y is the enzyme activity, x is the inhibitor concentration, and s is a slope factor. The equation assumes that y falls with increasing x.

### 2.3.3. Mutagenicity studies

**2.3.3.1. Cytokinesis-block micronucleus assay (chromosomal mutation analysis).** The cytokinesis-block micronucleus assay was performed in CHO-K1 cell line, to assess the potential of the synthetic compounds to induce DNA damage (chromosomal mutations) *in vitro*. The procedures were developed as described by Fenech [27,28], with adaptations. Briefly, the cells were seeded in 24-well plates ( $2.5 \times 10^5$  cells/well) and maintained at 37 °C in a humid atmosphere with 5% CO<sub>2</sub> in culture medium Ham F-12 with serum. After 24 h, the cells were washed twice with PBS, and the treatments were performed in culture media without serum for 3 h. Each treatment was performed in triplicate. The negative control group was treated with culture media without serum, and a positive control group was established with the treatment of the cells with methyl methanesulfonate (MMS-400 µM).

After completing treatments with three concentrations lower than the  $IC_{50}$  of the compounds **13** (6.41, 12.82, and 25.63 µM) and **14** (14.51, 29.02 and 58.04 µM) diluted in culture media, the cells were washed twice with PBS, trypsinized and centrifuged for 5 min at 1500 rpm. The pellet was then resuspended in chilled hypotonic solution (1% sodium citrate) together with one drop of 1% formaldehyde and carefully homogenized with a Pasteur pipette. This cell suspension was centrifuged for 5 min at 1500 rpm and resuspended in 2 mL of fixative, methanol/acetic acid (3:1 v/v). Next, the tubes were centrifuged for 5 min, and the supernatant was discarded; the cell suspension was spread onto slides previously cleaned and covered with a film of chilled distilled water.

At the moment of cytogenetic analysis, the slides were stained with DAPI (4',6-diamidino-2-phenylindole) diluted in phosphate buffer (0.06 M Na<sub>2</sub>HPO<sub>4</sub> and 0.06 M KH<sub>2</sub>PO<sub>4</sub>, pH 6.8) for 2 min, washed with distilled water and analysed under a fluorescent microscope (Zeiss, Axioscope) with an excitation filter of 365 nm and a barrier filter of 445/450 nm. One thousand cells with a well-preserved cytoplasm were analysed for each treatment in a blind test. Cells containing 1–4 micronuclei were scored. The criterion for the identification of MNs was according to a previous report [28].

**2.3.3.2. Nuclear division index (NDI).** The influence of the alkyl-triazoles **13** and **14** on cell division was assessed by calculating the Nuclear division index (NDI) in CHO-K1 cells. The same slides prepared for the micronucleus assay were used, and 300 cells with a well-preserved cytoplasm were counted using fluorescence microscopy, as described above. The NDI was calculated according Eastmond and Tucker [29]:

$$\text{NDI} = (\text{M1} + 2(\text{M2}) + 3(\text{M3}) + 4(\text{M4}))/\text{N}$$

where M1–M4 represent the number of cells with one to four nuclei and N is the total number of viable cells scored. The NDI and the proportion of binucleated cells are useful parameters for comparing the mitogenic response of cells and cytostatic effects of agents examined in the assay [27,28].

**2.3.3.3. Ames mutagenicity assay (gene mutation analysis).** The Ames mutagenicity assay was performed using the micro-suspension procedure modified by Kado et al. [30] and revised by Mortelmans and Zeiger [31]. This protocol is a modification of the traditional Ames test and provided to the assay a higher sensitivity than the original methodology. Overnight culture of *Salmonella typhimurium* strains TA98, TA100, TA97a and TA102 ( $1 \times 10^9$  cells/mL) was concentrated by centrifugation ( $4000 \times g$  at  $4^\circ\text{C}$ ) for 15 min and resuspended in 0.2 M sodium phosphate buffer pH 7.4. After,  $50 \mu\text{L}$  of each concentrate overnight bacterial culture ( $1 \times 10^{10}$  cells/mL) were mixed with  $50 \mu\text{L}$  of 0.2 M sodium phosphate buffer and five concentrations of the compounds in a test tube. Compound **13** was evaluated in concentrations ranging between 150.98 and 700.00  $\mu\text{M}$  and compound **14** was assessed in concentrations between 313.73 and 1454.55  $\mu\text{M}$ . The mixture was incubated at  $37^\circ\text{C}$  for 90 min without shaking. After this period, 2.5 mL molten surface agar (0.6% agar, 0.5% NaCl, 0.5 mM L-histidine, 0.5 mM biotin, pH 7.4,  $44^\circ\text{C}$ ) was added to the tube and this mixture was poured into a Petri plate containing minimal agar (1.5% agar, Vogel–Bonner E medium, containing 10% glucose). The Petri plates were incubated at  $37^\circ\text{C}$  for 72 h, and the His + revertant colonies were counted. For tests with metabolic activation, the sodium phosphate buffer was replaced by 50  $\mu\text{L}$  of S9 fraction, before pre-incubation.

To establish negative control, was used dimethyl sulfoxide (DMSO) for all strains. The positive controls used for this assay in the absence and presence of S9 fraction, respectively, were 4-nitro-o-phenylenediamine (NPD) and 2-aminoanthracene (2AA), for TA98 and TA97a; sodium azide (SA) and 2AA for TA100; and mitomycin C (MitC) and 2AA for TA102.

The concentrations used were based on the bacterial toxicity of each preparation, estimated in a preliminary test. In all subsequent assays, the upper limit of the dose range tested was either the highest non-toxic dose or the lowest toxic dose determined in this preliminary assay. Toxicity was apparent either as a reduction in the number of His + revertants, or as an alteration in the auxotrophic background (i.e. background lawn).

#### 2.4. Statistical analysis

The leishmanicidal activities of compounds were expressed as the concentration that inhibits the growth of 50.0% of protozoan form. Statistical analysis was performed using nonlinear regression to obtain the values of IC<sub>50</sub> and CC<sub>50</sub> (cytotoxic concentration for 50.0% of macrophages), followed by variance analyses and Tukey's test. Differences were significant when the p value was lower than 0.05.

Statistical analysis from antiproteolytic activity, cytokinesis-block micronucleus assay and index of nuclear division assays were performed using Graftit 5.0. Statistical significance was determined using one-way analysis of variance (ANOVA) followed by Tukey post hoc test. Values of  $p < 0.05$  were considered statistically significant. Data are expressed as mean  $\pm$  standard deviation (SD) unless otherwise specified.

For Ames assays, the statistical analysis was performed with the Salanal software, adopting the Bernstein et al. [32] model. The

mutagenic index (MI), which is the average number of revertant mutants per plate for treated groups divided by the average number of revertant mutants per plate for the negative control (solvent), was calculated for each concentration.

#### 2.5. Evaluation of lipophilicity by LogP (oct/water)

Lipophilicity values were estimated through theoretical determination of cLogP (oct/wat) by using the ChemDraw Ultra version 11.0 program. Calculated lipophilicity expressed by cLogP (oct/wat) of compounds **4**, **10**, **11**, **13**, **14**, **16**, **18** and **25** are showed on Table 2.

### 3. Results and discussion

#### 3.1. Synthesis

There are many protocols in the literature for the synthesis of alkylphospholipid analogues [33,34]. The best procedure we had access to was using the calcium salt of phosphorylcholine **1** as starting material (Scheme 1). The phosphate tetra-n-butylammonium **2** was prepared by treatment of **1** with an aqueous solution of oxalic acid followed by titration of a phosphoric acid derivative obtained with tetra-n-butylammonium hydroxide [35]. To obtain the compounds **3** and **4**, a solution of **2** in acetonitrile was treated with alkylating compounds (**8a** or **8b**), producing the alkylphosphocholines **3** and **4**, with 19% yield after purification on silica gel.

The synthesis of **8a** and **8b** compounds is depicted in Scheme 2. The mesylate compounds (**8a–b**) were prepared using 1,9-nonanediol or 1,12-dodecanediol as starting materials [16].

Compound **8b** in dichloromethane was treated with a solution of copper sulphate pentahydrate (8 mol%) and sodium ascorbate (20 mol%) in water. The reaction mixture was stirred for 24 h at room temperature, exclusively producing a high yield of the 1,4-disubstituted 1,2,3-triazole **9**. To obtain the alkyltriazoles **10** and **11**, a solution of alkyltriazoles **9** (Scheme 3) in acetone was treated with 4-DMAP and acetic anhydride. The reaction mixture was stirred for 24 h at room temperature, exclusively producing the alkyltriazole **11**, with 73% yield. To obtain the compound **10**, a

**Table 1**  
Leishmanicidal activity *in vitro* against promastigote forms of *Leishmania amazonensis* compared to amphotericin B.

Compounds	Promastigotes <sup>a</sup> IC <sub>50</sub> ( $\mu\text{M}$ )
<b>2</b>	$141.20 \pm 9.49^{\text{A}}$
<b>3</b>	$136.38 \pm 14.65^{\text{A}}$
<b>4</b>	$25.56 \pm 1.89^{\text{B,C}}$
<b>11</b>	$4.01 \pm 0.38^{\text{H}}$
<b>10</b>	$30.34 \pm 0.34^{\text{B,C}}$
<b>12</b>	$82.23 \pm 16.55^{\text{D}}$
<b>13</b>	$28.52 \pm 0.73^{\text{B,C,F}}$
<b>14</b>	$37.17 \pm 4.5^{\text{B,F}}$
<b>15</b>	$67.68 \pm 8.73^{\text{D,E}}$
<b>16</b>	$19.26 \pm 6.52^{\text{C}}$
<b>17</b>	$81.73 \pm 26.18^{\text{D}}$
<b>18</b>	$37.06 \pm 0.86^{\text{B}}$
<b>19</b>	$75.89 \pm 5.26^{\text{D,E}}$
<b>20</b>	$51.70 \pm 0.29^{\text{D,F}}$
<b>21</b>	$229.35 \pm 13.19^{\text{G}}$
<b>22</b>	$225.31 \pm 42.37^{\text{G}}$
<b>23</b>	$219.49 \pm 15.44^{\text{G}}$
<b>24</b>	$47.64 \pm 1.53^{\text{E,F}}$
<b>25</b>	$27.95 \pm 9.62^{\text{B,C}}$
<b>Amphotericin B</b>	$4.70 \pm 0.36^{\text{H}}$

<sup>a</sup> Same letters = non-statistical difference ( $p < 0.05$ ) by Tukey's test.

<sup>a</sup> Each IC<sub>50</sub> value represents the mean  $\pm$  standard deviation of triplicate determined by the software Graftit 5.0.

**Table 2**

Leishmanicidal activity *in vitro* against amastigote forms of *Leishmania amazonensis*, cytotoxicity, selectivity index values, cLogP, and r-CPB2.8 enzyme of *L. (L.) mexicana* data of compounds **4**, **10**, **11**, **13**, **14**, **16**, **18**, and **25** compared to pentamidine, amphotericin B, and E64.

Compounds	Amastigotes <sup>a</sup> IC <sub>50</sub> (μM)	Macrophages <sup>b</sup> CC <sub>50</sub> (μM)	Selectivity index (SI)*	cLogP <sup>c</sup>	r-CPB2.8 <sup>d</sup> IC <sub>50</sub> (μM)
<b>4</b>	3.81 ± 0.1 <sup>A</sup>	128.62 ± 10.99	33.76	6.90	8.3474 ± 0.5543 <sup>A</sup>
<b>11</b>	56.1 ± 4.3 <sup>D</sup>	26.55 ± 1.06	2.11	2.85	1.0226 ± 0.1761 <sup>B</sup>
<b>10</b>	70.25 ± 5.8 <sup>C</sup>	156.2 ± 9.61	2.14	3.54	4.5309 ± 0.2315 <sup>E</sup>
<b>13</b>	14.25 ± 0.92 <sup>B</sup>	163.4 ± 14.85	11.47	3.31	8.1841 ± 0.7048 <sup>A</sup>
<b>14</b>	76.68 ± 4.76 <sup>C</sup>	983.34 ± 37.98	12.82	2.23	0.8571 ± 0.0269 <sup>B</sup>
<b>16</b>	23.67 ± 5.17 <sup>B</sup>	66.15 ± 5.26	2.79	5.50	1.2220 ± 0.1005 <sup>B,C</sup>
<b>18</b>	15.05 ± 4.03 <sup>B</sup>	162.81 ± 16.56	9.83	4.47	2.2605 ± 0.0739 <sup>C</sup>
<b>25</b>	17.67 ± 0.88 <sup>B</sup>	93.35 ± 8.56	5.28	5.68	6.0772 ± 0.7588 <sup>D</sup>
<b>Pentamidine</b>	6.62 ± 0.03 <sup>A</sup>	11.22 ± 1.3	1.69	—	—
<b>Amphotericin B</b>	6.10 ± 1.0 <sup>A</sup>	27.10 ± 2.1	4.44	—	—
<b>E64</b>	—	—	—	—	0.125 ± 0.006

nd = not determined.

\*SI = ratio CC<sub>50</sub>(Macrophages)/IC<sub>50</sub>(Amastigotes).

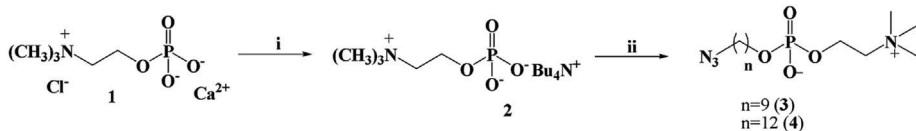
Same letters = non-statistical difference ( $p < 0.01$ ) by Tukey's test.

<sup>a</sup> Concentration for decrease of 50% infected macrophages in treated vs. non-treated wells.

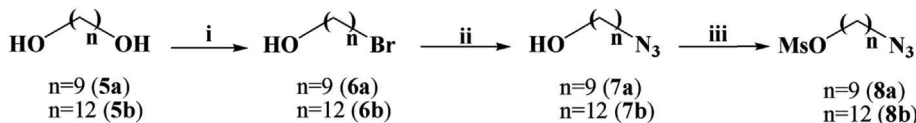
<sup>b</sup> Cytotoxicity concentration for 50% macrophages.

<sup>c</sup> Calculated lipophilicity expressed as cLogP (oct/wat) by using ChemDraw Ultra program version 11.0.

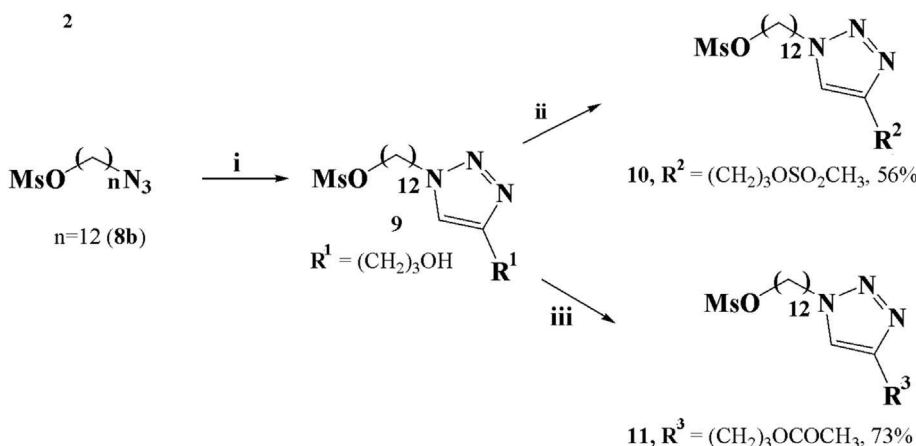
<sup>d</sup> Each IC<sub>50</sub> value represents the mean ± standard deviation of triplicate determined by the software Graftit 5.0.



**Scheme 1.** Reagents and conditions: (i) Oxalic acid, tetra-n-butylammonium hydroxide, pH 9; (ii) methanesulfonate alkylazide (**8a** or **8b**), acetonitrile, rt, 24 h and reflux, 3 h; 19%.



**Scheme 2.** Reagents and conditions: (i) HBr (48%), toluene, 110 °C, 24 h, 65–87%; (ii) NaN<sub>3</sub>, DMSO, rt, 24 h, 48–85%; (iii) CH<sub>2</sub>Cl<sub>2</sub>, methanesulfonyl chloride, triethylamine, rt, 24 h, 37–90%.



**Scheme 3.** Reagents and conditions: (i) NaAsc (20 mol%), CuSO<sub>4</sub>•5H<sub>2</sub>O (8 mol%), pent-4-yn-1-ol, CH<sub>2</sub>Cl<sub>2</sub>:H<sub>2</sub>O (1:1), rt, 24 h, 46–93%; (ii) 4-DMAP, acetic anhydride, acetone, rt, 24 h, 73%; (iii) CH<sub>2</sub>Cl<sub>2</sub>, methanesulfonyl chloride, triethylamine, rt, 24 h, 56%.

solution of alkyltriazoles **9** in dichloromethane was treated with mesyl chloride and triethylamine. The reaction mixture was stirred for 24 h at room temperature, producing the alkytriazole **10**, with 56% yield.

The triazoles **12–25** were obtained as previously described by Gontijo et al. (2014) [16].

All synthesized compounds were initially evaluated *in vitro* for their antileishmanial activities against promastigote forms of *Leishmania amazonensis*. The compounds showed IC<sub>50</sub> values ranging from  $4.01 \pm 0.38 \mu\text{M}$  (**11**) to  $229.35 \pm 13.19 \mu\text{M}$  (**21**). Only eight compounds (**4, 10, 11, 13, 14, 16, 18**, and **25**) exhibited inhibitory activities up to the limit of ten times less than amphotericin B's IC<sub>50</sub> (Table 1).

The eight compounds that were found to be more active against promastigote forms were also tested against the non-motile amastigote forms of *Leishmania amazonensis*. The IC<sub>50</sub> values of the active alkyltriazole compounds (**10, 11, 13, 14, 16, 18**, and **25**) and of alkylphosphocholine derivative **4**, pentamidine, and amphotericin B, are listed in Table 2. The cytotoxic effects of all compounds against murine peritoneal macrophages (CC<sub>50</sub>) were also evaluated to determine the Selectivity Index (SI).

Similar to previous observations [35], the leishmanicidal activity of the compounds against promastigotes was substantially different from the activity detected against amastigotes. This confirms that it is not appropriate to extrapolate the activities obtained for one form of the parasite to the other. The modulation of cell-mediated response and the cellular and biochemical pathways of amastigotes differ considerably from those of promastigotes, suggesting that the chemotherapeutic potential of anti-leishmanial drugs depend on their action against amastigotes.

Among the compounds tested, the phospholipid derivative **4** was the most potent against amastigote forms of *Leishmania amazonensis*, with an IC<sub>50</sub> of  $3.81 \mu\text{M}$ . Its IC<sub>50</sub> shows that its activity is comparable to that of the control drugs pentamidine (IC<sub>50</sub> =  $6.62 \mu\text{M}$ ) and amphotericin B (IC<sub>50</sub> =  $6.10 \mu\text{M}$ ). Additionally, this compound was found to be the least toxic to human macrophages, with a CC<sub>50</sub> of  $128.62 \mu\text{M}$  and folds more selective (SI = 33.76) than the standard drugs pentamidine (CC<sub>50</sub> =  $11.22 \mu\text{M}$ , SI = 1.69) and amphotericin B (CC<sub>50</sub> =  $27.10 \mu\text{M}$ , SI = 4.44). Considering the SI, expressed as the ratio of cytotoxicity (CC<sub>50</sub>) and antileishmanial potency (IC<sub>50</sub>), the compound **4** exhibited the best biological profile. This result is very important for developing novel

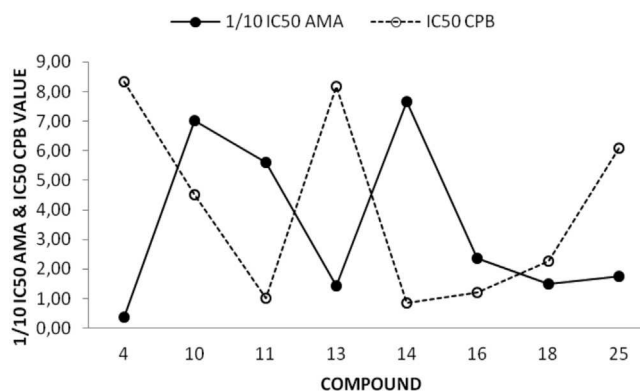


**Fig. 3.** Relation between leishmanicidal effect against amastigote forms (1/10 IC<sub>50</sub> AMA) and antiproteolytic activity for cysteine protease r-CPB2.8 (IC<sub>50</sub> CPB) for compounds **4, 10, 11, 13, 14, 16, 18**, and **25**.

phospholipid antileishmanial drugs. A large number of studies have reported the synthesis and biological screening of several ether phospholipids [36–42] derivatives for their *in vitro* leishmanicidal activity and citotoxicity. Avlonitis et al. [36] described the synthesis of a series of ring-substituted ether phospholipids and the evaluation of antileishmanial activity of the new compounds against the promastigote forms of *Leishmania donovani* and *Leishmania infantum*. Among the 37 compounds tested, 14 were more potent than miltefosine (IC<sub>50</sub>  $22.56 \mu\text{M}$ ) against *L. donovani*, but only two with IC<sub>50</sub> lower than  $3.81 \mu\text{M}$ . Cogghi et al. [42] also obtained 18 analogues of ether-linked phospholipids, but all compounds exhibited IC<sub>50</sub> values higher than miltefosine against amastigote forms of *L. donovani*. As observed by many authors [36–38], the length of alkyl chain on alkylphospholipid derivatives demonstrates to be important for the activity of this class of compounds. This could explain the higher activity of **4** ( $n = 12$ ) in comparison with compound **3** ( $n = 9$ ) against both promastigote and amastigote stages of *L. amazonensis* in the present study.

Among the alkyltriazole compounds obtained, the compound **13** was the more potent against amastigote forms of *L. amazonensis* ( $14.25 \mu\text{M}$ , SI = 11.47), followed by compound **18** ( $15.05 \mu\text{M}$ , SI = 9.83), and compound **25** ( $17.67 \mu\text{M}$ , SI = 5.28) (Table 2). For compounds **13, 18** and **25**, the length of carbon long-chain is the

**Table 3**

Absence of mutagenicity in *Salmonella typhimurium* strains, without (−S9) and with (+S9) metabolic activation. Data are shown as revertants/plate, standard deviation, and mutagenicity index (in parentheses), after treatment with five different concentrations of compound **13**.

Treatment ( $\mu\text{M}/\text{plate}$ )	TA98		TA100		TA97a		TA102	
	−S9	+S9	−S9	+S9	−S9	+S9	−S9	+S9
<b>0<sup>a</sup></b>	$41.00 \pm 8.54$	$34.33 \pm 3.06$	$164.33 \pm 23.43$	$181.33 \pm 17.04$	$135.50 \pm 3.54$	$128.67 \pm 4.51$	$313.33 \pm 23.86$	$272.67 \pm 42.34$
<b>150.98</b>	$40.67 \pm 5.03$ (1.0)	$39.33 \pm 8.33$	$174.67 \pm 18.82$ (1.1)	$162.67 \pm 13.50$ (0.9)	$175.50 \pm 10.61$ (1.3)*	$119.33 \pm 23.86$ (0.9)	$353.33 \pm 17.93$ (1.1)	$307.33 \pm 12.06$ (1.1)
<b>296.15</b>	$47.33 \pm 5.03$ (1.2)	$38.33 \pm 7.02$	$210.50 \pm 7.78$ (1.3)	$163.00 \pm 8.72$	$151.00 \pm 9.54$ (1.1)	$112.33 \pm 27.23$ (0.9)	$267.33 \pm 18.15$ (0.9)	$354.67 \pm 37.87$ (1.3)
<b>435.85</b>	$46.67 \pm 9.29$ (1.1)	$39.00 \pm 4.00$	$201.67 \pm 33.56$ (1.2)	$126.00 \pm 14.53$ (0.7)	$157.00 \pm 8.00$ (1.2)	$114.33 \pm 10.69$ *	$278.00 \pm 8.00$ (0.9)	$312.00 \pm 21.07$ (1.1)
<b>570.37</b>	$55.33 \pm 5.86$ (1.3)	$29.00 \pm 9.54$ (0.8)	$207.67 \pm 23.29$ (1.3)	$141.00 \pm 7.55$ (0.8)	$124.00 \pm 10.82$ (0.9)	$132.33 \pm 17.01$ (1.0)	$298.67 \pm 26.03$ (1.0)	$388.67 \pm 21.50$ (1.4)*
<b>700.00</b>	$53.67 \pm 5.51$ (1.3)	$40.33 \pm 40.33$	$164.50 \pm 2.12$ (1.0)	$159.00 \pm 31.48$	$141.00 \pm 4.24$ (1.1)	$109.00 \pm 13.45$ (0.8)	$306.00 \pm 25.06$ (1.0)	$376.33 \pm 3.21$ (1.4)*
<b>Ctrl+</b>	$1350.00 \pm 413.14^b$	$812.00 \pm 149.29^c$	$2808.00 \pm 344.43^d$	$1019.00 \pm 144.65^c$	$1101.33 \pm 169.77^b$	$803.33 \pm 164.08^c$	$1828.67 \pm 583.01^e$	$2512.00 \pm 325.00^c$

\*Representation of a significant response ( $P \leq 0.01$ ).

<sup>a</sup> Negative control (DMSO – 10  $\mu\text{L}$ ).

<sup>b</sup> NPD (10  $\mu\text{g}/\text{plate}$ ).

<sup>c</sup> 2AA (5  $\mu\text{g}/\text{plate}$ ).

<sup>d</sup> SA (5  $\mu\text{g}/\text{plate}$ ).

<sup>e</sup> MitC (0.5  $\mu\text{g}/\text{plate}$ ).

**Table 4**

Absence of mutagenicity in *Salmonella typhimurium* strains, without (−S9) and with (+S9) metabolic activation. Data are shown as Revertants/plate, standard deviation and mutagenicity index (in parentheses), after treatment with five different concentrations of compound **14**.

Treatment (μM/plate)	TA98		TA100		TA97a		TA102	
	−S9	+S9	−S9	+S9	−S9	+S9	−S9	+S9
<b>0<sup>a</sup></b>	41.00 ± 8.54	34.33 ± 3.06	164.33 ± 23.43	181.33 ± 17.04	117.33 ± 5.86	128.66 ± 4.51	295.33 ± 11.24	272.67 ± 42.34
<b>313.73</b>	61.67 ± 5.77 (1.5)	34.00 ± 6.56 (1.0)	193.00 ± 37.40 (1.2)	167.67 ± 27.02 (0.9)	151.00 ± 6.56 (1.3)**	102.67 ± 4.73 (0.8)	347.33 ± 41.00 (1.2)	376.00 ± 9.17 (1.4)*
<b>616.38</b>	50.67 ± 5.77 (1.2)	28.00 ± 2.65 (0.8)	200.00 ± 36.77 (1.3)	173.50 ± 19.09 (1.0)	192.00 ± 7.55 (1.6)**	114.33 ± 26.58 (0.9)	311.33 ± 59.00 (1.1)	446.33 ± 12.66 (1.7)**
<b>905.66</b>	47.67 ± 3.51 (1.2)	33.33 ± 5.86 (1.0)	197.00 ± 0 (1.2)	177.50 ± 28.99 (1.0)	207.00 ± 7.02 (1.8)**	117.33 ± 6.11 (0.9)	258.67 ± 40.07 (0.9)	364.33 ± 34.27 (1.3)
<b>1185.19</b>	63.00 ± 15.72 (1.5)	27.33 ± 2.08 (0.8)	217.00 ± 31.11 (1.3)	157.33 ± 13.58 (0.9)	155.00 ± 17.09 (1.3)	95.00 ± 5.29 (0.7)	364.00 ± 37.04 (1.2)	389.33 ± 14.29 (1.4)*
<b>1454.55</b>	56.67 ± 6.11 (1.4)	26.67 ± 9.45 (0.8)	192.33 ± 8.39 (1.2)	168.00 ± 14.18 (0.9)	159.33 ± 15.04 (1.4)*	105.67 ± 5.13 (0.8)	331.00 ± 13.61 (1.1)	326.00 ± 22.52 (1.2)
<b>Crtol+</b>	1350.00 ± 413.14 <sup>b</sup>	812.00 ± 149.29 <sup>c</sup>	2808.00 ± 344.43 <sup>d</sup>	1019.00 ± 144.65 <sup>b</sup>	924.00 ± 104.23 <sup>c</sup>	803.33 ± 164.08 <sup>d</sup>	2714.50 ± 284.96 <sup>e</sup>	2512.67 ± 325.00 <sup>c</sup>

\*\*Representation of a significant response ( $P \leq 0.01$ ).

\*Representation of a significant response ( $P \leq 0.05$ ).

<sup>a</sup> Negative control (DMSO – 10 μL).

<sup>b</sup> NPD (10 μg/plate).

<sup>c</sup> 2AA (5 μg/plate).

<sup>d</sup> SA (5 μg/plate).

<sup>e</sup> MitC (0.5 μg/plate).

same ( $n = 12$ ), which suggest the importance of this structural feature for activity (compare **12** versus **13**, for example). Additionally, the substituent in the position 4 of triazole nucleus also contains only three carbon atoms. A few studies have described the synthesis and leishmanicidal activity of triazoles compounds in the last decade. Corrales et al. [39] synthesized a series of novel 6-thiopurine derivatives containing 1,2,3-triazoles and evaluated the leishmanicidal activity against promastigote forms of *L. amazonensis*. Neither compound was more active than amphotericin B, used as control. Ferreira et al. [40] also synthesized and evaluated

new triazole compounds carrying either the carbaldehyde or the difluoromethylene functionalities against promastigote forms of *L. amazonensis*. Neither compound was more active than pentamidine, used as control. Tahghighi et al. [41] synthesized 5-(5-nitrofuran-2-yl)-1,3,4-thiadiazol-2-amines containing triazole moieties to examine the leishmanicidal potency. The anti-promastigote activity against *Leishmania major* ranged between 12.2 μM and 107.7 μM. In sum, compared to these examples, the structurally simple long-chain alkyltriazoles described in our work are attractive because they are easy to synthesize and may

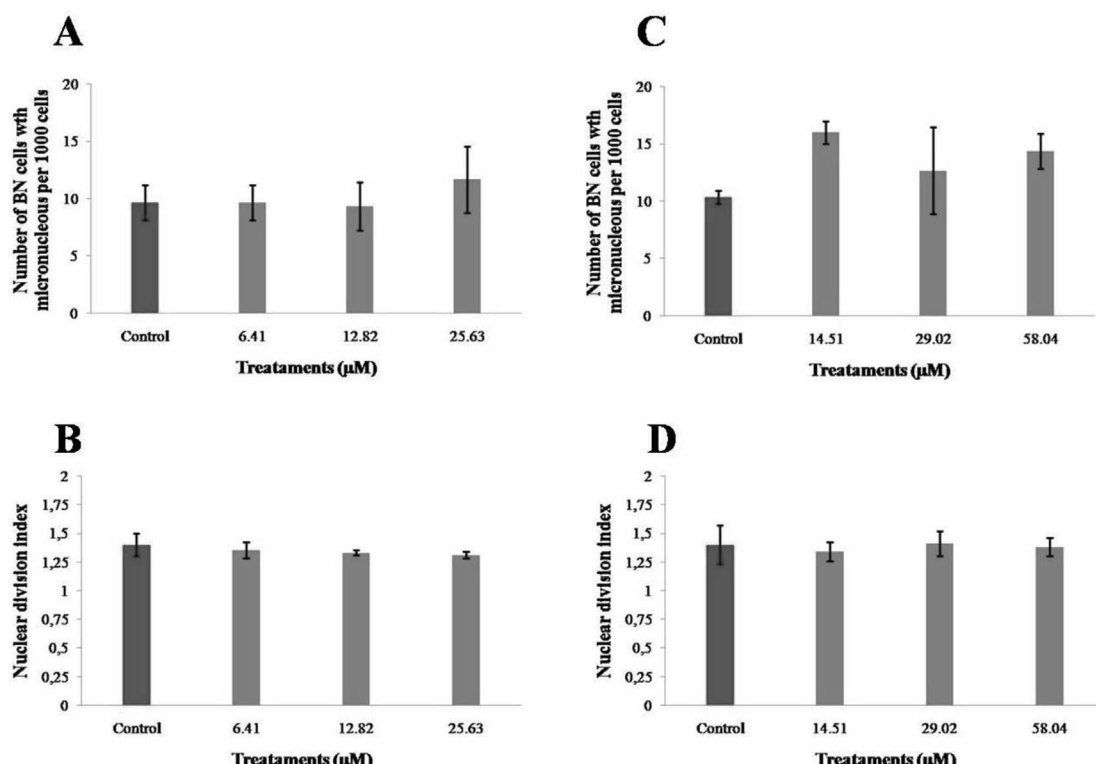


Fig. 4. Results obtained in cytokinesis-block micronucleus assay performed with CHO-K1 cells treated with different concentrations of compounds **13** and **14**.

represent a new and promising scaffold for the development of new leishmanicidal substances.

In order to investigate a possible mechanism of action, the antiproteolytic activity of compounds **4**, **10**, **11**, **13**, **14**, **16**, **18**, and **25** against the *L. (L.) mexicana* cysteine protease r-CPB2.8 was evaluated. The results are shown in Table 2 and Fig. 3. The compound **14** was observed to be the most potent inhibitor with an IC<sub>50</sub> value of 0.8571 μM; however, it was almost seven-fold less active than the standard compound E64 (IC<sub>50</sub> = 0.125 μM). We observed that almost all compounds exhibited an inverse correlation between anti-amastigote and antiproteolytic activities as shown in Fig. 3, since a smaller IC<sub>50</sub> enzyme inhibition value consistently correlates with a greater IC<sub>50</sub> anti-amastigote action. This led to the speculation that the compounds' proteolytic action is not essential to avoid macrophage infection by amastigote forms.

According to Abad-Zapatero and Metz [43], potent compounds do not necessarily result in promising drugs and other fundamental parameters can be related to optimal pharmacological properties. As observed in Table 2, compounds **4**, **13**, and **14** presented the best SI values of the series. Though compound **4** exhibits potent activity against amastigotes, its cLogP value is higher than 5, indicating high lipophilicity. Hann [44] affirms that compounds with this characteristic are correlated with poor oral drug-like properties, have more difficulty being excreted, and tend to be more toxic. For instance, in a series of compounds, increased microsomal clearance and pharmacological promiscuity are often associated with higher cLogP values, while limited cell permeation and absorption are linked with low lipophilicity. To achieve a compromise between absorption and first-pass clearance, a cLogP value between 2 and 3 is often considered optimal in an oral drug program [45]. Because of this, only compounds **13** and **14**, which presented promising properties as leishmanicidal agents having SI values higher than 10 and cLogP values between 2 and 3, were evaluated for their mutagenicity *in vitro* by employing the Ames assay (gene mutation analysis) and the micronucleus assay (chromosomal mutation analysis). As observed in Tables 3 and 4 and Fig. 4, these compounds did not induce DNA damage in the biological systems used in this study. The Ames Microsuspension Test verifies that, in some conditions, compounds **13** and **14** increased the frequency of revertant colonies in comparison with the negative control. However, all the mutagenicity index (MI) values were lower than 2, which show that these compounds were not mutagenic.

As observed, the micronucleus frequency in 1000 binucleated cells treated with all concentrations of compounds **13** and **14** was not statistically higher than the values identified in the control group, indicating absence of mutagenic activity at this concentration (shown in A and C, respectively). B and D show the influence of treatments in the nuclear division process (compounds **13** and **14**, respectively). There were no significant differences observed in the Nuclear division index (NDI) values when compared with that of the control group.

Evaluation of mutagenicity for compounds **13** and **14** is also important because, as affirmed in a previous work [16], these compounds were effective against HeLa (human uterine tumour) and RKO (human colon tumour) cell lines, with pro-apoptotic effect induced by the compound **13** in RKO [16].

#### 4. Conclusions

In summary, a series of alkyltriazoles and two new alkylphosphocholines were evaluated for their *in vitro* inhibitory activity against the *Leishmania* parasite. Several target compounds exhibited moderate anti-leishmanial activity against the promastigote forms of *Leishmania amazonensis*. The most cytotoxic compound against promastigotes was found to be the compound **11** and,

against amastigote form, the compound **4**. Considering the lipophilicity aspect of the assessed compounds, compound **13** presented the best characteristics, which were low IC<sub>50</sub> in promastigotes and amastigotes, low toxicity to murine macrophages (high Selectivity Index), and absence of mutagenicity. These compounds could represent a promising template for developing a new class of leishmanicidal agents, and deserve further investigation of derived scaffolds.

#### Acknowledgements

The authors are grateful to the Fundação de Amparo a Pesquisa o Estado de Minas Gerais (FAPEMIG, BR), Conselho Nacional de Desenvolvimento Científico e Tecnológico (CNPq, BR) and Coordenação de Aperfeiçoamento de Pessoal de Nível Superior (CAPES, BR) for fellowships and financial support.

#### Appendix A. Supplementary data

Supplementary data related to this article can be found at <http://dx.doi.org/10.1016/j.ejmech.2015.06.005>.

#### References

- [1] World Health Organization. Website: <http://www.who.int/leishmaniasis/en/> (Accessed April 2015).
- [2] A. Awasthi, R.K. Mathur, B. Saha, Immune response to *Leishmania* infection, Indian J. Med. Res. 119 (2004) 238–258.
- [3] J.Q. Reimão, A.G. Tempone, Investigation into *in vitro* anti-leishmanial combinations of calcium channel blockers and current anti-leishmanial drugs, Mem. Inst. Oswaldo Cruz 106 (8) (2011) 1032–1038.
- [4] L.F. Oliveira, A.O. Schubach, M.M. Martins, S.L. Passos, R.V. Oliveira, M.C. Marzochi, Systematic review of the adverse effects of cutaneous leishmaniasis treatment in the New World, Acta Trop. 118 (2011) 87–96.
- [5] A. Khatami, R. Talaee, M. Rahshenas, A. Khamesipour, P. Mehryan, S. Tehrani, Y. Dowlati, A. Firooz, Dressings combined with injection of meglumine antimoniate in the treatment of cutaneous leishmaniasis: a randomized controlled clinical trial, PLoS One 8 (6) (2013) 123.
- [6] A.H.A. Mohamed-Ahmed, K.A. Les, S.L. Croft, S. Brocchini, Preparation and characterisation of amphotericin B-copolymer complex for the treatment of leishmaniasis, Polym. Chem. 4 (2013) 584.
- [7] M. Shalev, J. Kondo, D. Kopelyanskiy, C.L. Jaffe, N. Adir, T. Baasov, Identification of the molecular attributes required for aminoglycoside activity against *Leishmania*, PNAS 110 (33) (2013) 13333–13338.
- [8] R.A.O. Castro, N.M. Silva-Barcellos, C.S.A. Licio, J.B. Souza, M.C. Souza-Testas, F.M. Ferreira, M.A. Batista, D. Silveira-Lemos, S.L. Moura, F. Frezard, S.A. Rezende, Association of liposome-encapsulated trivalent antimarial with ascorbic acid: an effective and safe strategy in the treatment of experimental visceral leishmaniasis, PLoS One 9 (8) (2014) 104055.
- [9] C.J. Hawker, K.L. Wooley, The convergence of synthetic organic and polymer chemistries, Science 309 (2005) 1200–1205.
- [10] J.E. Moses, A.D. Moorhouse, The growing applications of click chemistry, Chem. Soc. Rev. 36 (2007) 1249–1262.
- [11] S.G. Agalave, S.R. Majjan, V.S. Pore, Click chemistry: 1,2,3-triazoles as pharmacophores, Chem. Asian. J. 6 (2011) 2696–2718.
- [12] B. Schulze, U.S. Schubert, Beyond click chemistry -supramolecular interactions of 1,2,3-triazoles, Chem. Soc. Rev. 43 (2014) 2522.
- [13] L.B.O. Freitas, F.A. Ruela, G.R. Pereira, R.B. Alves, R.P. Freitas, A reação "click" na síntese de 1,2,3-triazóis: aspectos químicos e aplicações, Quím. Nova 34 (10) (2011) 1791–1804.
- [14] A. Tahghighi, S. Razmi, M. Mahdavi, P. Foroumadi, S.K. Ardestani, S. Emami, F. Kobarfard, S. Dastmalchi, A. Shafiee, A. Foroumadi, Synthesis and anti-leishmanial activity of 5-(5-nitrofuran-2-yl)-1,3,4-thiadiazol-2-amines containing N-[1-(benzyl-1H-1,2,3-triazol-4-yl)methyl] moieties, Eur. J. Med. Chem. 50 (2012) 124–128.
- [15] K. Kumar, B. Pradines, M. Madamet, R. Amalvict, V. Kumar, 1*H*-1,2,3-triazole tethered mono- and bis-ferrocenylchalcone-blactam conjugates: synthesis and antimalarial evaluation, Eur. J. Med. Chem. 8 (2014) 113–121.
- [16] V.S. Gontijo, M.É. Oliveira, R.J. Resende, A.L. Fonseca, R.R. Nunes, M.C. Júnior, A.G. Taranto, N.M.P.O. Torres, G.H.R. Viana, L.M. Silva, R.B. Alves, F.P. Varotti, R.P. Freitas, Long-chain alkyltriazoles as antitumor agents: synthesis, physicochemical properties, and biological and computational evaluation, Med. Chem. Res. 24 (2014) 430–441.
- [17] J. Alexander, G.H. Coombs, J.C. Mottram, *Leishmania mexicana* cysteine proteinase-deficient mutants have attenuated virulence for mice and potentiate a Th1 response, J. Immunol. 161 (1998) 6794–6801.
- [18] Juliano, J.C. Mottram, G.H. Coombs, Expression and characterization of a

- recombinant cysteine proteinase of *Leishmania mexicana*, *Biochem. J.* 347 (2000) 383–388.
- [19] C.R. Caffrey, S. Scory, D. Steverding, Cysteine proteinases of trypanosome parasites: novel targets for chemotherapy, *Curr. Drug Targets* 1 (2000) 155–162.
- [20] G.R. Wasson, V.J. McKelvey-Martin, C.D. Downes, The use of the comet assay in the study of human nutrition and cancer, *Mutagenesis* 23 3 (2008) 153–162.
- [21] R.J. Albertini, D. Anderson, G.R. Douglas, L. Hagmaar, K. Hemminki, F. Merlo, A. Aitio, IPCS guidelines for the monitoring of genotoxic effects of carcinogens in humans, *Mutat. Res.* 463 (2000) 111–172.
- [22] T.R. Calvo, D. Demarco, F.V. Santos, H.P. Moraes, T. Bauab, E.A. Varanda, I.M.S. Cólus, W. Vilegas, Phenolic compounds in leaves of alchornea triplinervia: anatomical localization, mutagenicity, and antibacterial activity, *Nat. Prod. Commun.* 5 (8) (2010) 1225–1232.
- [23] F.T. Martins, D.M. Assis, Santos, M.H. Dos Santos, I. Camps, M.P. Veloso, M.A. Juliano, L.C. Alves, A.C. Doriguetto, Natural poly-prenylatedbenzophenones inhibiting cysteine and serine proteases, *Eur. J. Med. Chem.* 44 (2009) 1230–1239.
- [24] T. Mosmann, Rapid colorimetric assay for cellular growth and survival: application to proliferation and cytotoxic assays, *J. Immunol. Methods* 65 (1983) 55–63.
- [25] S.J. Sanderson, K.G. Pollock, J.D. Hilley, M. Meldal, P.S. Hilaire, M.A. Juliano, Expression and characterization of a recombinant cysteine proteinase of *Leishmania mexicana*, *Biochem. J.* 347 (2000) 383–388, 15.
- [26] L.C. Alves, R.L. Melo, S.J. Sanderson, J.C. Mottram, G.H. Coombs, G. Caliendo, V. Santagada, L. Juliano, M.A. Juliano, S1 subsite specificity of a recombinant cysteine proteinase, CPB, of *Leishmania mexicana* compared with cruzain, human cathepsin L and papain using substrates containing non-natural basic amino acids, *Eur. J. Biochem.* 268 (2001) 1206–1212.
- [27] M. Fenech, The *in vitro* micronucleus technique, *Mutat. Res.* 455 (2000) 81–95.
- [28] M. Fenech, Cytokinesis-block micronucleus cytome assay, *Nat. Protoc.* 2 5 (2007) 1084–1104.
- [29] D.A. Eastmond, J.D. Tucker, Identification of aneuploidy-inducing agents using cytokinesis-blocked human lymphocytes and an antikinetochore antibody, *Environ. Mol. Mutagen* 13 (1989) 34–43.
- [30] N.Y. Kado, D. Langley, E. Eisenstadt, A simple modification of the *Salmonella* liquid incubation assay: increased sensitivity for detecting mutagens in human urine, *Mutat. Res.* 122 (1983) 25–32.
- [31] K. Mortelmans, E. Zeiger, The Ames *Salmonella* mutagenicity assay, *Mutat. Res.* 455 1–2 (2000) 29–60.
- [32] L. Bernstein, J. Kaldor, J. Me Carm, M.C. Pike, An empirical approach to the statistical analysis of mutagenesis data from the *Salmonella* test, *Mutat. Res.* 97 (1982) 267–281.
- [33] V. Hornillos, J.M. Saugar, B.G. Torre, D.A.L. Rivas, A.U. Acuña, F. Amant-Guerri, Synthesis of 16-mercaptopohexadecylphosphocholine, a miltefosine analog with leishmanicidal activity, *Bioorg. Med. Chem. Lett.* 16 19 (2006) 5190–5193.
- [34] R.R. Ravu, Ying-Lien Chen, M.R. Jacob, X. Pan, A.K. Agarwal, S.I. Khan, J. Heintman, A.M. Clark, Xing-Cong Li, Synthesis and antifungal activities of miltefosine analogs, *Bioorg. Med. Chem. Lett.* 23 17 (2013) 4828–4831.
- [35] S. Robledo, E. Osorio, D. Muñoz, L.M. Jaramillo, A. Restrepo, G. Arango, I. Vélez, In vitro and *in vivo* cytotoxicities and antileishmanial activities of thymol and hemisynthetic derivatives, *Antimicrob. Agents Chemother.* 49 4 (2005) 1652–1655.
- [36] N. Avlonitis, E. Lekka, A. Detsi, M. Koufaki, T. Calogeropoulou, E. Scoulica, E. Siapi, I. Kyrikou, T. Mamvromoustakos, A. Tsotinis, S.G. Grdadolnik, A. Makriyannis, Antileishmanial ring-substituted ether phospholipids, *J. Med. Chem.* 46 (2003) 755–767.
- [37] T. Calogeropoulou, P. Angelou, A. Detsi, I. Fragiadaki, E. Scoulica, Design and synthesis of potent antileishmanial cycloalkylidene-substituted ether phospholipid derivatives, *J. Med. Chem.* 51 (2008) 897–908.
- [38] I. Papanastasiou, K.C. Prousis, K. Georgikopoulou, T. Pavlidis, E. Scoulica, N. Kolocouris, T. Calogeropoulou, Design and synthesis of new adamantly-substituted antileishmanial ether phospholipids, *Bioorg. Med. Chem. Lett.* 20 (2010) 5484–5487.
- [39] R.C.N.R. Corrales, N.B. de Souza, L.S. Pinheiro, C. Abramo, E.S. Coimbra, A.D. Da Silva, Thiopurine derivatives containing triazole and steroid: synthesis, antimarial and antileishmanial activities, *Biomed. Pharmacother.* 65 (2011) 198–203.
- [40] S.B. Ferreira, M.S. Costa, N. Boechat, R.J.S. Bezerra, M.S. Genestra, M.M. Canto-Cavalheiro, W.B. Kover, V.F. Ferreira, Synthesis and evaluation of new difluoromethyl azoles as antileishmanial agents, *Eur. J. Med. Chem.* 42 (2007) 1388–1395.
- [41] A. Tahaghghi, S. Razmi, M. Mahdavi, P. Foroumadi, S.K. Ardestani, S. Emami, F. Kobarfard, S. Dastmalchi, A. Shafiee, A. Foroumadi, Synthesis and antileishmanial activity of 5-(5-nitrofuran-2-yl)-1,3,4-thiadiazol-2-amines containing N-[{(1-benzyl-1*H*-1,2,3-triazol-4-yl)methyl}] moieties, *Eur. J. Med. Chem.* 50 (2012) 124–128.
- [42] P. Coghi, N. Vaiana, M.G. Pezzano, L. Rizzi, M. Kaiser, R. Brun, S. Romeo, Parallel synthesis and antileishmanial activity of ether-linked phospholipids, *Bioorg. Med. Chem. Lett.* 18 (2008) 4658–4660.
- [43] C. Abad-Zapatero, J.T. Metz, Ligand efficiency indices as guideposts for drug discovery, *Drug Discov. Today* 10 (2005) 464–469.
- [44] M.M. Hann, Molecular obesity, potency and other addictions in drug discovery, *Med. Chem. Commun.* 2 5 (2011) 349.
- [45] T. Ryckmans, M.P. Edwards, V. Horne, A.M. Correia, D.R. Owen, L.R. Thompson, T. Young, Rapid assessment of a novel series of selective CB(2) agonists using parallel synthesis protocols: a lipophilic efficiency (LipE) analysis, *Bioorg. Med. Chem. Lett.* 19 15 (2009) 4406–4409.

# Long-chain alkyltriazoles as antitumor agents: synthesis, physicochemical properties, and biological and computational evaluation

Vanessa Silva Gontijo · Michael Éder Oliveira · Rafael José Resende ·  
Amanda Luisa Fonseca · Renata Rachide Nunes · Moacyr Comar Júnior ·  
Alex Gutterres Taranto · Natalia Machado Pereira Oliveira Torres ·  
Gustavo Henrique Ribeiro Viana · Luciana Maria Silva · Rosemeire Brondi Alves ·  
Fernando Pilla Varotti · Rossimiriam Pereira Freitas

Received: 27 March 2014 / Accepted: 25 June 2014 / Published online: 15 July 2014

© Springer Science+Business Media New York 2014

**Abstract** A series of novel long-chain alkyltriazoles were prepared from commercial diols in a rapid process with good yields. The compounds were evaluated in vitro for their anticancer potential against two human cancer cell lines: colon carcinoma (RKO) and uterine carcinoma (HeLa). The results of colorimetric MTT assays showed that six of fourteen compounds tested decreased cell viability in these cell lines. Compounds **5e** and **6a** were the most active against RKO cells, with IC<sub>50</sub> values of 16.70 and 14.57 μM, respectively. The same compounds, **5e** and **6a**, were the most active in HeLa cells as well, with IC<sub>50</sub> values of 11.05 and 12.77 μM, respectively. In addition, compound **5e** was found to induce apoptosis in RKO cells, as assessed by TUNEL assay. The results suggest that compound **5e** may be a promising prototype anticancer agent.

---

**Electronic supplementary material** The online version of this article (doi:10.1007/s00044-014-1137-3) contains supplementary material, which is available to authorized users.

V. S. Gontijo · N. M. P. O. Torres · R. B. Alves ·

R. P. Freitas (✉)

Departamento de Química, ICEX, UFMG, Av. Pres. Antônio Carlos 6627, Pampulha, Belo Horizonte, MG 31270-901, Brazil  
e-mail: rossimiriam@pq.cnpq.br

M. É. Oliveira · R. J. Resende · A. L. Fonseca ·

R. R. Nunes · M. C. Júnior · A. G. Taranto ·

G. H. R. Viana · F. P. Varotti (✉)

Universidade Federal de São João del-Rei, Campus Centro-Oeste, Av. Sebastião Gonçalves Coelho, 400, Divinópolis, MG 35501-296, Brazil  
e-mail: varotti@ufsj.edu.br

L. M. Silva

Laboratório de Biologia Celular, Fundação Ezequiel Dias, Belo Horizonte, MG 30535-380, Brazil

**Keywords** Alkyltriazoles · Antitumoral · Click chemistry · Heterocycles

## Introduction

Cancer is the second leading cause of death in the world. Most of the anticancer drugs currently available for cancer treatment have well-established shortcomings, such as poor efficiency and selectivity, and high toxicity. Therefore, the identification of potent, selective, and less toxic anticancer agents remains an important and challenging goal of medicinal chemistry (Hilário *et al.*, 2011; Correale *et al.*, 2011).

Single long-chain alkylphospholipids (APLs) are a relatively new class of structurally related antitumor agents that, unlike conventional chemotherapeutic drugs, induce apoptosis in tumor cells by acting on cell membranes rather than on DNA. APLs accumulate in the cell and interfere with lipid-dependent survival signaling pathways, notably the PI3K-Akt and Raf-Erk1/2 pathways, and de novo phospholipid biosynthesis (Blitterswijk and Verheij, 2012). Alkyllysophospholipids and alkylphosphocholines (APCs) are two classes of APL ether lipids that could be potential anticancer agents. Miltefosine, perifosine, erucylphosphocholine, and erufosine (Fig. 1) are APCs, which are derived from alkyllysophospholipids by the removal of the glycerol group. In the APC edelfosine, however, the glycerol backbone is maintained. Hexadecylphosphocholine (**1**) is a lipid analog that exerts antiproliferative activity against a broad spectrum of established tumor cell lines (Blitterswijk and Verheij, 2012; Wieder *et al.*, 1998). Studies on cytotoxic APLs revealed that a long alkyl chain and a polar group are essential for antitumor activity (Rakotomanga *et al.*, 2007).

In the last decade, a large number of studies have reported the synthesis and biological screening of several

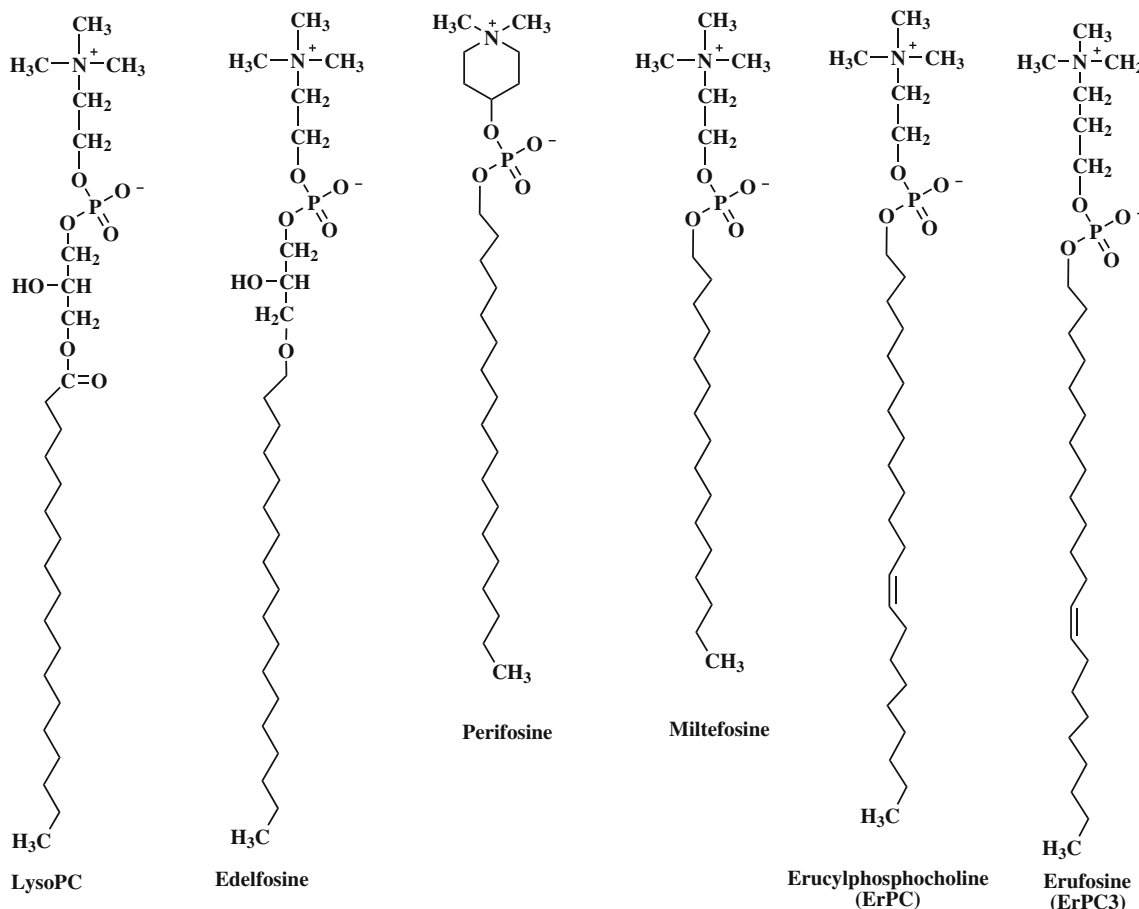


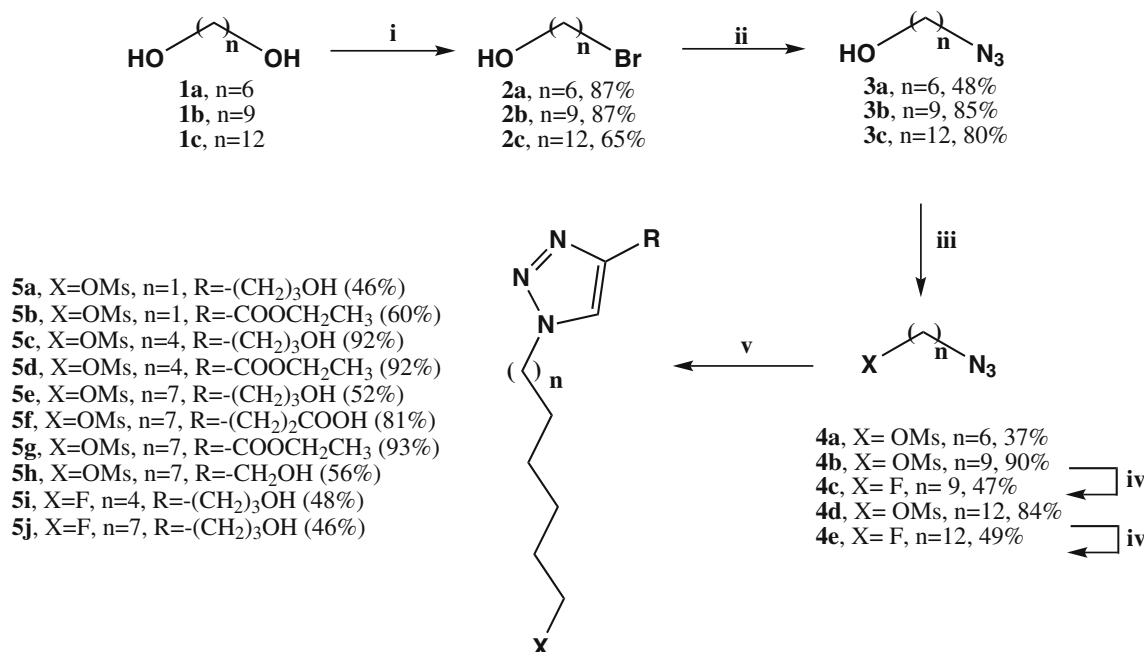
**Fig. 1** Structures of natural lysophosphatidylcholine and some synthetic alkyl-phospholipid (APL) analogs. (Adapted of Blitterswijk and Verheij, 2012)

APC compounds (Ungera and Eibl, 1991; Van der Luit *et al.*, 2007; Vink *et al.*, 2007). Although they are structurally simple, the purification of these highly polar compounds is very difficult, time-consuming, expensive, and frequently results in low yields.

1,2,3-Triazoles are a very important class of synthetic heterocycles that have received widespread attention in recent years because of their broad range of pharmacological properties and easy synthetic accessibility by click chemistry. They are found in various bioactive molecules, including antifungal (Aher *et al.*, 2009), antibacterial (Demaray *et al.*, 2008; Wang *et al.*, 2010), antiallergic (Buckle *et al.*, 1983), anti-HIV (Whiting *et al.*, 2006; Giffin *et al.*, 2008), antitubercular (Costa *et al.*, 2006; Patpi *et al.*, 2012), and anti-inflammatory agents (Simone *et al.*, 2011). In addition, the synthesis of different 1,2,3-triazoles with anticancer activity has also been increasingly noted (Alam *et al.*, 2013; Praveena *et al.*, 2014; Kurumurthy *et al.*, 2014). Triazoles are often considered bioisosteres of amide functionalities in bioactive compounds due to similarities in spatial structure and electronic effect. Furthermore, these

heterocycles are resistant to metabolic degradation and can interact with biological structures in several noncovalent ways (Deiters *et al.*, 2003; Wang *et al.*, 2003; Dirks *et al.*, 2005; Kosiova *et al.*, 2007; Santos *et al.*, 2008). Finally, they have a large dipole moment and are capable of hydrogen bonding, which could allow them to act as a polar head group.

Considering the potential anticancer activity of APCs and the speculation that their activity is linked to the presence of a hydrophobic tail attached to a hydrophilic polar head group, we focused our attention on synthesizing simpler potentially antitumoral compounds containing a 1,2,3-triazole ring and alkyl chains with different lengths and functionalizations. These compounds can be prepared using a 1,3-dipolar cycloaddition reaction between an alkyne and an azide (Struthers *et al.*, 2010). This cyclization reaction, developed in the early 1960s by Huisgen (1961), became highly popular when Sharpless (Rostovtsev *et al.*, 2002) and Meldal (Tornøe *et al.*, 2002) separately reported its Cu(I)-catalyzed version (Scheme 1). The reaction is now known as the Cu-catalyzed azide–alkyne



**Scheme 1** Reagents and conditions: (i) HBr (48 %), toluene, 110 °C, 24 h, 65–87 %; (ii) NaN<sub>3</sub>, DMSO, rt, 24 h, 48–85 %; (iii) CH<sub>2</sub>Cl<sub>2</sub>, mesyl chloride, triethylamine, rt, 24 h, 37–90 %; (iv) KF/18-crown-6,

DMSO, 110 °C, 24 h, 47–49 %; (v) NaAsc (20 mol%), CuSO<sub>4</sub>·5H<sub>2</sub>O (8 mol%), alkyne: pent-4-yn-1-ol, ethyl propiolate, 4-pentynoic acid, or propargyl alcohol, CH<sub>2</sub>Cl<sub>2</sub>:H<sub>2</sub>O (1:1), rt., 24 h, 46–93 %

cycloaddition (CuAAC) (Amblard *et al.*, 2009; Meldal and Tornoe, 2008) or click reaction. Sharpless strongly defended its use in drug discovery, reasoning that, in this field, all searches must be restricted to molecules that are easy to make (Kolb *et al.*, 2001). In addition to synthesizing alkyltriazoles, we also evaluated the antitumoral activity *in vitro* of the new compounds against two human cancer cell lines: colon carcinoma (RKO-AS451) cells and uterine carcinoma (HeLa).

## Methods and materials

### General

Reagents and solvents were purchased as reagent grade and used without further purification. All melting points were measured on Fisher–Jonhs and are uncorrected. IR spectra were recorded on Perkin-Elmer *Spectrum One SP-IR Spectrometer*. <sup>1</sup>H and <sup>13</sup>C NMR spectra were recorded on a *Bruker AVANCE DRX 200* MHz spectrometer using TMS as an internal standard. The results are presented as chemical shift  $\delta$  in ppm, number of protons, multiplicity,  $J$  values in Hertz (Hz), proton position, and carbon position. Multiplicities are abbreviated as follows: s (singlet), d (doublet), t (triplet), m (multiplet), and qn (quintet). High resolution mass spectra were recorded on ESI-MS—Bruker Daltonics Micro TOF mass spectrometer with electrospray

ionization coupled to time-of-flight (Solvent: MeOH). The progress of the reactions was monitored by TLC on Merck silica plates (GF254). Column chromatography was performed over silica gel 60, 70–230 mesh (Merck).

### Synthesis

#### General procedure for the synthesis of methanesulfonate alkylazides (**4a**, **4b**, and **4d**)

To a stirred solution of 1,6-hexanediol **1a** (1.00 equiv.), 1,9-nonenediol **1b** (1.00 equiv.), or 1,12-dodecanediol **1c** (1.00 equiv.), in 30 mL of toluene was added HBr 48 % (2.00 equiv.). The reaction was stirred at 110 °C for 24 h. The solvent was removed under reduced pressure, and the residue was purified by column chromatography over silica gel, eluting with hexane/EtOAc 9:1, to yield pure haloalcohol **2a–c**. These compounds were transformed into their corresponding azidoalcohols **3a–c** by S<sub>N</sub>2 substitution (Scheme 1). A stock solution of 0.5 M NaN<sub>3</sub> in DMSO was prepared by stirring the solution for 24 h at room temperature. To a 100-mL round-bottom flask equipped with a magnetic stir bar was added a 0.5 M solution of NaN<sub>3</sub> in DMSO at room temperature. To this solution was added the bromoalcohol **2a** (1.00 equiv.), **2b** (1.00 equiv.), or **2c** (1.00 equiv.), and the mixture was stirred for 24 h at room temperature. The reaction was quenched with H<sub>2</sub>O (50 mL) and stirred until it cooled to room temperature. The mixture was extracted with Et<sub>2</sub>O

( $3 \times 30$  mL), and the resulting extracts were washed with  $\text{H}_2\text{O}$  ( $3 \times 50$  mL) and brine (50 mL). The organic layer was dried ( $\text{Na}_2\text{SO}_4$ ) and filtered, and the residue obtained was purified by column chromatography over silica gel, eluting with hexane/EtOAc 9:1, to yield pure alkyl azidoalcohols **3a–c**. A solution of the azidoalcohol **3a** (1.00 equiv.), **3b** (1.00 equiv.), or **3c** (1.00 equiv.) in  $\text{CH}_2\text{Cl}_2$  (50 mL) was cooled to 0 °C.  $\text{Et}_3\text{N}$  (2.00 equiv.) and methanesulfonyl chloride (2.00 equiv.) was added. The reaction mixture was stirred for 24 h and then allowed to reach room temperature. The reaction mixture was poured into crushed ice (70 mL) and was then extracted with methylene chloride ( $3 \times 30$  mL). The organic layer was dried ( $\text{Na}_2\text{SO}_4$ ), filtered, and evaporated under reduced pressure. The residue obtained was purified by column chromatography over silica gel, eluting with hexane/EtOAc 9:1, to yield highly purified halo alcohol pure methanesulfonate alkylazides compounds **4a**, **4b**, and **4d**.

*General procedure for the synthesis of alkylfluoro (4c and 4e)*

To a stirred solution of 9-azidononyl methanesulfonate **4b** (1.00 equiv.) or 12-azidododecyl methanesulfonate **4d** (1.00 equiv.) in 4 mL of anhydrous DMSO was added KF (2.00 equiv.) and 18-crown-6 (2.00 equiv.). The reaction was maintained at 110 °C for 24 h. The solvent was removed under reduced pressure, and the residue was purified by column chromatography over silica gel, eluting with hexane/EtOAc 9:1, to yield pure alkylfluoro **4c** and **4e**.

**1-Azido-9-fluorononane (4c)** Yellow oil, 49 %; IR (neat)  $\nu_{\max}$  2929, 2857, 2091  $\text{cm}^{-1}$ ;  $^1\text{H}$  NMR ( $\text{CDCl}_3$ , 200 MHz):  $\delta = 1.20\text{--}1.49$  (12H, m,  $6 \times \text{CH}_2$ ), 1.52–1.81 (2H, m,  $-\text{CH}_2\text{CH}_2\text{F}$ ), 3.26 (2H, t,  $J = 6.0$  Hz,  $-\text{CH}_2\text{N}_3$ ), 4.43 (2H, td,  $J = 6.0$ , 48.0 Hz,  $-\text{CH}_2\text{F}$ ).  $^{13}\text{C}$  NMR ( $\text{CDCl}_3$ , 50 MHz):  $\delta = 25.2$  ( $-\text{CH}_2\text{CH}_2\text{N}_3$ ), 26.8 ( $-\text{CH}_2\text{CH}_2\text{F}$ ), 29.0, 29.2, 29.3, 29.5 ( $4 \times \text{CH}_2$ ), 30.6 (d,  $J = 19.0$ ,  $-\text{CH}_2\text{CH}_2\text{F}$ ), 51.6 ( $-\text{CH}_2\text{N}_3$ ), 84.3 (d,  $J = 163.0$ ,  $-\text{CH}_2\text{F}$ ).

**1-Azido-12-fluorododecane (4e)** Yellow oil, 47 %; IR (neat)  $\nu_{\max}$  2929, 2857, 2091  $\text{cm}^{-1}$ ;  $^1\text{H}$  NMR ( $\text{CDCl}_3$ , 200 MHz):  $\delta = 1.19\text{--}1.44$  (18H, m,  $9 \times \text{CH}_2$ ), 1.52–1.80 (2H, m,  $-\text{CH}_2\text{CH}_2\text{F}$ ), 3.26 (2H, t,  $J = 6.0$  Hz,  $-\text{CH}_2\text{N}_3$ ), 4.44 (2H, t,  $J = 6.0$  Hz,  $-\text{CH}_2\text{F}$ );  $^{13}\text{C}$  NMR ( $\text{CDCl}_3$ , 50 MHz):  $\delta = 25.3$  ( $-\text{CH}_2\text{CH}_2\text{N}_3$ ), 26.9 ( $-\text{CH}_2\text{CH}_2\text{F}$ ), 29.0, 29.3, 29.4, 29.7 ( $7 \times \text{CH}_2$ ), 30.6 (d,  $J = 19.5$  Hz,  $-\text{CH}_2\text{CH}_2\text{F}$ ), 51.7 ( $-\text{CH}_2\text{N}_3$ ), 84.5 (d,  $J = 156.5$  Hz,  $-\text{CH}_2\text{F}$ ).

*General procedure for the synthesis of alkyltriazoles (5a–j)*

The azide compound (**4a–e**) (1.00 equiv.) was added to a 10-mL round-bottom flask containing 1 mL of dichloromethane, 1 mL of water,  $\text{CuSO}_4 \cdot 5\text{H}_2\text{O}$  (0.08 equiv.), sodium

ascorbate (0.20 equiv.), and alkyne (pent-4-yn-1-ol, propargyl alcohol, 4-pentynoic acid, or ethyl propiolate (1.00 equiv.). The reaction mixture was vigorously stirred at room temperature for 24 h. After completion of the reaction, 5 mL of water were added, followed by extraction with dichloromethane ( $3 \times 8$  mL). The resulting organic layer was washed three times with a 25 % EDTA solution buffered with  $\text{NH}_4\text{Cl}$  at pH 9.5. The organic layer was dried with  $\text{Na}_2\text{SO}_4$  and the solvent was removed under reduced pressure. The crude product was purified by column chromatography over silica gel, eluting with dichloromethane, dichloromethane:EtOAc (8:2 v/v; 5:5 v/v; 2:8 v/v), EtOAc and EtOAc/MeOH (8:2 v/v; 5:5 v/v; 2:8 v/v), to give pure compounds **5a–j**.

**6-(4-(3-Hydroxypropyl)-1*H*-1,2,3-triazol-1-yl)hexyl methanesulfonate (5a)** Yellow oil, 46 %; IR (neat)  $\nu_{\max}$  3276, 2916, 2850, 1331, 1162, 1052–848  $\text{cm}^{-1}$ ;  $^1\text{H}$  NMR ( $\text{CDCl}_3$ , 200 MHz):  $\delta = 1.24\text{--}1.96$  (10H, m,  $5 \times \text{CH}_2$ ), 2.79 (2H, t,  $J = 6.0$  Hz,  $-\text{CH}_2\text{C}_{\text{triazole}}$ ), 2.98 (3H, s,  $-\text{CH}_3\text{SO}_2$ ), 3.66 (2H, t,  $J = 6.0$  Hz,  $-\text{CH}_2\text{N}_{\text{triazole}}$ ), 4.18 (2H, t,  $J = 6.0$  Hz,  $-\text{CH}_2\text{OH}$ ), 4.30 (2H, t,  $J = 6.0$  Hz,  $-\text{CH}_2\text{OMs}$ ), 7.33 (1H, s,  $-\text{C}=\text{CH}_{\text{triazole}}$ );  $^{13}\text{C}$  NMR ( $\text{CDCl}_3$ , 50 MHz):  $\delta = 21.5, 24.4, 25.4, 28.4, 29.6$  and 31.8 ( $6 \times \text{CH}_2$ ), 36.9 ( $-\text{CH}_3\text{SO}_2$ ), 49.6 ( $-\text{CH}_2\text{N}_{\text{triazole}}$ ), 60.8 ( $-\text{CH}_2\text{OH}$ ), 69.9 ( $-\text{CH}_2\text{OMs}$ ), 121.1 ( $-\text{C}=\text{CH}_{\text{triazole}}$ ), 147.2 ( $-\text{C}=\text{C}_{\text{triazole}}$ ); HRESIMS  $m/z$  [M+H]<sup>+</sup>: 306.1350  $\text{C}_{12}\text{H}_{24}\text{N}_3\text{O}_4\text{S}$  (calcd. 306.1487).

**6-(4-(Ethoxycarbonyl)-1*H*-1,2,3-triazol-1-yl)hexyl methanesulfonate (5b)** Yellow–white solid, 60 %; m.p. = 70–72 °C; IR (neat)  $\nu_{\max}$  2945, 2915, 2869, 1728, 1344, 1197, 1097–957, 1166, 1156, 1097, 915  $\text{cm}^{-1}$ ;  $^1\text{H}$  NMR ( $\text{CDCl}_3$ , 200 MHz):  $\delta = 1.30\text{--}1.38$  (7H, m,  $-\text{OCH}_2\text{CH}_3$  and  $2 \times \text{CH}_2$ ), 1.68 (2H, qn,  $J = 6.0$  Hz,  $-\text{CH}_2\text{CH}_2\text{N}_{\text{triazole}}$ ), 1.90 (2H, qn,  $J = 6.0$  Hz,  $-\text{CH}_2\text{CH}_2\text{OMs}$ ), 2.95 (3H, s,  $-\text{CH}_3\text{SO}_2$ ), 4.15 (2H, t,  $J = 6.0$  Hz,  $-\text{CH}_2\text{OMs}$ ), 4.26–4.42 (4H, m,  $-\text{CH}_2\text{N}_{\text{triazole}}$  and  $-\text{OCH}_2\text{CH}_3$ ), 8.08 (1H, s,  $-\text{C}=\text{CH}_{\text{triazole}}$ );  $^{13}\text{C}$  NMR ( $\text{CDCl}_3$ , 50 MHz):  $\delta = 14.2$  ( $-\text{OCH}_2\text{CH}_3$ ), 24.7, 25.6, 28.7 and 29.8 ( $4 \times \text{CH}_2$ ), 37.2 ( $-\text{CH}_3\text{SO}_2$ ), 50.3 ( $-\text{CH}_2\text{N}_{\text{triazole}}$ ), 61.1 ( $-\text{OCH}_2\text{CH}_3$ ), 69.7 ( $-\text{CH}_2\text{OMs}$ ), 127.3 ( $-\text{C}=\text{CH}_{\text{triazole}}$ ), 140.1 ( $-\text{C}=\text{C}_{\text{triazole}}$ ), 160.6 ( $-\text{CO}$ ); HRESIMS  $m/z$  [M+H]<sup>+</sup>: 320.1138  $\text{C}_{12}\text{H}_{22}\text{N}_3\text{O}_5\text{S}$  (calcd. 320.1280).

**9-(4-3-Hydroxypropyl)-1*H*-1,2,3-triazol-1-yl)nonyl methanesulfonate (5c)** White solid, 39 %; m.p. = 64–66 °C; IR (neat)  $\nu_{\max}$  3276, 2919, 2851, 1332, 1164, 1059–848  $\text{cm}^{-1}$ ;  $^1\text{H}$  NMR ( $\text{CDCl}_3$ , 200 MHz):  $\delta = 1.02\text{--}1.45$  (10H, m,  $5 \times \text{CH}_2$ ), 1.57–1.71 (m,  $-\text{CH}_2\text{CH}_2\text{N}_{\text{triazole}}$ ), 1.70–1.99 (4H, m,  $-\text{CH}_2\text{CH}_2\text{OMs}$  and  $-\text{CH}_2\text{CH}_2\text{OH}$ ), 2.76 (2H, t,  $J = 6.0$  Hz,  $-\text{CH}_2\text{C}_{\text{triazole}}$ ), 2.94 (3H, s,  $-\text{CH}_3\text{SO}_2$ ), 3.63 (2H, t,  $J = 6.0$  Hz,  $-\text{CH}_2\text{OH}$ ), 4.15 (2H, t,  $J = 6.0$  Hz,  $-\text{CH}_2\text{OMs}$ ), 4.24 (2H, t,  $J = 6.0$  Hz,  $-\text{CH}_2\text{N}_{\text{triazole}}$ ), 7.24 (1H, s,  $-\text{C}=\text{CH}_{\text{triazole}}$ );  $^{13}\text{C}$  NMR ( $\text{CDCl}_3$ , 50 MHz):  $\delta =$

21.8, 24.9, 25.9, 28.5, 28.9, 29.8 and 31.9 ( $9 \times \text{CH}_2$ ), 36.9 ( $-\text{CH}_3\text{SO}_2$ ), 49.5 ( $-\text{CH}_2-\text{N}_{\text{triazole}}$ ), 61.4 ( $-\text{CH}_2\text{OH}$ ), 70.1 ( $-\text{CH}_2\text{OMs}$ ), 120.7 ( $-\text{C}=\text{C}_{\text{triazole}}$ ), 147.4 ( $-\text{C}=\text{C}_{\text{triazole}}$ ); HRESIMS  $m/z$  [M+H]<sup>+</sup>: 348.1834 C<sub>15</sub>H<sub>30</sub>N<sub>3</sub>O<sub>4</sub>S (calcd. 348.1957).

**9-(4-(Ethoxycarbonyl)-1*H*-1,2,3-triazol-1-yl)nonyl methanesulfonate (5d)** Yellow solid, 92 %; m.p. = 72–74 °C; IR (neat)  $\nu_{\text{max}}$  2936, 2912, 2852, 1713, 1352, 1215, 1168, 1051–979 cm<sup>−1</sup>; <sup>1</sup>H NMR (CDCl<sub>3</sub>, 200 MHz):  $\delta$  = 1.14–1.33 (10H, m,  $5 \times \text{CH}_2$ ), 1.39 (2H, t,  $J$  = 6.0 Hz,  $-\text{OCH}_2\text{CH}_3$ ), 1.71 (2H, qn,  $J$  = 6.0,  $-\text{CH}_2\text{CH}_2\text{OMs}$ ), 1.81–1.99 (2H, m,  $-\text{CH}_2\text{CH}_2\text{N}_{\text{triazole}}$ ), 2.90 (3H, s,  $-\text{CH}_3\text{SO}_2$ ), 4.19 (2H, t,  $J$  = 6.0 Hz,  $-\text{CH}_2\text{OMs}$ ), 4.30–4.50 (2H, m,  $-\text{CH}_2-\text{N}_{\text{triazole}}$ ), 8.08 (1H, s,  $-\text{C}=\text{C}_{\text{triazole}}$ ); <sup>13</sup>C NMR (CDCl<sub>3</sub>, 50 MHz):  $\delta$  = 13.7 ( $-\text{OCH}_2\text{CH}_3$ ), 24.9, 26.3, 28.6, 29.0 and 29.8 ( $5 \times \text{CH}_2$ ), 37.4 ( $-\text{CH}_3\text{OMs}$ ), 49.9 ( $-\text{CH}_2-\text{N}_{\text{triazole}}$ ), 60.9 ( $-\text{OCH}_2\text{CH}_3$ ), 69.7 ( $-\text{CH}_2\text{OMs}$ ), 127.3 ( $-\text{C}=\text{C}_{\text{triazole}}$ ), 140.2 ( $-\text{C}=\text{C}_{\text{triazole}}$ ), 160.6 ( $-\text{CO}$ ); HRESIMS  $m/z$  [M+H]<sup>+</sup>: 362.1861 C<sub>15</sub>H<sub>28</sub>N<sub>3</sub>O<sub>5</sub>S (calcd. 362.1749).

**12-(4-(3-Hydroxypropyl)-1*H*-1,2,3-triazol-1-yl)dodecyl methanesulfonate (5e)** White solid, 52 %; m.p. = 80–82 °C; IR (neat)  $\nu_{\text{max}}$  3389, 2916, 2850, 1332, 1163, 1045, 956 cm<sup>−1</sup>; <sup>1</sup>H NMR (CDCl<sub>3</sub>, 200 MHz):  $\delta$  = 1.25–1.44 (16H, m,  $2 \times \text{CH}_2$ ), 1.75 (2H, qn,  $J$  = 6.0 Hz,  $-\text{CH}_2\text{CH}_2\text{OMs}$ ), 1.84–1.99 (4H,  $-\text{CH}_2\text{CH}_2\text{N}_{\text{triazole}}$  and  $-\text{CH}_2\text{CH}_2\text{OH}$ ), 2.84 (2H, t,  $J$  = 6.0 Hz,  $-\text{CH}_2-\text{C}_{\text{triazole}}$ ), 3.01 (3H, s,  $-\text{CH}_3\text{OMs}$ ), 3.71 (2H, t,  $J$  = 6.0 Hz,  $-\text{CH}_2\text{OH}$ ), 4.22 (2H, t,  $J$  = 6.0 Hz,  $-\text{CH}_2-\text{N}_{\text{triazole}}$ ), 4.31 (2H, t,  $J$  = 6.0 Hz,  $-\text{CH}_2\text{OMs}$ ), 7.74 (1H, s,  $-\text{C}=\text{C}_{\text{triazole}}$ ); <sup>13</sup>C NMR (CDCl<sub>3</sub>, 50 MHz):  $\delta$  = 21.2 ( $-\text{CH}_2(\text{CH}_2)_2\text{OMs}$ ), 24.8, 25.9, 28.5, 28.6, 28.8, 29.0, 29.8 and 31.9 ( $11 \times \text{CH}_2$ ), 35.5 ( $-\text{CH}_3\text{OMs}$ ), 49.8 ( $-\text{CH}_2-\text{N}_{\text{triazole}}$ ), 60.5 ( $-\text{CH}_2\text{OH}$ ), 70.2 ( $-\text{CH}_2\text{OMs}$ ), 121.7 ( $-\text{C}=\text{C}_{\text{triazole}}$ ), 150.1 ( $-\text{C}=\text{C}_{\text{triazole}}$ ); HRESIMS  $m/z$  [M+H]<sup>+</sup>: 390.2572 C<sub>18</sub>H<sub>34</sub>N<sub>3</sub>O<sub>5</sub>S (calcd. 390.2426).

**3-(1-(12-Methanesulfonyldodecyl)-1*H*-1,2,3-triazol-1-yl)propanoic acid (5f)** Yellow solid, 81 %; IR (neat)  $\nu_{\text{max}}$  2916, 2850, 1729, 1331, 1163, 1052–952, 850 cm<sup>−1</sup>; <sup>1</sup>H (CDCl<sub>3</sub>, 200 MHz):  $\delta$  = 1.18–1.26 (16H, m,  $8 \times \text{CH}_2$ ), 1.50–1.69 (4H, m,  $-\text{CH}_2\text{CH}_2\text{N}_{\text{triazole}}$  and  $-\text{CH}_2\text{CH}_2\text{OMs}$ ), 2.19–2.50 (4H, m,  $\text{CH}_2\text{CH}_2\text{COOH}$ ), 3.19 (2H, t,  $J$  = 6.0 Hz,  $-\text{CH}_2-\text{N}_{\text{triazole}}$ ), 4.15 (2H, t,  $J$  = 6.0 Hz,  $-\text{CH}_2\text{OMs}$ ), 7.98 (1H, s,  $-\text{C}=\text{C}_{\text{triazole}}$ ); <sup>13</sup>C NMR (CDCl<sub>3</sub>, 50 MHz):  $\delta$  = 25.3 ( $-\text{CH}_2(\text{CH}_2)_2\text{OMs}$ ), 26.6, 28.5, 28.7, 28.9, 29.0 and 29.4 ( $11 \times \text{CH}_2$ ), 33.2 ( $-\text{CH}_2\text{COOH}$ ), 37.1 ( $-\text{CH}_3\text{OMs}$ ), 51.0 ( $-\text{CH}_2-\text{N}_{\text{triazole}}$ ), 70.3 ( $-\text{CH}_2\text{OMs}$ ), 115.6 ( $-\text{C}=\text{C}_{\text{triazole}}$ ), 136.3 ( $-\text{C}=\text{C}_{\text{triazole}}$ ), 178.9 ( $-\text{CO}$ ); HRESIMS  $m/z$  [M+H]<sup>+</sup>: 404.2464 C<sub>18</sub>H<sub>34</sub>N<sub>3</sub>O<sub>5</sub>S (calcd. 404.2219).

**12-(4-(Ethoxycarbonyl)-1*H*-1,2,3-triazol-1-yl)dodecyl methanesulfonate (5g)** White solid, 93 %; m.p. = 78–80 °C; IR (neat)  $\nu_{\text{max}}$  2916, 2850, 1717, 1341, 1226, 1207, 1168, 1046–943, 848 cm<sup>−1</sup>; <sup>1</sup>H NMR (CDCl<sub>3</sub>, 200 MHz):  $\delta$  = 1.20–1.30 (16H, m,  $8 \times \text{CH}_2$ ), 1.41 (2H, t,  $J$  = 6.0 Hz,  $-\text{OCH}_2\text{CH}_3$ ), 1.74 (2H, qn,  $J$  = 6.0 Hz,  $-\text{CH}_2\text{CH}_2\text{OMs}$ ), 1.87–1.98 (2H, m,  $-\text{CH}_2\text{CH}_2\text{N}_{\text{triazole}}$ ), 2.97 (3H, s,  $-\text{CH}_3\text{OMs}$ ), 4.18 (2H, t,  $J$  = 6.0 Hz,  $-\text{CH}_2-\text{N}_{\text{triazole}}$ ), 4.39–4.45 (4H, m,  $-\text{CH}_2\text{OMs}$  and  $-\text{OCH}_2\text{CH}_3$ ), 8.05 (1H, s,  $-\text{C}=\text{C}_{\text{triazole}}$ ); <sup>13</sup>C NMR (CDCl<sub>3</sub>, 50 MHz):  $\delta$  = 14.2 ( $-\text{OCH}_2\text{CH}_3$ ), 25.2, 26.2, 29.0, 29.2, 29.5, 29.8 and 30.3 ( $8 \times \text{CH}_2$ ), 37.0 ( $-\text{CH}_3\text{OMs}$ ), 50.8 ( $-\text{CH}_2-\text{N}_{\text{triazole}}$ ), 61.5 ( $-\text{OCH}_2\text{CH}_3$ ), 70.4 ( $-\text{CH}_2\text{OMs}$ ), 127.2 ( $-\text{C}=\text{C}_{\text{triazole}}$ ), 140.1 ( $-\text{C}=\text{C}_{\text{triazole}}$ ), 160.7 ( $-\text{CO}$ ); HRESIMS  $m/z$  [M+H]<sup>+</sup>: 404.2464 C<sub>18</sub>H<sub>34</sub>N<sub>3</sub>O<sub>5</sub>S (calcd. 404.2219).

**12-(4-(Hydroxymethyl)-1*H*-1,2,3-triazol-1-yl)dodecyl methanesulfonate (5h)** Yellow solid, 56 %; m.p. = 86–88 °C; IR (neat)  $\nu_{\text{max}}$  3117, 3023, 2916, 2850, 1331, 1162, 1120, 1052–951 cm<sup>−1</sup>; <sup>1</sup>H NMR (CDCl<sub>3</sub>, 200 MHz):  $\delta$  = 1.16–1.38 (16H, m,  $8 \times \text{CH}_2$ ), 1.62–1.88 (4H, m,  $\text{CH}_2\text{CH}_2\text{OMs}$  and  $\text{CH}_2\text{CH}_2\text{N}_{\text{triazole}}$ ), 2.95 (3H, s,  $-\text{CH}_3\text{OMs}$ ), 4.16 (2H, t,  $J$  = 6.0 Hz,  $-\text{CH}_2\text{OMs}$ ), 4.27 (2H, t,  $J$  = 6.0 Hz,  $-\text{CH}_2-\text{N}_{\text{triazole}}$ ), 4.70 (2H, s,  $-\text{CH}_2\text{OH}$ ), 7.54 (1H, s,  $-\text{C}=\text{C}_{\text{triazole}}$ ); <sup>13</sup>C NMR (CDCl<sub>3</sub>, 50 MHz):  $\delta$  = 25.4, 26.3, 28.8, 28.9, 29.2, 30.1 and 31.2 ( $10 \times \text{CH}_2$ ), 37.2 ( $-\text{CH}_3\text{OMs}$ ), 50.3 ( $-\text{CH}_2-\text{N}_{\text{triazole}}$ ), 55.9 ( $-\text{CH}_2\text{OH}$ ), 70.3 ( $-\text{CH}_2\text{OMs}$ ), 121.8 ( $-\text{C}=\text{C}_{\text{triazole}}$ ), 147.8 ( $-\text{C}=\text{C}_{\text{triazole}}$ ); HRESIMS  $m/z$  [M+H]<sup>+</sup>: 362.2047 C<sub>16</sub>H<sub>32</sub>N<sub>3</sub>O<sub>4</sub>S (calcd. 362.2113).

**3-(1-(9-Fluorononyl)-1*H*-1,2,3-triazol-1-yl)propan-1-ol (5i)** White solid, 48 %; m.p. = 62–64 °C; IR (neat)  $\nu_{\text{max}}$  3312, 2913, 2848, 1050 cm<sup>−1</sup>; <sup>1</sup>H NMR (CDCl<sub>3</sub>, 200 MHz):  $\delta$  = 1.29–1.40 (10H, m,  $5 \times \text{CH}_2$ ), 1.68 (2H, qnd,  $J$  = 2.0 Hz,  $J$  = 24.0 Hz,  $-\text{CH}_2\text{CH}_2\text{F}$ ), 1.83–1.98 (4H, m,  $-\text{CH}_2\text{CH}_2\text{OH}$  and  $\text{CH}_2\text{CH}_2\text{N}_{\text{triazole}}$ ), 2.83 (2H, t,  $J$  = 8.0 Hz,  $-\text{CH}_2-\text{C}_{\text{triazole}}$ ), 3.66–3.74 (2H, m,  $-\text{CH}_2\text{OH}$ ), 4.31 (2H, t,  $J$  = 8.0 Hz,  $-\text{CH}_2-\text{N}_{\text{triazole}}$ ), 4.43 (2H, td,  $J$  = 8.0 Hz,  $J$  = 48.0 Hz,  $-\text{CH}_2\text{F}$ ), 7.54 (1H, s,  $-\text{C}=\text{C}_{\text{triazole}}$ ); <sup>13</sup>C NMR (CDCl<sub>3</sub>, 50 MHz):  $\delta$  = 21.85 ( $-\text{CH}_2(\text{CH}_2)_2\text{F}$ ), 24.9, 26.3, 28.7, 28.9, 29.0 and 30.1 ( $6 \times \text{CH}_2$ ), 30.22 (d,  $J$  = 13.5 Hz,  $-\text{CH}_2\text{F}$ ), 33.3 ( $\text{HOCH}_2\text{CH}_2-\text{C}_{\text{triazole}}$ ), 51.5 ( $-\text{CH}_2-\text{N}_{\text{triazole}}$ ), 62.8 ( $-\text{CH}_2\text{OH}$ ), 85.4 (d,  $J$  = 163.0 Hz,  $-\text{CH}_2\text{F}$ ), 122.0 ( $-\text{C}=\text{C}_{\text{triazole}}$ ), 148.0 ( $-\text{C}=\text{C}_{\text{triazole}}$ ); HRESIMS  $m/z$  [M+H]<sup>+</sup>: 272.1973 C<sub>14</sub>H<sub>27</sub>FN<sub>3</sub>O (calcd. 272.2138).

**3-(1-(12-Fluorododecyl)-1*H*-1,2,3-triazol-1-yl)propano-1-ol (5j)** White solid, 46 %; m.p. = 88–90 °C; IR (neat)  $\nu_{\text{max}}$  3321, 2917, 2846, 1006 cm<sup>−1</sup>; <sup>1</sup>H NMR (CDCl<sub>3</sub>, 200 MHz):  $\delta$  = 1.21–1.44 (16H, m,  $2 \times \text{CH}_2$ ), 1.56–2.05 (6H,  $3 \times \text{CH}_2$ ), 2.86 (2H, t,  $J$  = 6.0 Hz,  $-\text{CH}_2-\text{C}_{\text{triazole}}$ ), 3.70 (2H, t,  $J$  = 6.0 Hz,  $-\text{CH}_2\text{OH}$ ), 4.32 (2H, t,  $J$  =

6.0 Hz,  $-\text{CH}_2\text{N}$ <sub>triazole</sub>), 4.55 (2H, td,  $J = 6.0$  Hz,  $J = 46.0$  Hz,  $-\text{CH}_2\text{F}$ ), 7.34 (1H, s,  $-\text{C}=\text{CH}$ <sub>triazole</sub>);  $^{13}\text{C}$  NMR ( $\text{CDCl}_3$ , 50 MHz):  $\delta = 21.7$  ( $-\text{CH}_2(\text{CH}_2)_2\text{F}$ ), 25.2, 26.6, 29.6, 29.0 and 30.4 ( $9 \times \text{CH}_2$ ), 30.5 (d,  $J = 19.0$  Hz,  $-\text{CH}_2\text{F}$ ), 32.2 ( $\text{HOCH}_2\text{CH}_2\text{CH}_2\text{N}$ <sub>triazole</sub>), 49.8 ( $-\text{CH}_2\text{N}$ <sub>triazole</sub>), 61.1 ( $-\text{CH}_2\text{OH}$ ), 84.2 (d,  $J = 179.5$  Hz,  $-\text{CH}_2\text{F}$ ), 121.0 ( $-\text{C}=\text{CH}$ <sub>triazole</sub>), 147.3 ( $-\text{C}=\text{C}$ <sub>triazole</sub>); HRESIMS  $m/z$  [M+H]<sup>+</sup>: 314.2458  $\text{C}_{17}\text{H}_{33}\text{FN}_3\text{O}$  (calcd. 314.2608).

#### General procedure for the synthesis of **6a–d**

To a solution of compounds **5c**, **5d**, **5e**, or **5g** (1.00 equiv.) in acetone (5 mL), was added sodium iodide (2.00 equiv.). The mixture was heated at reflux for 24 h. Afterward the reaction mixture was diluted with water and extracted with dichloromethane ( $3 \times 15$  mL). The organic extracts were combined and dried ( $\text{Na}_2\text{SO}_4$ ), and the solvent was removed under reduced pressure. The residue obtained was purified by column chromatography over silica gel, eluting with mixtures of EtOAc/MeOH (100:0; 80:20, and 0:100), to give pure compounds **6a–d**.

**3-(1-(9-Iodononyl)-1*H*-1,2,3-triazol-4-yl)propan-1-ol (**6a**)** Yellow solid, 84 %; m.p. = 88–90 °C; IR (neat)  $\nu_{\max}$  3350, 2924, 2851 cm<sup>−1</sup>;  $^1\text{H}$  NMR ( $\text{CDCl}_3$ , 200 MHz):  $\delta = 1.24\text{--}1.34$  (10H, m,  $5 \times \text{CH}_2$ ), 1.74–1.94 (6H, m,  $-\text{CH}_2\text{CH}_2\text{N}$ <sub>triazole</sub>,  $-\text{CH}_2\text{CH}_2\text{OH}$  and  $-\text{CH}_2\text{CH}_2\text{I}$ ), 2.80 (2H, t,  $J = 6.0$  Hz,  $-\text{CH}_2\text{C}$ <sub>triazole</sub>), 3.17 (2H, t,  $J = 6.0$  Hz,  $-\text{CH}_2\text{I}$ ), 3.67 (2H, t,  $J = 6.0$  Hz,  $-\text{CH}_2\text{OH}$ ), 4.29 (2H, t,  $J = 6.0$  Hz,  $-\text{CH}_2\text{N}$ <sub>triazole</sub>), 7.31 (1H, s,  $-\text{C}=\text{CH}$ <sub>triazole</sub>);  $^{13}\text{C}$  NMR ( $\text{CDCl}_3$ , 50 MHz):  $\delta = 7.5$  ( $-\text{CH}_2\text{I}$ ), 22.0 ( $-\text{CH}_2(\text{CH}_2)_3\text{I}$ ), 26.6, 28.5, 29.00, 29.3, 30.4, 32.2, 33.6 (8  $\times \text{CH}_2$ ), 50.7 ( $-\text{CH}_2\text{N}$ <sub>triazole</sub>), 61.6 ( $-\text{CH}_2\text{OH}$ ), 121.0 ( $-\text{C}=\text{CH}$ <sub>triazole</sub>), 147.6 ( $-\text{C}=\text{C}$ <sub>triazole</sub>); HRESIMS  $m/z$  [M+H]<sup>+</sup>: 380.1170  $\text{C}_{14}\text{H}_{27}\text{IN}_3\text{O}$  (calcd. 380.1199).

**3-(1-(12-Iodododecyl)-1*H*-1,2,3-triazol-4-yl)propan-1-ol (**6b**)** Yellow solid, 73 %; m.p. = 84–86 °C; IR (neat)  $\nu_{\max}$  3308, 2917, 2848 cm<sup>−1</sup>;  $^1\text{H}$  NMR ( $\text{CDCl}_3$ , 200 MHz):  $\delta = 1.12\text{--}1.46$  (16H, m,  $8 \times \text{CH}_2$ ), 1.62–2.04 (6H, m,  $-\text{CH}_2\text{CH}_2\text{N}$ <sub>triazole</sub>,  $-\text{CH}_2\text{CH}_2\text{OH}$  and  $-\text{CH}_2\text{CH}_2\text{I}$ ), 2.83 (2H, t,  $J = 6.0$  Hz,  $-\text{CH}_2\text{C}$ <sub>triazole</sub>), 3.18 (2H, t,  $J = 6.0$  Hz,  $-\text{CH}_2\text{I}$ ), 3.70 (2H, t,  $J = 6.0$  Hz,  $-\text{CH}_2\text{OH}$ ), 4.30 (2H, t,  $J = 6.0$  Hz,  $-\text{CH}_2\text{N}$ <sub>triazole</sub>), 7.31 (1H, s,  $-\text{C}=\text{CH}$ <sub>triazole</sub>);  $^{13}\text{C}$  NMR ( $\text{CDCl}_3$ , 50 MHz):  $\delta = 7.34$  ( $-\text{CH}_2\text{I}$ ), 21.91 ( $-\text{CH}_2(\text{CH}_2)_3\text{I}$ ), 26.3, 28.3, 28.8, 29.2, 29.3, 30.2, 30.3, 31.9 and 34.0 ( $9 \times \text{CH}_2$ ), 49.9 ( $-\text{CH}_2\text{N}$ <sub>triazole</sub>), 61.3 ( $-\text{CH}_2\text{OH}$ ), 120.8 ( $-\text{C}=\text{CH}$ <sub>triazole</sub>), 147.4 ( $-\text{C}=\text{C}$ <sub>triazole</sub>); HRESIMS  $m/z$  [M+H]<sup>+</sup>: 422.1637  $\text{C}_{17}\text{H}_{33}\text{IN}_3\text{O}$  (calcd. 422.1668).

**Ethyl-1-(9-iodononyl)-1*H*-1,2,3-triazole-4-carboxylate (**6c**)** White solid, 97 %; m.p. = 90–92 °C; IR (neat)  $\nu_{\max}$  2919, 2848, 1723, 1216, 1197, 1164 cm<sup>−1</sup>;  $^1\text{H}$  NMR ( $\text{CDCl}_3$ , 200 MHz):  $\delta = 1.22\text{--}1.28$  (10H, m,  $5 \times \text{CH}_2$ ), 1.41 (3H, t,  $J = 6.0$  Hz,  $-\text{OCH}_2\text{CH}_3$ ), 1.71–1.96 (4H, m,  $-\text{CH}_2\text{CH}_2\text{N}$ <sub>triazole</sub> and  $-\text{CH}_2\text{CH}_2\text{I}$ ), 3.18 (2H, t,  $J = 6.0$  Hz,  $-\text{CH}_2\text{I}$ ), 4.30–4.51 (4H, m,  $-\text{CH}_2\text{N}$ <sub>triazole</sub> and  $-\text{OCH}_2\text{CH}_3$ ), 8.07 (1H, s,  $-\text{C}=\text{CH}$ <sub>triazole</sub>);  $^{13}\text{C}$  NMR ( $\text{CDCl}_3$ , 50 MHz):  $\delta = 7.37$  ( $-\text{CH}_2\text{I}$ ), 14.5 ( $-\text{OCH}_2\text{CH}_3$ ), 26.5, 28.7, 29.1, 29.6, 30.3, 30.6 and 33.3 ( $7 \times \text{CH}_2$ ), 50.6 ( $-\text{CH}_2\text{N}$ <sub>triazole</sub>), 61.8 ( $-\text{CH}_2\text{OH}$ ), 127.4 ( $-\text{C}=\text{CH}$ <sub>triazole</sub>), 140.5 ( $-\text{C}=\text{C}$ <sub>triazole</sub>), 160.8 (CO); HRESIMS  $m/z$  [M+H]<sup>+</sup>: 394.1123  $\text{C}_{14}\text{H}_{25}\text{IN}_3\text{O}_2$  (calcd. 394.0991).

**Ethyl-1-(12-iodododecyl)-1*H*-1,2,3-triazole-4-carboxylate (**6d**)** Yellow solid, 90 %; m.p. = 80–82 °C. IR (neat)  $\nu_{\max}$  2919, 2848, 1723, 1224, 1207, 1164, 777 cm<sup>−1</sup>;  $^1\text{H}$  NMR ( $\text{CDCl}_3$ , 200 MHz):  $\delta = 1.15\text{--}1.39$  (16H, m,  $8 \times \text{CH}_2$ ), 1.41 (3H, t,  $J = 6.0$  Hz,  $-\text{OCH}_2\text{CH}_3$ ), 1.81 (2H, t,  $J = 6.0$  Hz,  $-\text{CH}_2\text{CH}_2\text{I}$ ), 1.95 (2H, qn,  $J = 6.0$  Hz,  $-\text{CH}_2\text{CH}_2\text{N}$ <sub>triazole</sub>), 3.18 (2H, t,  $J = 6.0$  Hz,  $-\text{CH}_2\text{I}$ ), 4.47 (4H, m,  $-\text{CH}_2\text{N}$ <sub>triazole</sub> and  $-\text{OCH}_2\text{CH}_3$ ), 8.06 (1H, s,  $-\text{C}=\text{CH}$ <sub>triazole</sub>);  $^{13}\text{C}$  NMR (50 MHz,  $\text{CDCl}_3$ ): 6.9 ( $-\text{CH}_2\text{I}$ ), 14.3 ( $-\text{OCH}_2\text{CH}_3$ ), 26.3, 28.3, 28.8, 29.1, 30.1, 30.4 and 33.4 ( $6 \times \text{CH}_2$ ), 50.9 ( $-\text{CH}_2\text{N}$ <sub>triazole</sub>), 61.1 ( $-\text{CH}_2\text{OH}$ ), 127.2 ( $-\text{C}=\text{CH}$ <sub>triazole</sub>), 140.09 ( $-\text{C}=\text{C}$ <sub>triazole</sub>), 160.8 (CO); HRESIMS  $m/z$  [M+H]<sup>+</sup>: 436.1419  $\text{C}_{17}\text{H}_{31}\text{IN}_3\text{O}_2$  (calcd. 436.1461).

#### Biological assays

##### Cytotoxicity assay

The cytotoxicity of the compounds was assessed with the human cell lines RKO (colon carcinoma ATCC# CRL-2577), uterine carcinoma (HeLa), and lung fibroblast (WI-26VA4) cells, using the MTT (3-(4,5-dimethylthiazol-2-yl)-2,5-diphenyltetrazolium bromide) (Sigma, St. Louis, MO, USA) colorimetric method. Briefly, the cells were plated in 96-well plates (1 × 105 cells/well) and incubated for 24 h at 37 °C in a humid atmosphere with 5 % CO<sub>2</sub> to adhesion. After this period, the wells were washed with culture medium (EMEM + 10 % inactivated fetal calf serum + 2 mM L-glutamine) and incubated with the compounds at different concentrations (0.01–500 μM). Control with etoposide (Sigma-Aldrich, St. Louis, MO) used as reference anticancer drug, was performed in parallel. After the incubation, the plates were treated with MTT. The reading was performed using a SpectraMax M5e microplate reader (Molecular Devices, Sunnyvale, CA, USA) at 550 nm. Cytotoxicity was scored as the percentage reduction in absorbance versus untreated control cultures (Hilário *et al.*, 2011). All experiments were performed in triplicate. The

results were expressed as the mean of the  $IC_{50}$  (the lethal drug concentration that reduced cell viability by 50 %).

#### DNA Nick-End labeling by the TUNEL method and immunofluorescence

Apoptotic cell death was measured using the APO-BrdU TUNEL assay kit (Invitrogen, CA, USA). Briefly, the effect of the compound **5e** and etoposide on DNA fragmentation was determined using RKO cells. The cells were incubated with the compounds during 48 h as described above, and fixed using a solution of ice-cold 70 % ethanol. The cells were then counterstained with 5-Bromo-2'-deoxyuridine 5'-triphosphate (BrdUTP) in the presence of the terminal deoxynucleotidyl transferase (TdT) and stained with Anti-BrdU monoclonal antibody PRB-1 Alexa Fluor 488 conjugate, as previous described (Pereira *et al.*, 2012). The loaded cells were visualized by fluorescence microscopy using a Zeiss Axiovert 200.

#### Virtual screening

All ligands were built and optimized using GaussView (Frisch *et al.*, 2009) and Parametric Method 6 (PM6) (Stewart, 2007) implemented in Gaussian 09W (Carregal *et al.*, 2012), respectively. Next, the inverse virtual screening approach was used to identify the molecular target of each ligand present in Our Own Molecular Targets Data Bank (OOMT) (Carregal *et al.*, 2013), OOMT is a data bank with 34 molecular targets from Protein Data Bank (PDB) (Berman *et al.*, 2013), and built by comparative homology modeling, which was parameterized for screening studies by redocked of respective crystallographic ligand (Nunes *et al.*, 2013). The parameterization of OOMT includes the construction of grid box, which was

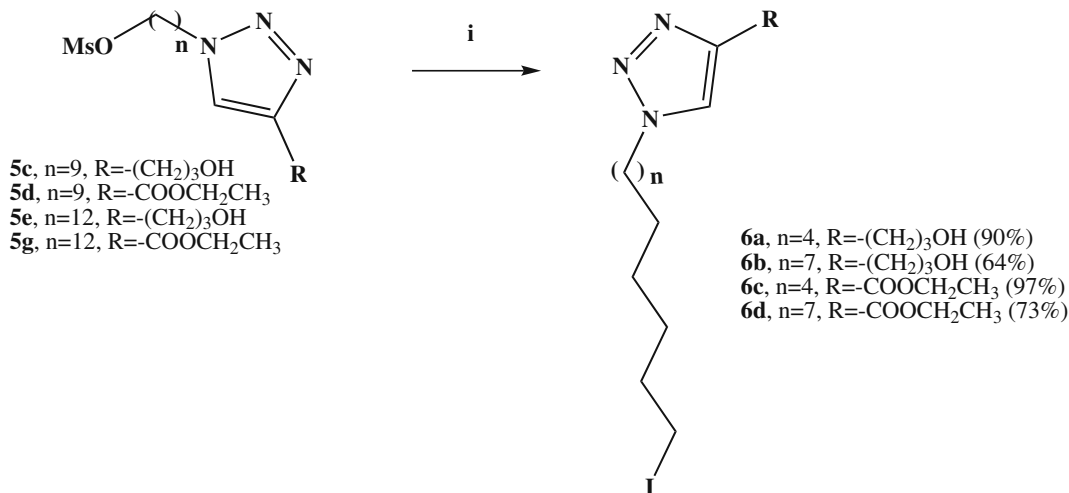
defined as a cube with the geometric center in the crystallographic ligand sufficiently to accommodate the whole binding site and with spaced points of 1 Å. Hence, all ligands were docked against molecular target using Auto-Dock Vina 1.1.2. The search algorithm used was Iterated Local Search Global Optimizer for global optimization. In this process, a succession of steps with a mutation and local optimization (the method of Broyden–Fletcher–Goldfarb–Shanno [BFGS]) were conducted, and each step followed the Metropolis criterion (Trott and Olson, 2010).

#### Statistical analysis

The average of  $IC_{50}$  was compared using Tukey's test. Differences between the values were evaluated with Origin 6.0. A *p* value of 0.05 was considered to be statistically significant.

#### Results and discussion

The synthesis of new long-chain alkyltriazole compounds is depicted in Scheme 1. The mesylate compounds (**4a–e**) were prepared using 1,6-hexanediol (**1a**), 1,9-nonanediol (**1b**), or 1,12-dodecanediol (**1c**) as starting materials (Hilário *et al.*, 2011; Chong *et al.*, 2000). These diols were converted in their monobrominated derivatives by treatment with hydrobromic acid. The haloalcohols obtained were transformed into azido alcohols by  $S_N2$  substitution. The azide compounds were transformed in their corresponding mesylates by reaction with mesyl chloride in alkaline conditions. Compounds **4b** and **4d** were treated with KF/18-crown-6 in dimethylsulfoxide to yield **4c** and **4e**. To obtain the alkyltriazoles **5a–j**, a solution of commercially available alkynes (pent-4-yn-1-ol, propargyl alcohol, 4-pentynoic acid, or



**Scheme 2** Reagents and conditions: (i) NaI, acetone, reflux, 24 h

ethyl propiolate) and alkylazides (**4a–e**) in dichloromethane was treated with a solution of copper sulfate pentahydrate (8 mol%) and sodium ascorbate (20 mol%) in water. The reaction mixture was stirred for 24 h at room temperature, exclusively producing high yields of the 1,4-disubstituted 1,2,3-triazoles (**5a–j**).

We synthesized four additional novel long-chain alkyltriazoles that contained an iodine atom (Scheme 2).

All synthesized compounds were evaluated in vitro for their anticancer potential against two human cancer cell lines (colon carcinoma RKO and uterine carcinoma HeLa). The compounds were also tested on a non-cancerous human cell line (lung fibroblast WI-26VA4) to determine the selectivity index. Colorimetric MTT assays determined that compounds **5e** and **6a** presented potent antitumor activity in vitro (Table 1). Against RKO cells, compounds **5e** and **6a** showed IC<sub>50</sub> values of 16.70 and 14.57 μM, respectively. These same compounds presented similar IC<sub>50</sub> values (11.05 and 12.77 μM, respectively) against the HeLa cell line. The cytotoxicity of compounds **5e** and **6a** was comparable to that of etoposide, an anticancer agent (Correale *et al.*, 2011).

The physicochemical properties of miltefosine and all the alkyltriazole compounds synthesized in this study are shown in Table 2. All new alkyltriazoles showed a desirable profile for an oral drug (Leeson and Springthorpe, 2007). Based on IC<sub>50</sub> values and physicochemical properties, one of the most

active compounds, i.e., **5e**, was selected for further investigation of its cytotoxic mode of action.

Apoptosis via cytotoxicity is considered an efficient strategy for the identification of potential antitumor drugs

**Table 2** Physicochemical properties of miltefosine and the alkyltriazole compounds **5a–j** and **6a–d**

Compounds	cLog P	MW	HBD	HBA
Miltefosine	6.0	407.56	0	4
<b>5a</b>	0.59	305.39	1	4
<b>5b</b>	1.24	319.37	0	5
<b>5c</b>	1.67	347.47	1	4
<b>5d</b>	2.32	361.45	0	5
<b>5e</b>	2.74	389.55	1	4
<b>5f</b>	2.36	403.53	1	5
<b>5g</b>	3.57	403.53	0	5
<b>5h</b>	2.12	361.5	1	4
<b>5i</b>	2.70	271.37	1	2
<b>5j</b>	3.77	313.45	1	2
<b>6a</b>	3.37	379.28	1	1
<b>6b</b>	4.45	421.36	1	1
<b>6c</b>	3.86	393.26	0	2
<b>6d</b>	4.93	435.34	0	2

MW molecular weight, HDB hydrogen-bond donors, HBA hydrogen-bond acceptors

**Table 1** In vitro cytotoxic activity of the alkyltriazole compounds against human colon carcinoma (RKO) cells, uterine carcinoma (HeLa) cells, and lung fibroblast (WI-26VA4) cells

Compounds	IC <sub>50</sub> (μM) ± SD <sup>a</sup>			SI	
	HeLa	RKO	WI	WI/HeLa	WI/RKO
Miltefosine	13.80 ± 4.2	>100	ND	ND	ND
<b>5a</b>	210.10 ± 5.18	397.90 ± 6.54	489.15 ± 4.02	2.33	1.23
<b>5b</b>	202.18 ± 0.31	198.23 ± 18.02	339.34 ± 27.86	1.67	1.71
<b>5c</b>	24.48 ± 5.20	182.03 ± 28.4	ND	ND	ND
<b>5d</b>	37.10 ± 3.90	20.49 ± 5.80	ND	ND	ND
<b>5e</b>	11.05 ± 3.70	16.70 ± 3.40	ND	ND	ND
<b>5f</b>	35.95 ± 7.38	99.94 ± 0.89	39.45 ± 10.42	1.09	0.39
<b>5g</b>	208.17 ± 25.12	180.16 ± 5.92	490.41 ± 4.03	2.35	2.72
<b>5h</b>	21.87 ± 0.78	19.87 ± 4.22	36.54 ± 3.21	1.67	1.84
<b>5i</b>	84.25 ± 9.92	307.21 ± 8.77	184.43 ± 1.51	2.19	0.60
<b>5j</b>	25.82 ± 9.19	90.82 ± 0.83	80.48 ± 12.66	3.11	1.13
<b>6a</b>	12.77 ± 1.16	14.57 ± 2.18	21.40 ± 3.36	1.67	1.47
<b>6b</b>	145.33 ± 13.22	138.16 ± 10.10	27.68 ± 4.08	0.19	0.20
<b>6c</b>	52.22 ± 12.74	199.01 ± 26.30	253.82 ± 59.95	4.87	2.27
<b>6d</b>	26.61 ± 2.20	62.23 ± 2.55	71.84 ± 14.10	2.70	1.15
Etoposide	11.35 ± 2.73	10.66 ± 2.23	4.30 ± 1.34	0.39	0.40

ND not determined, SI selectivity index

<sup>a</sup> Values are average ± Standard Deviation

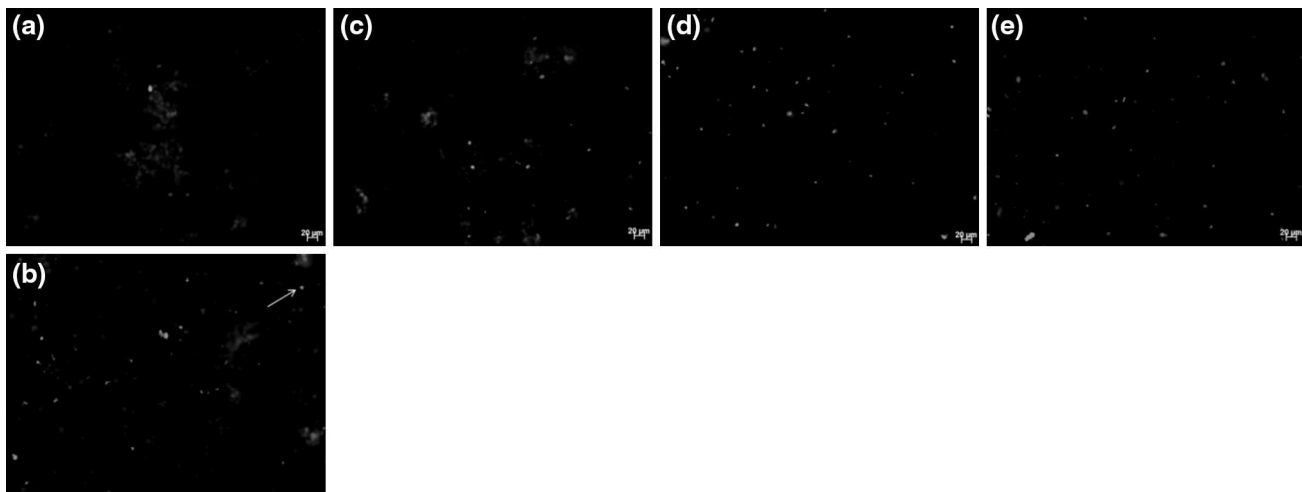


**Fig. 2** Apoptosis in human colon carcinoma (RKO) cells. Cells were incubated (48 h) with compound **5e** in different concentrations. (a) control of life, (b) etoposide at 1  $\mu$ M, and **5e** 1  $\mu$ M, (d) 10  $\mu$ M,

and (e) 100  $\mu$ M. The arrow indicates cell death by apoptosis (green). Viable cells are stained red. Scale bar: 20  $\mu$ m (Color figure online)

(Essack *et al.*, 2011). To investigate the possible apoptosis-inducing action of these compounds, specific DNA fragments on RKO cells were detected by a TUNEL assay using compound **5e** and etoposide, an apoptosis-inducing drug (Liu *et al.*, 2011). The results presented here indicate that compound **5e** promoted apoptosis in RKO cells (Fig. 2), reducing the number of viable cells in a concentration-dependent manner (Fig. 2a–e). The mechanism by which long-chain APLs trigger apoptosis is, as yet, unclear.

APLs interact with signaling proteins, membrane lipids, or lipid microdomains (Strassheim *et al.*, 2000; Samadder *et al.*, 2003; Kondapaka *et al.*, 2003). The ability of cells to proliferate or initiate apoptosis relies on signaling pathways that produce anti- or pro-apoptotic signals (Ruiter *et al.*, 1999; Dineva *et al.*, 2012). Anti-apoptotic pathways can comprise the Ras–Raf–MAPK/ERK proliferative pathway (Ruiter *et al.*, 2002). Other targets, such as transmembrane proteins, are also involved in the apoptosis process. In this context, galectins (galactoside-binding glycoproteins) were shown to modulate many functions in cell survival, including proliferation and metastasis (Vladouli *et al.*, 2014). In an attempt to understand the mode of action of the compounds synthesized in this work, we performed a virtual screening against 34 potential antitumor targets. All synthesized compounds exhibited the best docking scores against galectin-1 (PDB: 1W6M) and ERK1 (PDB: 2ZOQ) (Table 3). The compound **5e**, an apoptosis inducer, showed a better binding energy for galectin-1 ( $-4.4 \text{ kcal mol}^{-1}$ ) and ERK-1 ( $-6.2 \text{ kcal mol}^{-1}$ ) than miltefosine, used as reference compound. Figure 3 shows 3D and 2D diagrams of the intermolecular interactions between **5e** and galectin-1 and ERK1.

**Table 3** Docking results between miltefosine and alkyltriazoles alkyltriazole compounds **5a–j** and **6a–d** against the molecular targets Galectin-1 and ERK1 carried out by Autodock Vina

Compounds	Binding Energy ( $\text{kcal mol}^{-1}$ )	
	Galectin-1 (PDB: 1W6M)	ERK1 (PDB: 2ZOQ)
Miltefosine	-3.3	-5.7
<b>5a</b>	-4.3	-5.7
<b>5b</b>	-4.4	-6.0
<b>5c</b>	-4.4	-6.2
<b>5d</b>	-4.5	-6.0
<b>5e</b>	-4.1	-5.7
<b>5f</b>	-3.7	-5.6
<b>5g</b>	-3.8	-5.7
<b>5h</b>	-4.0	-6.2
<b>5i</b>	-4.7	-6.4
<b>5j</b>	-4.5	-6.3
<b>6a</b>	-4.7	-5.9
<b>6b</b>	-4.5	-6.3
<b>6c</b>	-4.0	-6.1
<b>6d</b>	-4.7	-5.9

## Conclusions

In conclusion, this preliminary investigation demonstrates that very simple long-chain alkyltriazoles may be a promising class of substances with cytotoxic activity, and that this activity can be modified significantly by classical chemical modifications. Among the synthesized compounds, **5e** was the most active, could represent a promising template for developing a new class of antitumor

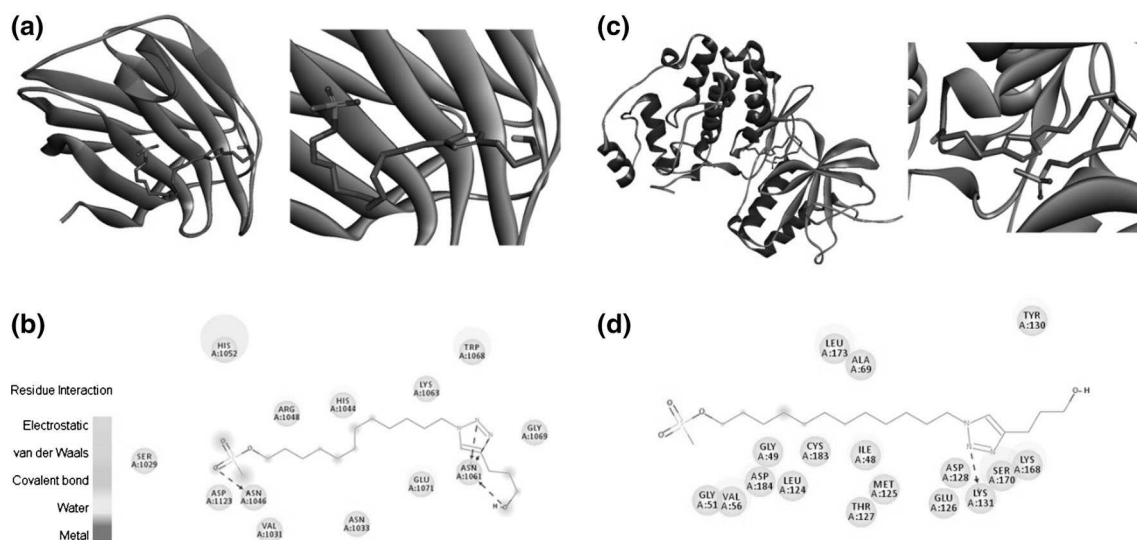


**Fig. 3** 3D and 2D diagrams of the intermolecular interactions between **5e** and galectin-1 and ERK1. **a** 3D diagram of **5e** and galectin-1 (PDB: 1W6M). **b** Intermolecular interactions between **5e** and galectin-1 (PDB: 1W6M): electrostatic interactions, hydrogen bonds (ASN A:1046), and van der Waals interactions (ASP A:1123) with the mesyl group. The triazole ring and hydroxyl group form

electrostatic interactions and hydrogen bonds (ASN A:1061). **c** 3D diagram of **5e** and ERK1 (PDB: 2Z0Q). **d** Intermolecular interactions between **5e** and ERK1 (PDB: 2Z0Q): the triazole ring forms electrostatic interactions and hydrogen bonds (LYS A:131), electrostatic interactions (SER A:170 e LYS A:168), and van der Waals interactions (ASP A:128)

agents, and deserves further investigation of derived scaffolds.

**Acknowledgments** The authors thank Fundação de Amparo a Pesquisa do Estado de Minas Gerais (FAPEMIG) and Conselho Nacional de Desenvolvimento Científico e Tecnológico (CNPq) for financial support. We further thank Pró-Reitoria de Pesquisa (UFMG) for the financial aid to publish the results.

## References

- Aher NG, Pore VS, Mishra NN, Kumar A, Shukla PK, Sharma A, Bhat MK (2009) Synthesis and antifungal activity of 1,2,3-triazole containing fluconazole analogues. *Bioorg Med Chem Lett* 19:759–763
- Alam MDM, Eun-Ha Joh, Park H, Kim B, Dong-Hyun Kim, Lee YS (2013) Synthesis, characterization and Akt phosphorylation inhibitory activity of cyclopentanecarboxylate-substituted alkylphosphocholines. *Bioorg Med Chem Lett* 21:2018–2024
- Amblard F, Cho JH, Schinazi RF (2009) Cu(I)-catalyzed huisgen azide-alkyne 1,3-dipolar cycloaddition reaction in nucleoside, nucleotide, and oligonucleotide chemistry. *Chem Rev* 109: 4207–4220
- Berman HM, Kleywegt GJ, Nakamura H, Markley JL (2013) The future of the protein data bank. *Biopolymers* 99(3):218–222
- Blitterswijk WJV, Verheij M (2012) Anticancer mechanisms and clinical application of alkylphospholipids. *Biochim Biophys Acta* 1831:663–674
- Buckle DR, Outred DJ, Rockell CJM, Smith H, Spicer BA (1983) Studies on v-triazoles. 7. Antiallergic 9-oxo-1*H*,9*H*-benzopyrano[2,3-*d*]-v-triazoles. *J Med Chem* 26:251–254
- Carregal AP, Comar M, Alves SN, De Siqueira JM, Lima LA, Taranto AG (2012) Inverse virtual screening studies of selected natural compounds from cerrado. *Int J Quantum Chem* 112(20):3333–3340
- Carregal AP, JrM Comar, Taranto AG (2013) Our Own Molecular Targets Data Bank (OOMT). *Biochem Biotechnol Rep* 2(2): 14–16
- Chong JM, Heuft MA, Rabbat F (2000) Solvent effects on the monobromination of  $\alpha,\omega$ -diols: a convenient preparation of  $\omega$ -bromoalkanols. *J Org Chem* 65:5837–5838
- Correale P, Botta C, Basile A, Pagliuchi M, Licchetta A, Martellucci I, Bestoso E, Apollinari S, Addeo R, Misso G, Romano O, Abbruzzese A, Lamberti M, Luzzi L, Gotti G, Rotundo MS, Caraglia M, Tagliaferri P (2011) Phase II trial of bevacizumab and dose/dense chemotherapy with cisplatin and metronomic daily oral etoposide in advanced non-small-cell-lung cancer patients. *Can Biol Ther* 2:112–118
- Costa MS, Boechat N, Rangel EA, Silva FDCC, Souza AMTD, Rodrigues CR, Castro HC, Junior IN, Lourenç MCS, Wardell SMSV, Ferreira VF (2006) Synthesis, tuberculosis inhibitory activity, and SAR study of *N*-substituted-phenyl-1,2,3-triazole derivatives. *Bioorg Med Chem* 14:8644–8653
- Deiters A, Cropp TA, Mukherji M, Chin JW, Anderson JC, Schultz PG (2003) Adding amino acids with novel reactivity to the genetic code of *Saccharomyces cerevisiae*. *J Am Chem Soc* 125:11782–11783
- Demaray JA, Thuner JE, Dawson MN, Scheck SJ (2008) Synthesis of triazole-oxazolidinones via a one-pot reaction and evaluation of their antimicrobial activity. *Bioorg Med Chem Lett* 18:4868–4871
- Dineva IK, Zaharieva MM, Konstantinov SM, Eibl H, Berger MR (2012) Erafosine suppresses breast cancer in vitro and in vivo for its activity on PI3K, c-Raf and Akt proteins. *J Cancer Res Clin Oncol* 138:1909–1917
- Dirks AJT, Van Berkel SS, Hatzakis NS, Opsteen JA, van Delft FL, Cornelissen JJLM, Rowan AE, van Hest JCM, Rutjes FPJT, Nolte RJM (2005) Preparation of biohybrid amphiphiles via the copper catalysed Huisgen [3+2] dipolar cycloaddition reaction. *Chem Commun* 33:4172

- Essack M, Bajic V, Archer JAC (2011) Recently confirmed apoptosis-inducing lead compounds isolated from marine sponge of potential relevance in cancer treatment. *Mar Drugs* 9:1580–1606
- Frisch MJ, Trucks GW, Schlegel HB, Scuseria GE, Robb MA, Cheeseman JR, Scalmani G, Barone V, Mennucci B, Petersson GA, Nakatsuji H, Caricato M, Li X, Hratchian HP, Izmaylov AF, Bloino J, Zheng G, Sonnenberg JL, Hada M, Ehara M, Toyota K, Fukuda R, Hasegawa J, Ishida M, Nakajima T, Honda Y, Kitao O, Nakai H, Vreven T, Montgomery JA Jr, Peralta JE, Ogliaro F, Bearpark M, Heyd JJ, Brothers E, Kudin KN, Staroverov VN, Kobayashi R, Normand J, Raghavachari K, Rendell A, Burant JC, Iyengar SS, Tomasi J, Cossi M, Rega N, Millam NJ, Klene M, Knox JE, Cross JB, Bakken V, Adamo C, Jaramillo J, Gomperts R, Stratmann RE, Yazyev O, Austin AJ, Cammi R, Pomelli C, Ochterski JW, Martin RL, Morokuma K, Zakrzewski VG, Voth GA, Salvador P, Dannenberg JJ, Dapprich S, Daniels AD, Farkas Ö, Foresman JB, Ortiz JV, Cioslowski J, Fox DJ (2009) Gaussian 09, Revision D.01. Gaussian, Inc., Wallingford
- Giffin MJ, Heaslet H, Brik A, Lin YC, Cauvi G, Wong CH, McRee DE, Elder JH, Stout CD, Torbett EB (2008) AB2, an azide-alkyne click compound, is a potent inhibitor of a multidrug-resistant mutant protease arising from protease inhibitor selection. *J Med Chem* 51:6263–6270
- Hilário FF, de Paula RC, Silveira ML, Viana GHR, Alves RB, Pereira JR, Silva LM, Freitas RP, Varotti FP (2011) Synthesis and evaluation of antimalarial activity of oxygenated 3-alkylpyridine marine alkaloid analogues. *Chem Biol Drug Des* 78:477–482
- Huisgen R (1961) Centenary lecture-1,3 dipolar cycloadditions. *Proceed Chem Soc* 6:357–369
- Kolb HC, Finn MG, Sharpless KB (2001) Click chemistry: diverse chemical function from a few good reactions. *Angew Chem Int Ed* 40:2004
- Kondapaka SB, Singh SS, Dasmahapatra GP, Sausville EA, Roy KK (2003) Perifosine, a novel alkylphospholipid, inhibits protein kinase B activation. *Mol Cancer Ther* 2:1093–1103
- Kosiova I, Kovackova S, Kois P (2007) Synthesis of coumarin-nucleoside conjugates via Huisgen 1,3-dipolar cycloaddition. *Tetrahedron* 63:312–320
- Kurumurthy C, Veeraswamy B, Rao PS, Kumar GS, Rao PS, Reddy VL, Rao JV, Narasaiah B (2014) Synthesis of novel 1,2,3-triazole tagged pyrazolo[3,4-*b*]pyridine derivatives and their cytotoxic activity. *Bioorg Med Chem Lett* 24:746–749
- Leeson PD, Springthorpe B (2007) The influence of drug-like concepts on decision-making in medicinal chemistry. *Nat Rev Drug Discov* 6:881–890
- Liu J, Uematsu H, Tsuchida N, Ikeda MA (2011) Essential role of caspase-8 in p53/p73-dependent apoptosis induced by etoposide in head and neck carcinoma cells. *Molecular Cancer* 10:95
- Meldal M, Tornoe CW (2008) Cu-catalyzed azide–alkyne cycloaddition. *Chem Rev* 108:2952–3015
- Nunes RR, Fonseca AL, Alves RJ, Comar M Jr, Taranto AG (2013) Validação In silico do transportador de hexose do *Plasmodium falciparum* (Pfht). *Reports* 2(2):108–110
- Patpi SR, Pulipati L, Yogeeshwari P, Sriram D, Jain N, Sridhar B, Murthy R, Anjana DT, Kalivendi SV, Kantevari S (2012) Design, synthesis, and structure-activity correlations of novel dibenzo[*b,d*]furan, dibenzo[*b,d*]thiophene, and *N*-methylcarbazole clubbed 1,2,3-triazoles as potent inhibitors of *Mycobacterium tuberculosis*. *J Med Chem* 55:3911–3922
- Pereira JRCS, Hilário FF, Lima AB, Silveira MLT, Silva LM, Alves RB, de Freitas RP, Varotti FP, Viana GHR (2012) Cytotoxicity evaluation of marine alkaloid analogues of viscosaline and theonelladin C. *Biomed Prev Nutr* 2:145–148
- Praveena KSS, Durgadas S, Suresh N, Akkenapally S, Kumar CG, Deora GS, Murthy NYS, Mukkanti K, Pal S (2014) Synthesis of 2,2,4-trimethyl-1,2-dihydroquinolinyl substituted 1,2,3-triazole derivatives: their evaluation as potential PDE 4B inhibitors possessing cytotoxic properties against cancer cells. *Bioorg Chem* 53:8–14
- Rakotomanga M, Blanc S, Gaudin K, Chaminade P, Loiseau PM (2007) Miltefosine affects lipid metabolism in *Leishmania donovani* Promastigotes. *Antimicrob Agents Chemother* 51:1425–1430
- Rostovtsev VV, Green LG, Fokin VV, Sharpless BK (2002) A stepwise huisgen cycloaddition process: copper(I)-catalyzed regioselective ligation of azides and terminal alkynes. *Vsevolod V. Rostovtsev, Luke G. Green, Valery V. Fokin, K. Barry Sharpless. Angew Chem Int Ed* 41:2596
- Ruiter GA, Zerp SF, Bartelink H, Blitterswijk WJ, Verheij M (1999) Alkyl-lysophospholipids activate the SAPK/JNK pathway and enhance radiation-induced apoptosis. *Cancer Res* 59:2457–2463
- Ruiter GA, Verheij M, Zerp SF, Moolenaar WH, Blitterswijk WJ (2002) Submicromolar doses of alkyl-lysophospholipids induce rapid internalization, but not activation, of epidermal growth factor receptor and concomitant MAPK/ERK activation Inn A431 cells. *Int J Cancer* 102:343–350
- Samadder P, Richards C, Bittman R, Bhullar RP, Arthur G (2003) Synthesis and use of novel ether phospholipids enantiomers to probe the molecular basis of the antitumor effects of alkyllyso-phospholipids: differential activation of c-Jun NH2-terminal protein kinase in neuronal tumor cells. *Anticancer Res* 23:2291–2295
- Santos FC, Cunha AC, Souza MCBV, Tomé AC, Neves MGPMS, Ferreira VF, Cavaleiro JAS (2008) Synthesis of porphyrin-quinolone conjugates. *Tetrahedron Lett* 49:7268
- Simone R, Chini MG, Bruno I, Riccio R, Mueller D, Werz O, Bifulco G (2011) Structure-based discovery of inhibitors of microsomal prostaglandin E2 synthase-1,5-lipoxygenase and 5-lipoxygenase-activating protein: promising hits for the development of new anti-inflammatory agents. *J Med Chem* 54:1565–1575
- Stewart JJP (2007) Optimization of parameters for semiempirical methods V: Modification of NDDO approximations and application to 70 elements. *J Mol Model* 13(12):1173–1213
- Strassheim D, Shafer SH, Phelps SH, Williams CL (2000) Small cell lung carcinoma exhibits greater phospholipase C-β1 expression and edelfosine resistance compared with non-small cell lung carcinoma. *Cancer Res* 60:2730–2736
- Struthers H, Viertl D, Kosinski M, Spangler B, Buchegger F, Schibli R (2010) Metal chelating systems synthesized using the copper(I) catalyzed azide–alkyne cycloaddition. *Dalton Trans* 39:675–696
- Tornøe CW, Christensen C, Meldal M (2002) Peptidotriazoles on solid phase: [1,2,3]-triazoles by regiospecific copper(I)-catalyzed 1,3-dipolar cycloadditions of terminal alkynes to azides. *J Org Chem* 67(9):3057–3064
- Trott O, Olson AJ (2010) AutoDock Vina: improving the speed and accuracy of docking with a new scoring function, efficient optimization, and multithreading. *J Comput Chem* 31:455–461
- Ungera C, Eibl H (1991) Hexadecylphosphocholine: preclinical and the first clinical results of a new antitumor drug. *Lipids* 26(12):1412–1417
- Van der Luit AH, Vink SR, Klarenbeek JB, Perrissoud D, Solary E, Verheij M, Van Blitterswijk W (2007) A new class of anticancer alkylphospholipids uses lipid rafts as membrane gateways to induce apoptosis in lymphoma cells. *J Mol Cancer Ther* 6:2337
- Vink SR, van Blitterswijk WJ, Schellens JHM, Verheij M (2007) Rationale and clinical application of alkylphospholipid analogues in combination with radiotherapy. *Cancer Treat Rev* 33:191
- Vladoiu MC, Labrie M, St-Pierre Y (2014) Intracellular galectins in cancer cells: potential new targets for therapy (Review). *Int J Oncol* 21:1001–1014

- Wang Q, Chan TR, Hilgraf R, Fokin VV, Sharpless KB, Finn MG (2003) Bioconjugation by copper(I)-catalyzed azide–alkyne [3+2] cycloaddition. *J Am Chem Soc* 125:3192–3193
- Wang XL, Wan K, Zhou CH (2010) Synthesis of novel sulfanilamide-derived 1,2,3-triazoles and their evaluation for antibacterial and antifungal activities. *Eur J Med Chem* 45:4631–4639
- Whiting M, Tripp JC, Lin YC, Lindstrom W, Olson AJ, Elder JH, Sharpless K, Fokin VV (2006) Rapid discovery and structure–activity profiling of novel inhibitors of human immunodeficiency virus type 1 protease enabled by the copper(I)-catalyzed synthesis of 1,2,3-triazoles and their further functionalization. *J Med Chem* 49:7697–7710
- Wieder T, Orfanos CE, Geilen CC (1998) Induction of ceramide-mediated apoptosis by the anticancer phospholipid analog, hexadecylphosphocholine. *J Chem Biol* 273:11025–11031

## Efficacy of the Triazole SCH 56592 against *Leishmania amazonensis* and *Leishmania donovani* in Experimental Murine Cutaneous and Visceral Leishmaniasis

HAIL M. AL-ABDELY,<sup>1,2\*</sup> JOHN R. GRAYBILL,<sup>1,2</sup> DAVID LOEBENBERG,<sup>3</sup> AND PETER C. MELBY<sup>1,2</sup>

*Medical Service, Audie Murphy Veterans Administration Hospital,<sup>1</sup> and Division of Infectious Diseases, Department of Medicine, The University of Texas Health Science Center at San Antonio,<sup>2</sup> San Antonio, Texas 78284, and Schering-Plough Research Institute, Kenilworth, New Jersey 07833<sup>3</sup>*

Received 18 May 1999/Returned for modification 29 June 1999/Accepted 1 October 1999

**Current therapy for leishmaniasis is unsatisfactory. Efficacious and safe oral therapy would be ideal. We examined the efficacy of SCH 56592, an investigational triazole antifungal agent, against cutaneous infection with *Leishmania amazonensis* and visceral infection with *Leishmania donovani* in BALB/c mice. Mice were infected in the ear pinna and tail with *L. amazonensis* promastigotes and were treated with oral SCH 56592 or intraperitoneal amphotericin B for 21 days. At doses of 60 and 30 mg/kg/day, SCH 56592 was highly efficacious in treating cutaneous disease, and at a dose of 60 mg/kg/day, it was superior to amphotericin B at a dose of 1 mg/kg/day. The means of tail lesion sizes were  $0.32 \pm 0.12$ ,  $0.11 \pm 0.06$ ,  $0.17 \pm 0.07$ , and  $0.19 \pm 0.08$  mm for controls, SCH 56592 at 60 and 30 mg/kg/day, and amphotericin B recipients, respectively ( $P = 0.0003$ ,  $0.005$ , and  $0.01$ , respectively). Parasite burden in draining lymph nodes confirmed these efficacy findings. In visceral leishmaniasis due to *L. donovani* infection, mice treated with SCH 56592 showed a 0.5- to 1-log-unit reduction in parasite burdens in the liver and the spleen compared to untreated mice. Amphotericin B at 1 mg/kg/day was superior to SCH 56592 in the treatment of visceral infection, with a 2-log-unit reduction in parasite burdens in both the liver and spleen. These studies indicate very good activity of SCH 56592 against cutaneous leishmaniasis due to *L. amazonensis* infection and, to a lesser degree, against visceral leishmaniasis due to *L. donovani* infection in susceptible BALB/c mice.**

The protozoa of the genus *Leishmania*, which are distributed throughout the world, are the cause of various clinical syndromes. Visceral leishmaniasis (VL) is usually fatal if untreated (3). Cutaneous leishmaniasis (CL) can be associated with significant morbidity and occasional deforming scars. Pentavalent antimonial compounds (sodium stibogluconate and meglumine antimoniate) have been the drugs of first choice for decades for the treatment of these disorders. These drugs are parenteral and associated with significant side effects (14). Pentamidine and amphotericin B are other parenteral alternatives that may cause significant side effects, such as renal toxicity and pancreatitis (7). Antimonial compounds are also associated with significant failure and relapse rates, especially in immunocompromised hosts (2, 9, 13).

The search for safe and efficacious oral therapy has been ongoing for more than 2 decades. The azole antifungals ketoconazole and itraconazole have been used to treat cutaneous leishmaniasis with variable success rates (5, 6, 10). There have been conflicting reports of the success and failure of azoles in the treatment of VL (8, 12). Imidazole and triazole antifungals (Fig. 1) inhibit C-14 demethylation of lanosterol, which interferes with the production of leishmanial ergosterol, an essential component of their membrane structure (4).

SCH 56592 (Schering-Plough Research Institute, Kenilworth, N.J.) is an investigational triazole with broad-spectrum antifungal activity (Fig. 1) (11). We tested the activity of SCH

56592 against *Leishmania* promastigotes in vitro and against experimental CL caused by *Leishmania amazonensis* infection and VL caused by *Leishmania donovani* infection.

### MATERIALS AND METHODS

**Parasites.** *L. donovani* 1S (MHOM/SD/001S-2D) and *L. amazonensis* JOSEPHA were used for the in vitro and in vivo studies. *Leishmania major* KK, *L. mexicana* 68 and 390 (gifts from F. Andrade Narvaez, Merida, Mexico), and *Leishmania panamensis* LS94 and L334 (gifts from B. Travi, CI-DEIM, Cali, Colombia) were included in the in vitro testing. Parasites, in stationary phase, were washed in phosphate-buffered saline, were counted, and were resuspended in phosphate-buffered saline at the appropriate concentration prior to infection.

**Animals.** Age-matched 4- to 6-week-old female inbred BALB/c *nu/+* mice (Veterinary Medical Unit breeding colony of the Audie Murphy Veterans Administration Hospital, San Antonio, Tex.) were used in the *L. donovani* infections. Male BALB/c *nu/+* mice were used in the *L. amazonensis* study. Ten (*L. amazonensis* study) or 16 (*L. donovani* study) mice were included in each treatment or control group and were housed in populations of up to five per cage with free access to water and food.

**Drugs.** SCH 56592 is an investigational triazole antifungal provided by Schering-Plough Research Institute. The drug was reconstituted from powder in 0.3% Noble agar and was given in 0.2-ml volumes orally by gavage. Amphotericin B was purchased commercially (Bristol-Myers Squibb, Princeton, N.J.) and was injected intraperitoneally in 0.2-ml doses.

**In vitro susceptibility.** In vitro testing of *Leishmania* promastigotes was performed as described previously (1). In brief, *Leishmania* promastigotes were maintained in Grace's insect culture media and were harvested and counted with a hemacytometer. Promastigotes ( $5 \times 10^6$ /ml) were incubated at 26°C in 250 µl of medium per well containing twofold dilutions of each drug (0.125 to 8 µg/ml for amphotericin B and 0.25 to 32 µg/ml for SCH 56592 and fluconazole) and control media in microwell plates. The minimum protozoacidal concentration (MPC), as assessed by flagellar motility under indirect microscopy, was defined as the lowest concentration that reduced the number of viable promastigotes with respect to simultaneously growing controls by >90% after 18 h of incubation with the drug. In a few experiments, parasite death was also assessed by a [<sup>3</sup>H]thymidine incorporation assay.

***L. amazonensis* study.** Five groups of 10 male inbred BALB/c *nu/+* mice were selected randomly to receive SCH 56592 at doses of 60, 30, and 15 mg/kg orally;

\* Corresponding author. Present address: Division of Infectious Diseases, Department of Medicine (MBC 46), King Faisal Specialist Hospital and Research Center, P.O. Box 3354, Riyadh 11211, Saudi Arabia. Phone: (966) 1-442-7494. Fax: (966) 1-442-7499. E-mail: abdely@kfshrc.edu.sa.

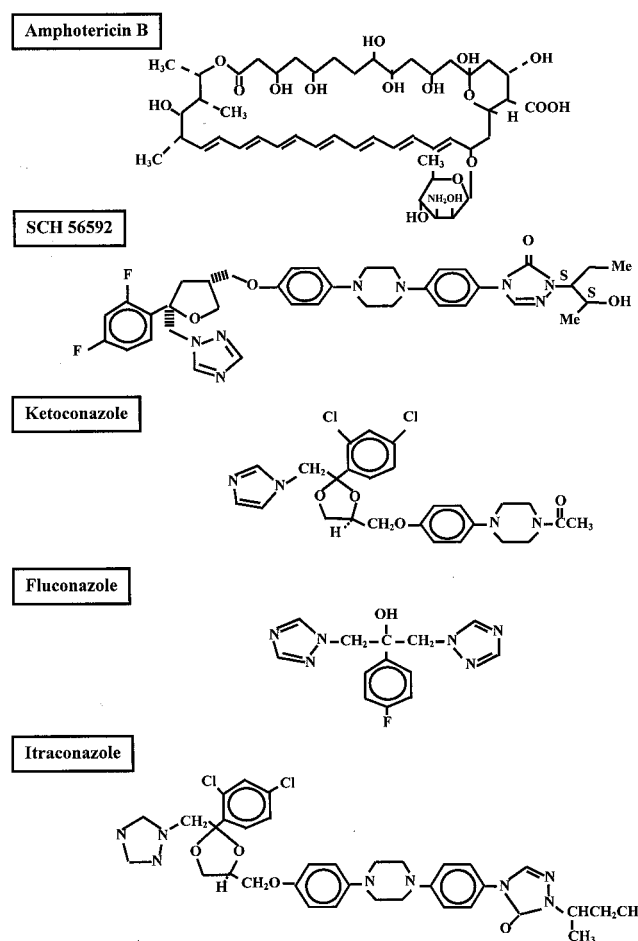


FIG. 1. Chemical structure of amphotericin B, SCH 56592, and other currently available azoles.

to receive amphotericin B at a dose of 1 mg/kg intraperitoneally; or to receive 0.3% Noble agar orally. Mice were injected with  $10^3$  promastigotes of *L. amazonensis* in a 0.01-ml volume into the right ear pinna and  $10^5$  promastigotes of *L. amazonensis* in a 0.02-ml volume injected subcutaneously into the proximal third of the tail. Treatments were started on the third day postinfection and were continued for 21 days. Measurements of ear pinna thickness and tail lesion thickness, using a fine scale (Fowler Precision Tools, Lux Scientific Instrument Corp., New York, N.Y.), were taken on the 4th day postinfection, and these measurements were taken weekly for the following 6 weeks. Lesion size was considered as the difference between the thickness of the infected ear pinna and uninfected ear pinna. The size of the tail lesion was obtained by subtracting the average measurement of tail diameter at points just rostral and caudal to the lesion site from the maximal tail diameter at the lesion site. At day 44 postinfection, mice (eight per group) were terminated. Right ears and the external sacral lymph nodes (ESLN) (which drain the tail) were harvested, and the parasite burdens were determined by the quantitative limiting dilution method. Ear tissue was disrupted with a rotator homogenizer, and lymph nodes were harvested and homogenized between the frosted ends of sterile slides in 1 ml of complete culture medium and were diluted with the same medium to a final concentration of 1 mg/ml. Fourfold serial dilutions of the homogenized tissue were then plated in a 96-well tissue culture plate and were cultured at 26°C for 3 weeks. The wells were examined for viable promastigotes at 3-day intervals, and the reciprocal of the highest dilution, which was positive for viable parasites, was considered to be the concentration of parasites in the organ (1).

***L. donovani* study.** Five groups of 16 female BALB/c mice were randomly selected to receive SCH 56592 at doses of 60, 30, and 15 mg/kg orally; to receive amphotericin B at a dose of 1 mg/kg intraperitoneally; or to receive 0.3% Noble agar orally. Mice were inoculated intravenously with  $10^6$  *L. donovani* promastigotes in a 0.2-ml volume through the lateral tail vein. Treatment was started on the 3rd day postinfection and was continued for 21 days. Half the mice (eight per group) were terminated at day 24, and the other half were terminated at day 44 postinfection. Hepatic and splenic parasite burdens were determined by the

TABLE 1. MPCs of SCH 56592, amphotericin B, and fluconazole against *Leishmania* spp.<sup>a</sup>

Organism	Concn (μg/ml) of:		
	Ampho B	SCH 56592	Fluconazole
<i>L. donovani</i>	0.5	16	>32
<i>L. amazonensis</i>	0.5	16	>32
<i>L. major</i>	0.125	8	>32
<i>L. mexicana</i> 68	0.5	8	>32
<i>L. mexicana</i> 390	1.0	16	>32
<i>L. panamensis</i> L334	0.25	8	>32
<i>L. panamensis</i> LS94	0.25	16	>32

<sup>a</sup> MPC of the drug is defined as the concentration which results in 90% inhibition of promastigote motility after 18 h of incubation.

quantitative limiting dilution method described above (a 30-mg piece of tissue was homogenized in 3 ml of medium).

**Statistical analysis.** For cutaneous infection, the means of the sizes of the ear and tail lesions of treatment groups and controls were compared using unpaired Student *t* test. For visceral infection, the mean log<sub>10</sub> values of parasites per gram of liver and spleen of treatment groups and controls were compared using unpaired Student *t* test. A *P* value of <0.05 was considered statistically significant.

## RESULTS

**In vitro susceptibility to SCH 56592, amphotericin B, and fluconazole.** In vitro, amphotericin B was more potent than SCH 56592 against *Leishmania* promastigotes of different species (Table 1). As previously reported, fluconazole was not effective against *Leishmania* promastigotes in culture media with MPCs of more than 32 μg/ml (1).

**Efficacy of SCH 56592 in experimental cutaneous leishmaniasis.** Six weeks postinfection with *L. amazonensis* promastigotes, tail lesions of the control group were significantly larger than those of any of the treatment groups. Lesion sizes were  $0.32 \pm 0.12$ ,  $0.11 \pm 0.06$ ,  $0.17 \pm 0.07$ ,  $0.21 \pm 0.06$ , and  $0.19 \pm 0.08$  mm for controls; SCH 56592 at 60, 30, and 15 mg/kg/day; and amphotericin B recipients, respectively (*P* = 0.0003, 0.005, 0.02, and 0.01, respectively). SCH 56592 at a dose of 60 mg/kg/day was superior to amphotericin B at a dose of 1 mg/kg/day (*P* = 0.03) (Fig. 2A). Parasite burdens in the ESLN of all treatment groups were significantly lower than the burdens in controls. The mean log<sub>10</sub> values of parasites per ESLN were  $6.25 \pm 1.14$ ,  $3.86 \pm 0.69$ ,  $4.16 \pm 0.53$ ,  $4.80 \pm 0.84$ , and  $4.47 \pm 0.87$  for controls; SCH 56592 at 60, 30, and 15 mg/kg/day; and amphotericin B recipients, respectively (*P* = 0.0002, 0.0003, 0.01, and 0.003, respectively) (Fig. 3A).

In ear infections, only recipients of SCH 56592 at a dose of 60 mg/kg/day had significantly smaller lesion sizes than controls. Lesion sizes were  $1.09 \pm 0.47$  mm for controls,  $0.65 \pm 0.20$  mm for groups treated with SCH 56592 at 60 mg,  $0.95 \pm 0.38$  mm for groups treated with SCH 56592 at 30 mg,  $0.90 \pm 0.37$  mm for groups treated with SCH 56592 at 15 mg/kg/day, and  $1.0 \pm 0.32$  mm for groups treated with amphotericin B (*P* = 0.03 for SCH 56592 at 60 mg/kg/day) (Fig. 2B). Parasite burdens in the ear were lower only in the recipients of SCH 56592 at a dose of 60 mg/kg/day. The mean log<sub>10</sub> values of parasites per ear were  $6.13 \pm 0.84$ ,  $5.24 \pm 0.70$ ,  $5.65 \pm 0.77$ ,  $5.80 \pm 0.71$ , and  $5.69 \pm 0.93$  for controls; SCH 56592 at 60, 30, and 15 mg/kg/day; and amphotericin B recipients, respectively (*P* = 0.04 for SCH 56592 at 60 mg/kg/day) (Fig. 3B).

**Efficacy of SCH 56592 in experimental VL.** *L. donovani*-infected mice were treated for 21 days. Visceral parasite burdens were determined at days 24 and 44 postinfection. Table 2 summarizes the parasite loads in the liver and spleen of treated and untreated mice. At a dose of 30 mg/kg/day, SCH 56592

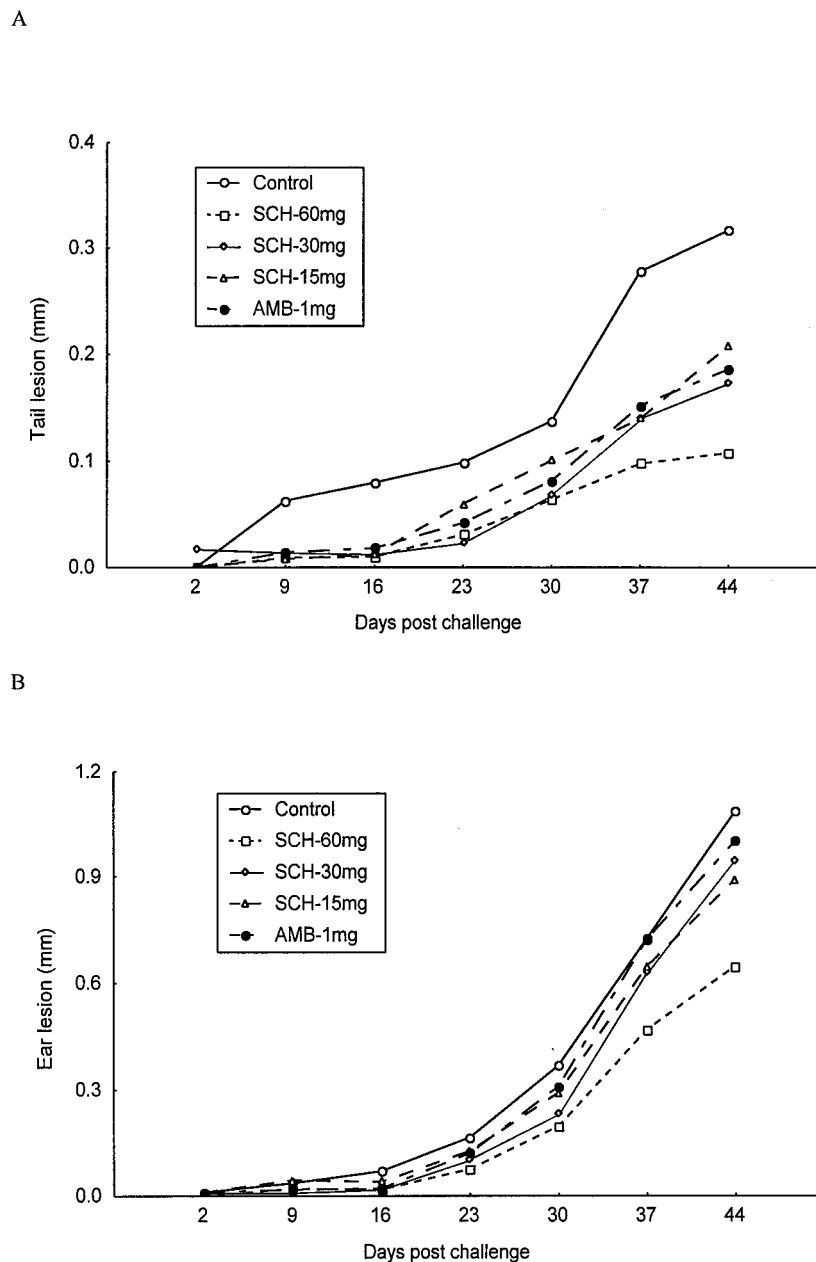


FIG. 2. Graph of the efficacy of a 21-day treatment course with SCH 56592 or amphotericin B in experimental CL caused by *L. amazonensis* infection. Sizes of tail lesions are shown in panel A and ear pinna lesions are shown in panel B for treated and untreated control mice. Treatments were started on the 3rd day postinfection and were continued for 21 days. The ear lesion size was considered as the difference between the thicknesses of the infected and uninfected ear pinnae. The size of the tail lesion was obtained by subtracting the average tail diameter at points just rostral and caudal to the lesion site from the maximal tail diameter at the lesion site.

reduced parasite burdens in the liver and spleen by 0.5 to 1 log unit ( $P < 0.05$ ). Amphotericin B reduced parasite burdens by 2 log units in both liver and spleen ( $P < 0.001$ ). There was no significant difference in parasite loads at days 24 and 44 postinfection. All mice that received SCH 56592 at a dose of 60 mg/kg/day died within 14 days of therapy for an unexplained reason, possibly due to drug toxicity.

## DISCUSSION

Inconvenience, toxicity, and a significant relapse rate are major problems associated with the currently used parenteral

drug therapy for the leishmaniasis (2, 7, 9, 13). Efficacious and safe oral therapy is greatly needed. In this study, we examined a new, orally administered triazole antifungal drug, SCH 56592, against *Leishmania*. In vitro studies showed that SCH 56592 had modest activity, inferior to amphotericin B but substantially better than fluconazole, against leishmanial promastigotes. The in vitro activity of a drug against the promastigote stage may not necessarily correlate with its activity against intracellular amastigotes. Our in vivo studies demonstrated that SCH 56592 was efficacious in the treatment of experimental CL. The mechanism of action of SCH 56592 against *Leishmania* spp. is probably similar to those of other azole antifun-

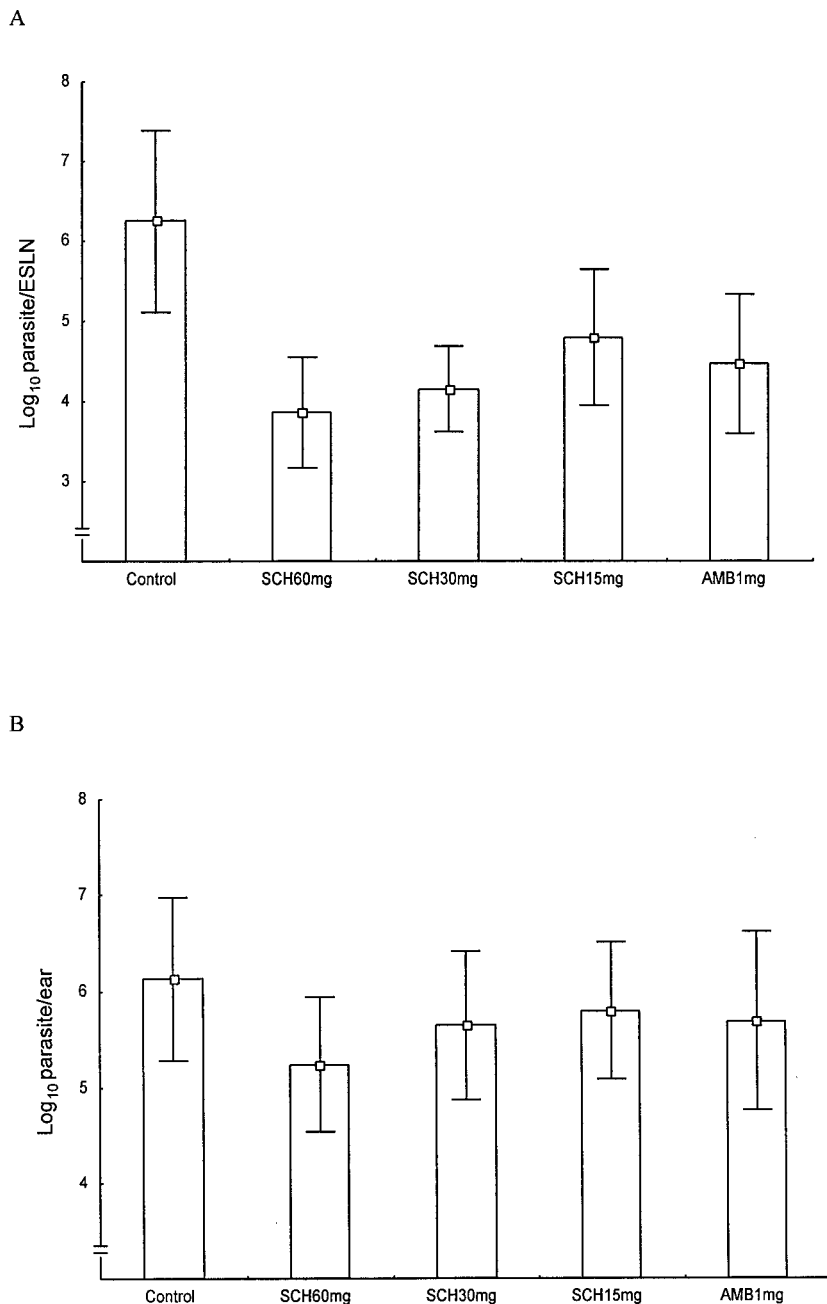


FIG. 3. Efficacy of a 21-day treatment course with SCH 56592 or amphotericin B in experimental CL caused by *L. amazonensis*. Parasite burdens in the ESLN are shown in panel A, and burdens in the ear are shown in panel B.

gals, i.e., inhibition of membrane sterol synthesis resulting in disruption of the cell membrane.

We studied the efficacy of SCH 56592 in an experimental model of CL caused by a highly virulent strain of *L. amazonensis*. Mice were infected at both relatively permissive (ear pinna) and nonpermissive (tail) sites (1), and the response to therapy was assessed by measurement of lesions and determination of parasite burdens in the ears and lymph nodes which drain the tail site of infection. SCH 56592, when used at higher doses (60 mg/kg/day), was superior to the standard, tolerated, doses of amphotericin B in reducing the size of cutaneous lesions. It is not clear if this superiority in treating cutaneous disease is

related to leishmanicidal activity or, as is more likely, due to a better distribution of the drug to the skin and subcutaneous tissue. The lower parasite burdens present in the ear tissue and lymph nodes in SCH 56592-treated mice were consistent with the results of the clinical response. The response observed in the ear infection was clearly less impressive than in the tail infection. This was previously observed in treated mice (1). In humans, leishmanial infections involving the ear are more chronic and progressive, and they are more difficult to treat than infections at other cutaneous sites (15). Amphotericin B demonstrated a reduced efficacy in treating cutaneous diseases. In future studies, it may be useful to compare SCH 56592 to

TABLE 2. Parasite burdens on days 24 and 44 in the liver and spleen of *L. donovani*-infected mice treated for 21 days

Treatment	Dose (mg/kg/ day)	Day of tissue burden	Log <sub>10</sub> of parasite/g of tissue <sup>a</sup>	
			Liver	Spleen
None		24	5.70 ± 0.55	5.53 ± 0.40
		44	5.15 ± 0.43	5.72 ± 0.24
SCH56592	30	24	4.86 ± 0.53*	4.82 ± 0.63*
		44	4.41 ± 0.81*	4.86 ± 0.53*
SCH56592	15	24	5.47 ± 0.42	5.38 ± 0.27
		44	5.15 ± 0.42	5.65 ± 0.32
Amphotericin B	1	24	3.88 ± 1.00**	3.89 ± 0.60**
		44	3.52 ± 0.70**	3.97 ± 0.39**

<sup>a</sup> Means ± standard deviations for eight mice. \*, Statistically significant ( $P < 0.05$ ); \*\*, highly significant ( $P < 0.0001$ ) compared to untreated mice.

other azoles to determine if it would be more efficacious than structurally related compounds.

In the model of VL due to *L. donovani* infection, SCH 56592 was modestly effective in reducing the parasite burdens in the liver and spleen compared to untreated controls. Amphotericin B was clearly superior to SCH 56592, resulting in reductions in parasite burdens of approximately 2 log units in the liver and spleen. These findings are consistent with the reported limited success achieved when treating patients with visceral disease with other azoles (12).

Our study indicates that SCH 56592 is efficacious against CL due to *L. amazonensis* infection and may serve as convenient oral therapy. However, this has to await formal toxicity testing. The study also indicates that SCH 56592 is less likely to be effective as a single drug in the treatment of VL. Perhaps this drug may be useful as part of a combination therapy for resistant disease.

#### ACKNOWLEDGMENTS

This work was supported in part by Schering-Plough Research Institute and by funding from the Veterans Administration to P.C. Melby.

We are grateful to L. Najvar, R. Bocanegra, and E. Montalbo for their help with measurement of lesions and with dosing animals; A. Fothergill (Fungus Testing Laboratory, San Antonio, Tex.) for her

help in preparing drugs for in vitro testing; and Weigou Zhao for his help with preparation of the culture media.

#### REFERENCES

- Al-Abdeley, H. M., J. R. Graybill, R. Bocanegra, L. Najvar, E. Montalbo, S. L. Regen, and P. C. Melby. 1998. Efficacies of KY62 against *Leishmania amazonensis* and *Leishmania donovani* in experimental murine cutaneous leishmaniasis and visceral leishmaniasis. *Antimicrob. Agents Chemother.* **42:** 2542–2548.
- Alvar, J., C. Canavate, B. Gutierrez-Solar, M. Jimenez, F. Laguna, R. Lopez-Velez, R. Molina, and J. Moreno. 1997. *Leishmania* and human immunodeficiency virus coinfection: the first 10 years. *Clin. Microbiol. Rev.* **10:**298–319.
- Berman, J. D. 1997. Human leishmaniasis: clinical, diagnostic, and chemotherapeutic developments in the last 10 years. *Clin. Infect. Dis.* **24:**684–703.
- Berman, J. D., L. J. Goad, D. H. Beach, and G. G. Holz, Jr. 1986. Effects of ketoconazole on sterol biosynthesis by *Leishmania mexicana mexicana* amastigotes in murine macrophage tumor cells. *Mol. Biochem. Parasitol.* **20:**85–92.
- Dan, M., E. Verner, J. el-On, F. Zuckerman, and D. Michaeli. 1986. Failure of oral ketoconazole to cure cutaneous ulcers caused by *Leishmania braziliensis*. *Cutis* **38:**198–199.
- Dogra, J., and V. N. Saxena. 1996. Itraconazole and leishmaniasis: a randomised double-blind trial in cutaneous disease. *Int. J. Parasitol.* **26:**1413–1415.
- Gasser, R. A., Jr., A. J. Magill, C. N. Oster, E. D. Franke, M. Grogl, and J. D. Berman. 1994. Pancreatitis induced by pentavalent antimonials during treatment of leishmaniasis. *Clin. Infect. Dis.* **18:**83–90.
- Halim, M. A., O. Alfurayh, M. E. Kalin, S. Dammas, A. al-Eisa, and G. Damanhour. 1993. Successful treatment of visceral leishmaniasis with allopurinol plus ketoconazole in a renal transplant recipient after the occurrence of pancreatitis due to stibogluconate. *Clin. Infect. Dis.* **16:**397–399.
- Mishra, M., U. K. Biswas, A. M. Jha, and A. B. Khan. 1994. Amphotericin versus sodium stibogluconate in first-line treatment of Indian kala-azar. *Lancet* **344:**1599–1600.
- Momeni, A. Z., T. Jalayer, M. Emamjomeh, N. Bashardost, R. L. Ghassemi, M. Meghdadi, A. Javadi, and M. Aminjavaheri. 1996. Treatment of cutaneous leishmaniasis with itraconazole. Randomized double-blind study. *Arch. Dermatol.* **132:**784–786.
- Oakley, K. L., C. B. Moore, and D. W. Denning. 1997. In vitro activity of SCH-56592 and comparison with activities of amphotericin B and itraconazole against *Aspergillus* spp. *Antimicrob. Agents Chemother.* **41:**1124–1126.
- Rashid, J. R., K. M. Wasunna, G. S. Gachihi, P. M. Nyakundi, J. Mbugua, and G. Kirigi. 1994. The efficacy and safety of ketoconazole in visceral leishmaniasis. *East Afr. Med. J.* **71:**392–395.
- Rosenthal, E., P. Marty, I. Poizot-Martin, J. Reynes, F. Pratlong, A. Lafeuillade, D. Jaubert, O. Boulat, J. Dereure, and F. Gambarelli. 1995. Visceral leishmaniasis and HIV-1 co-infection in southern France. *Trans. R. Soc. Trop. Med. Hyg.* **89:**159–162.
- Van Voorhis, W. C. 1990. Therapy and prophylaxis of systemic protozoan infections. *Drugs* **40:**176–202.
- Walton, B. C. 1987. American cutaneous and mucocutaneous leishmaniasis, p. 644. In W. Peters and R. Killick-Kendrick (ed.), *The leishmaniasis in biology and medicine*, vol. II. Academic Press, London, United Kingdom.

# In Vitro Activity of the Antifungal Azoles Itraconazole and Posaconazole against *Leishmania amazonensis*

Sara Teixeira de Macedo-Silva<sup>1,2</sup>, Julio A. Urbina<sup>3</sup>, Wanderley de Souza<sup>1,2,4</sup>, Juliany Cola Fernandes Rodrigues<sup>1,2,4,5\*</sup>

**1** Laboratório de Ultraestrutura Celular Hertha Meyer, Instituto de Biofísica Carlos Chagas Filho, Universidade Federal do Rio de Janeiro, Rio de Janeiro, Brazil, **2** Instituto Nacional de Ciência e Tecnologia de Biologia Estrutural e Bioimagem, Rio de Janeiro, Brazil, **3** Instituto Venezolano de Investigaciones Científicas, Centro de Bioquímica y Biofísica, Caracas, Venezuela, **4** Instituto Nacional de Metrologia, Qualidade e Tecnologia, Inmetro, Rio de Janeiro, Brazil, **5** Núcleo Multidisciplinar de Pesquisa em Biologia (NUMPEX-BIO), Polo Avançado de Xerém, Universidade Federal do Rio de Janeiro, Duque de Caxias, Brazil

## Abstract

Leishmaniasis, caused by protozoan parasites of the *Leishmania* genus, is one of the most prevalent neglected tropical diseases. It is endemic in 98 countries, causing considerable morbidity and mortality. Pentavalent antimonials are the first line of treatment for leishmaniasis except in India. In resistant cases, miltefosine, amphotericin B and pentamidine are used. These treatments are unsatisfactory due to toxicity, limited efficacy, high cost and difficult administration. Thus, there is an urgent need to develop drugs that are efficacious, safe, and more accessible to patients. Trypanosomatids, including *Leishmania* spp. and *Trypanosoma cruzi*, have an essential requirement for ergosterol and other 24-alkyl sterols, which are absent in mammalian cells. Inhibition of ergosterol biosynthesis is increasingly recognized as a promising target for the development of new chemotherapeutic agents. The aim of this work was to investigate the antiproliferative, physiological and ultrastructural effects against *Leishmania amazonensis* of itraconazole (ITZ) and posaconazole (POSA), two azole antifungal agents that inhibit sterol C14 $\alpha$ -demethylase (CYP51). Antiproliferative studies demonstrated potent activity of POSA and ITZ: for promastigotes, the IC<sub>50</sub> values were 2.74  $\mu$ M and 0.44  $\mu$ M for POSA and ITZ, respectively, and for intracellular amastigotes, the corresponding values were 1.63  $\mu$ M and 0.08  $\mu$ M, for both stages after 72 h of treatment. Physiological studies revealed that both inhibitors induced a collapse of the mitochondrial membrane potential ( $\Delta\Psi_m$ ), which was consistent with ultrastructural alterations in the mitochondrion. Intense mitochondrial swelling, disorganization and rupture of mitochondrial membranes were observed by transmission electron microscopy. In addition, accumulation of lipid bodies, appearance of autophagosome-like structures and alterations in the kinetoplast were also observed. In conclusion, our results indicate that ITZ and POSA are potent inhibitors of *L. amazonensis* and suggest that these drugs could represent novel therapies for the treatment of leishmaniasis, either alone or in combination with other agents.

**Citation:** de Macedo-Silva ST, Urbina JA, de Souza W, Rodrigues JCF (2013) In Vitro Activity of the Antifungal Azoles Itraconazole and Posaconazole against *Leishmania amazonensis*. PLoS ONE 8(12): e83247. doi:10.1371/journal.pone.0083247

**Editor:** Henk D. F. H. Schallig, Royal Tropical Institute, The Netherlands

**Received** June 17, 2013; **Accepted** October 31, 2013; **Published** December 23, 2013

**Copyright:** © 2013 de Macedo-Silva et al. This is an open-access article distributed under the terms of the Creative Commons Attribution License, which permits unrestricted use, distribution, and reproduction in any medium, provided the original author and source are credited.

**Funding:** This work was supported by Conselho Nacional de Desenvolvimento Científico (CNPq), Fundação Carlos Chagas Filho de Amparo à Pesquisa do Estado do Rio de Janeiro (FAPERJ), Financiadora de Estudos e Projetos (FINEP), and Coordenação de Aperfeiçoamento de Pessoal de Nível Superior (CAPES). The funders had no role in study design, data collection and analysis, decision to publish, or preparation of the manuscript.

**Competing Interests:** The authors have declared that no competing interests exist.

\* E-mail: juliany.rodrigues@xerem.ufrj.br

## Introduction

The leishmaniases, which are among the most prevalent neglected tropical diseases, are caused by protozoan parasites of the *Leishmania* genus. The disease is endemic in 98 countries worldwide, and more than 2 million new cases occur annually, with high levels of morbidity and mortality [1]. There are three major clinical manifestations of the disease: visceral, mucocutaneous and cutaneous leishmaniases. Other cutaneous manifestations include diffuse cutaneous leishmaniasis, recidivans leishmaniasis and post-kala-azar dermal leishmaniasis [2]. The pathology caused by *Leishmania* depends on several factors, which include the infecting species and the host immune response [3,4]. More than 90% of cases of visceral leishmaniasis and cutaneous leishmaniases occur in India, Sudan, Bangladesh, Nepal, Brazil, Afghanistan, Saudi Arabia, Algeria, Iran, Iraq and Syria [1]. In Brazil, *Leishmania amazonensis* is one of the species responsible for the cutaneous form of the disease [5] and it is important for the

epidemiology of the leishmaniasis in the Amazon region [6]. When the immune system fails to mount an appropriate response against the parasite, *L. amazonensis* can cause clinical manifestations of diffuse cutaneous leishmaniasis [5]. It is a serious public health problem in Brazil, because the lesions cover a large part of the body, sometimes producing mutilated lesions, and is devastating for the patients, because it is incurable using currently available treatments.

Pentavalent antimonial compounds (e.g., sodium stibogluconate and meglumine antimoniate) have been the drugs of choice for the treatment of leishmaniasis for decades worldwide despite their severe side effects [7,8]. However, they have been recently discontinued in India. In addition, antimoniales are associated with significant failure and relapse rates, especially in immunocompromised hosts [9–11]. Pentamidine and amphotericin B are other parenteral alternatives that can cause significant side effects [8,12]. Miltefosine (Impavido) is the first oral drug available for treatment of visceral leishmaniasis in India [12–13], but it is

teratogenic, and there are indications that resistance to the drug is appearing in endemic areas [13]. In addition, miltefosine also has significant effects against cutaneous leishmaniasis in human [12] and in murine models of cutaneous leishmaniasis by infection with *L. amazonensis* [14]. Thus, there is an urgent need to develop new drugs that are efficacious, safe, and more accessible to patients.

Sterols are constituents of cellular membranes that are essential for their normal structure and function. Trypanosomatids have an essential requirement for ergosterol and other 24-alkyl sterols, which are absent in mammalian cells [15–16], and ergosterol biosynthesis inhibitors (EBIs) have proved to be potential candidates for the treatment of leishmaniasis and other diseases caused by protozoan parasites, such as Chagas disease (17–21). Itraconazole (ITZ) and posaconazole (POSA) are two known azoles that inhibit sterol C14 $\alpha$ -demethylase (CYP51), an essential enzyme in the sterol biosynthesis pathway, with potent effects against fungi and trypanosomatids [22–28]. In particular, POSA has shown potent activity in murine models of acute and chronic Chagas' disease [17,29]. In addition, POSA and ITZ have also been studied in murine models of cutaneous and visceral leishmaniases by infection with *L. amazonensis*, *L. donovani* [18] and *L. infantum* [30]. Furthermore, there are some studies describing the effect of ITZ on patients with cutaneous leishmaniasis [31–33]. Thus, we decided to investigate the *in vitro* effects of POSA and ITZ on the proliferation and ultrastructure of *L. amazonensis*. We found that both compounds are potent inhibitors of *L. amazonensis* growth and induced multiple severe alterations in the ultrastructure of promastigotes and intracellular amastigotes. In particular, these drugs affected the structure and function of the single giant mitochondrion present in these cells and induced an accumulation of lipid bodies and autophagosomes.

## Materials and Methods

### Ethics Statement

The experiments using animal models to obtain macrophages and *Leishmania* were approved by the Ethics Committee for Animal Experimentation of the Health Sciences Centre, Federal University of Rio de Janeiro (Protocols n. IBCCF 096/097/106), according to the Brazilian federal law (11.794/2008, Decreto n° 6.899/2009). All animals received humane care in compliance with the "Principles of Laboratory Animal Care" formulated by the National Society for Medical Research and the "Guide for the Care and Use of Laboratory Animals" prepared by the National Academy of Sciences, USA.

### Parasites

The MHOM/BR/75/Josefa strain of *L. amazonensis* used in this study was isolated in 1975 by Dr. Cesar A. Cuba-Cuba (Brasilia University, Brazil) from a patient with diffuse cutaneous leishmaniasis and kindly provided by the *Leishmania* Collection of the Instituto Oswaldo Cruz (Code IOCL 0071 - FIOCRUZ). The strain was maintained by inoculation into the base of the tails of Balb/C mice. Axenic promastigotes were cultured at 25°C in Warren's medium (brain heart infusion plus hemin and folic acid) [34] supplemented with 10% fetal bovine serum (Cultilab, Brazil). Infective metacyclic promastigotes of the Josefa strain were used to obtain intracellular amastigotes in macrophage cultures.

### Drugs and Reagents

Posaconazole (POSA) was provided by the Schering Plough Research Institute (United States). Itraconazole (ITZ) was purchased from Janssen Pharmaceutical Companies (Brazil). Both drugs were dissolved in a 10 mM stock of dimethyl sulfoxide

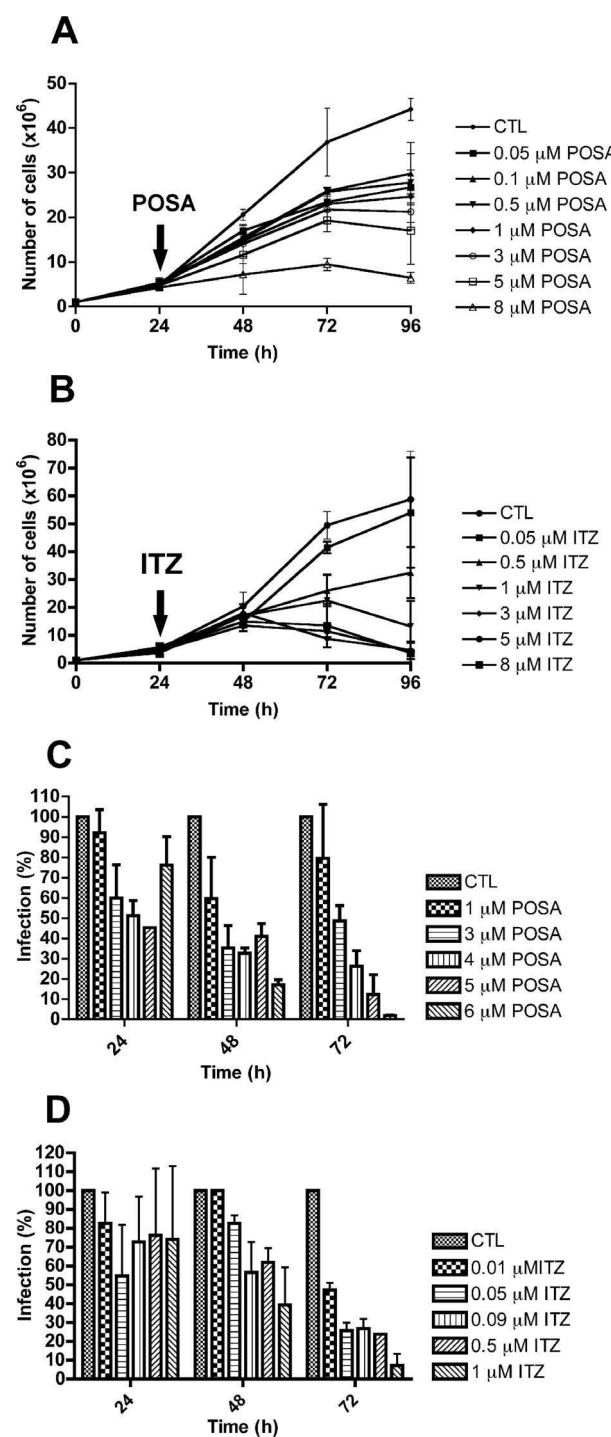


**Figure 1. Antiproliferative effects of posaconazole and itraconazole on *Leishmania amazonensis*.** *L. amazonensis* promastigotes (A, B) and intracellular amastigotes (C, D) were treated with posaconazole (POSA) (A, C) or itraconazole (ITZ) (B, D) to evaluate the parasite growth. The arrows indicate the time of the addition of the drugs at the indicated concentrations. The results were plotted as the mean of three independent experiments and the bars represent the standard deviation.

doi:10.1371/journal.pone.0083247.g001

(DMSO) and stored at -20°C. For experiments, new dilutions were prepared in culture medium to ensure that the DMSO concentration in the culture medium did not exceed 0.1%. All the

**Table 1.** IC<sub>50</sub>, CC<sub>50</sub> and selective indexes (SI) for the treatment of *L. amazonensis* promastigotes and intracellular amastigotes with posaconazole (POSA) and itraconazole (ITZ).

Time of incubation	Promastigotes (IC <sub>50</sub> - μM)		Intracellular amastigotes (IC <sub>50</sub> - μM)		CC <sub>50</sub> (μM)*	Selectivity Index (SI)**
	48 h	72 h	48 h	72 h		
<b>Posaconazole</b>	3.94	2.74	1.95	1.63	20	12.2
<b>Itraconazole</b>	0.88	0.44	0.64	0.08	15	187.5

\*CC<sub>50</sub> was obtained after 72 h of treatment with both compounds.

\*\*Selectivity Index (SI) was calculated dividing the CC<sub>50</sub> by the IC<sub>50</sub> values obtained after treatment for 72 h.

doi:10.1371/journal.pone.0083247.t001

reagents for electron microscopy were from Electron Microscopy Sciences (England).

### In vitro Antiproliferative Effects

Promastigote cultures were initiated at a cell density of  $1.0 \times 10^6$  cells/ml. After 24 h of growth, POSA or ITZ was added at different concentrations (0.05; 0.1; 0.5; 1; 3; 5; 8 μM for POSA, and 0.05; 0.5; 1; 3; 5; 8 μM for ITZ) from concentrated stock solutions. Cell densities were evaluated daily over 96 h of growth using a Neubauer chamber. To evaluate the effects of POSA and ITZ on *L. amazonensis* intracellular amastigotes, macrophages from the peritoneal cavity of CF1 mice were harvested by washing with Hank's solution, plated in 24-well tissue culture chamber slides and allowed to adhere to the slides for 24 h at 37°C, 5% CO<sub>2</sub>, in RPMI medium (Gibco, Brazil) supplemented with 10% fetal bovine serum. Adherent macrophages were infected with metacyclic promastigotes at a macrophage-to-parasite ratio of 1:10 at 35°C, 5% CO<sub>2</sub>, for 2 h and then washed two times with RPMI medium to remove non-ingested parasites. Infected cultures were incubated in RPMI medium supplemented with 10% fetal bovine serum without drugs. After 24 h of infection when the number of amastigotes per macrophage was in the range of two to four, different concentrations of POSA (1; 3; 4; 5; 6 μM) or ITZ (0.01; 0.05; 0.09; 0.5; 1 μM) were added. Fresh medium with POSA or ITZ was added daily for 3 days (72 h of treatment). The cultures were fixed in Bouin's solution (70% picric acid, 5% acetic acid and 25% formaldehyde in aqueous solution), washed in 70% ethanol and in distilled water. The cultures were then stained with Giemsa for 1 h. To determine the percentage of infected cells, 600 macrophages (infected and non-infected) were counted in a bright field optical microscope using a 100× immersion oil objective. Association indexes (mean number of parasites internalized per cell, multiplied by the number of infected macrophages and divided by the total number of macrophages) were determined and used to calculate the percentage of infection in each study condition. The concentration that inhibited 50% of the growth (IC<sub>50</sub> value) was calculated and the control infection (without treatment) was used as reference parameter (100% of infection). The results are expressed as the mean of three independent experiments.

### IC<sub>50</sub> Calculations

For the calculation of the IC<sub>50</sub> values, percentage of growth inhibition was plotted as a function of drug concentration by fitting the values to a non-linear curve analysis where  $f = \min + (\max - \min) / (1 + (x/EC_{50})^{HillSlope})$ , where the IC<sub>50</sub> is the concentration that inhibits 50% of the growth. The regression analyses were performed with Graphpad Prism 4 Software (United States).

### Cytotoxicity Assay

Cytotoxicity effects of ITZ and POSA against murine macrophages were evaluated using the CellTiter 96® Aqueous MTS Reagent Powder (Promega, United States). Murine macrophages obtained as explained above were cultivated in a 96-well plate with RPMI medium containing 10% fetal bovine serum (Gibco, Brazil) and maintained at 37°C in 5% CO<sub>2</sub>. After 24 h of cultivation, different concentrations of the drugs (5, 15, 25 and 35 μM for POSA and ITZ) were added every 24 h until 72 h of treatment, when the cytotoxicity was measured. Cell viability was assessed by the MTS/PMS assay reaction and results were expressed as optical density measured at 492 nm in a microplate reader and spectrophotometer SpectraMax M2/M2e (Molecular Devices, United States) [35]. The cytotoxicity concentration to reduce 50% of viable macrophages (CC<sub>50</sub>) was determined.

### Electron Microscopy

Control, ITZ- or POSA-treated promastigotes and intracellular amastigotes inside macrophages were fixed in 2.5% glutaraldehyde in 0.1 M cacodylate buffer (pH 7.2) and postfixed in a solution containing 1% OsO<sub>4</sub>, 1.25% potassium ferrocyanide and 0.1 M cacodylate buffer, pH 7.2. For transmission electron microscopy, cells were dehydrated in acetone and embedded in epoxy resin. Ultrathin sections were stained with uranyl acetate and lead citrate and observed under a Zeiss 900 electron microscope. For scanning electron microscopy, promastigotes were dehydrated in ethanol, critical point-dried in CO<sub>2</sub>, mounted on stubs, sputtered with a thin gold layer and observed under a FEI Quanta 250 scanning electron microscope.

### Estimation of Mitochondrial Transmembrane Electric Potential ( $\Delta\Psi_m$ )

The mitochondrial membrane potential ( $\Delta\Psi_m$ ) of *L. amazonensis* promastigotes was analyzed after 48 h of treatment with POSA or ITZ (1 and 5 μM), using the JC-1 fluorochrome (Molecular Probes, United States) [36]. This fluorochrome is a lipophilic, cationic, mitochondrial vital dye that accumulates in the mitochondria in response to  $\Delta\Psi_m$ . At low concentrations, the dye exists as a monomer, which emits at 530 nm (green fluorescence); at higher concentrations the dye accumulates in the mitochondrion and forms J-aggregates, which emit at 590 nm (red fluorescence). Control, POSA and ITZ-treated promastigotes were harvested, washed in PBS, pH 7.2, added to the reaction medium containing 125 mM sucrose, 65 mM KCl, 10 mM HEPES/K<sup>+</sup> pH 7.2, 2 mM Pi, 1 mM MgCl<sub>2</sub> and 500 μM EGTA and counted using a Neubauer chamber. To evaluate the  $\Delta\Psi_m$  for each experimental condition,  $1.0 \times 10^7$  parasites were incubated with 10 μg/mL JC-1 for 40 min, with readings made every minute using a microplate reader and spectrophotometer SpectraMax

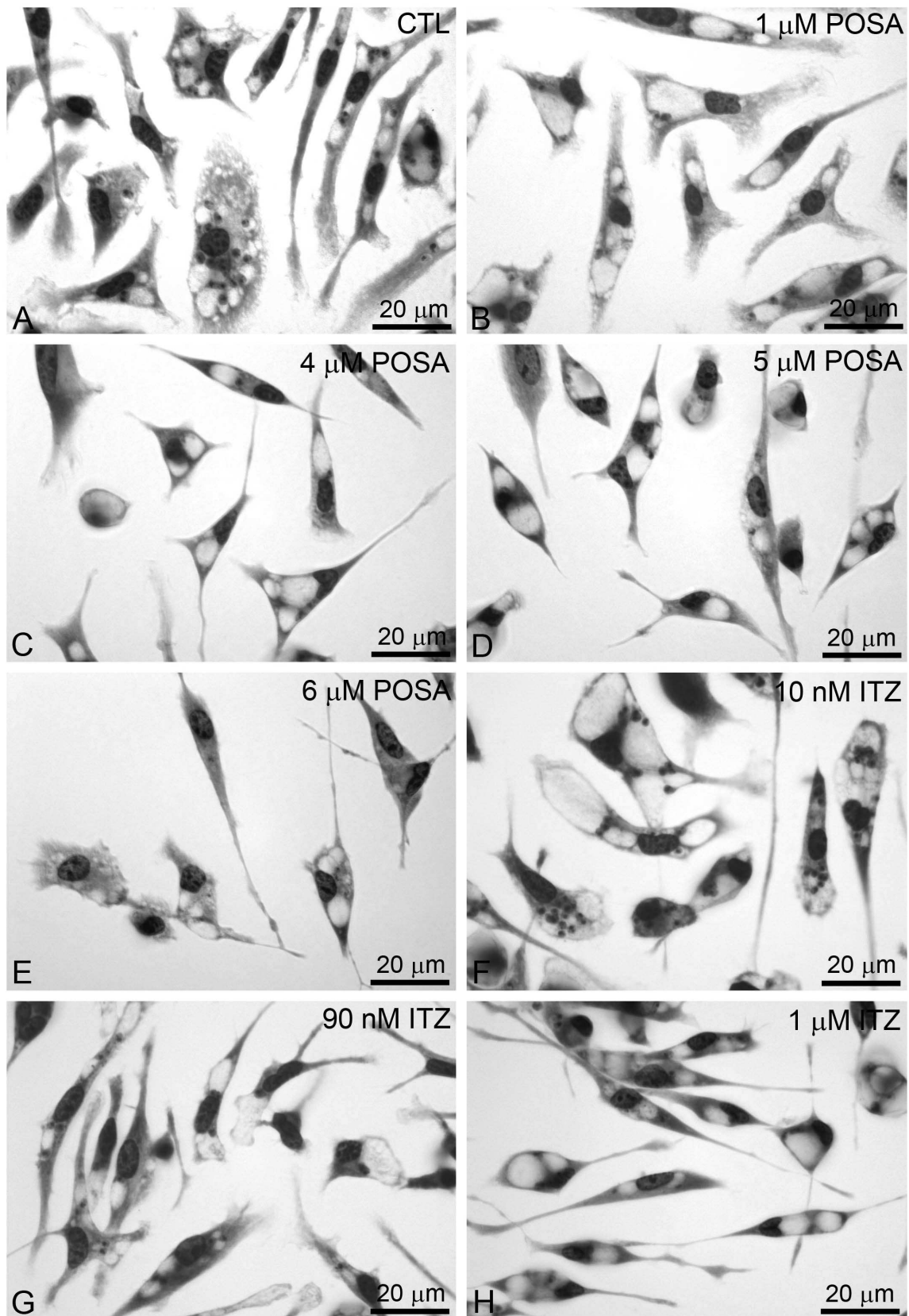


**Figure 2. Light microscopy of murine macrophages infected with *L. amazonensis* amastigotes.** (A) Control culture with many amastigotes inside parasitophorous vacuoles. (B–H) After 72 h of treatment with different concentrations of POSA and ITZ, a significant reduction in the number of parasites and the presence of several empty parasitophorous vacuoles was observed.

doi:10.1371/journal.pone.0083247.g002

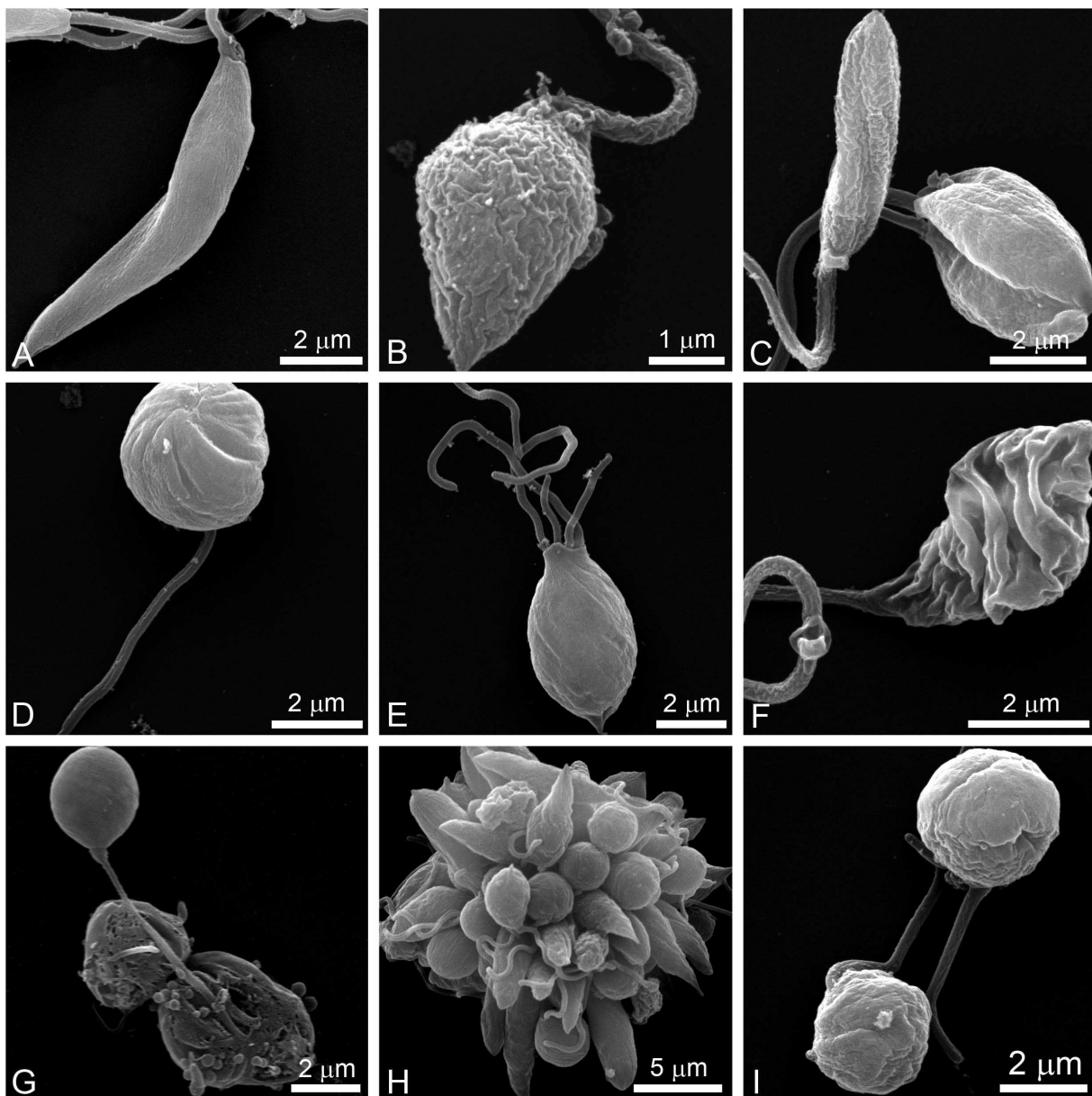


**Figure 3. Scanning electron microscopy (SEM) of *L. amazonensis* promastigotes.** Control parasites (A) and promastigotes that were treated with different concentrations of POSA and ITZ for 48 h (B–I) were observed by SEM. (B, C) 1  $\mu$ M ITZ; (D–F) 1  $\mu$ M POSA; (G) 5  $\mu$ M ITZ; (H, I) 5  $\mu$ M POSA. The images show dramatic alterations in promastigote shape (B–I), a promastigote with four flagella (E), and profound changes in the plasma membrane (B, C, F).

doi:10.1371/journal.pone.0083247.g003

M2/M2<sup>c</sup>. After 36 min of readings, 2  $\mu$ M FCCP was added to abolish the  $\Delta\Psi_m$ . For the positive control, cells were incubated in the presence of 2  $\mu$ M FCCP, a mitochondrial protonophore. The relative  $\Delta\Psi_m$  value was obtained by calculating the ratio between the reading at 590 nm and the reading at 530 nm (590:530 ratio). Each experiment was repeated at least three times in triplicate using a black 96-well plate, and the figures shown are representative of these experiments.

#### Evaluation of Membrane Integrity and the Presence of Lipid Bodies via Nile Red Accumulation

Control and treated promastigotes were harvested, washed in PBS, pH 7.2, and counted using a Neubauer chamber. Cells

( $1.0 \times 10^7$ ) were then incubated with 10  $\mu$ g/mL Nile Red (Sigma, Brazil) for 20 min and 1  $\mu$ M Sytox Blue for 20 min. The experiments were performed in triplicate, using a black 96-well plate. The cells were washed twice before analysis. The final volume in each well was 200  $\mu$ L of cell suspension in PBS. Readings were taken with a microplate reader and spectrophotometer SpectraMax M2/M2<sup>c</sup> using the following wavelengths for excitation and emission, respectively: 485 and 538 nm for Nile Red, and 444 and 560 nm for Sytox Blue. Each experiment was repeated at least three times in triplicate, and the figures shown are representative of these experiments. After the readings, control and treated-parasites incubated with Nile Red were fixed with 4% nascent formaldehyde in 0.1 M phosphate buffer, pH 7.2, before

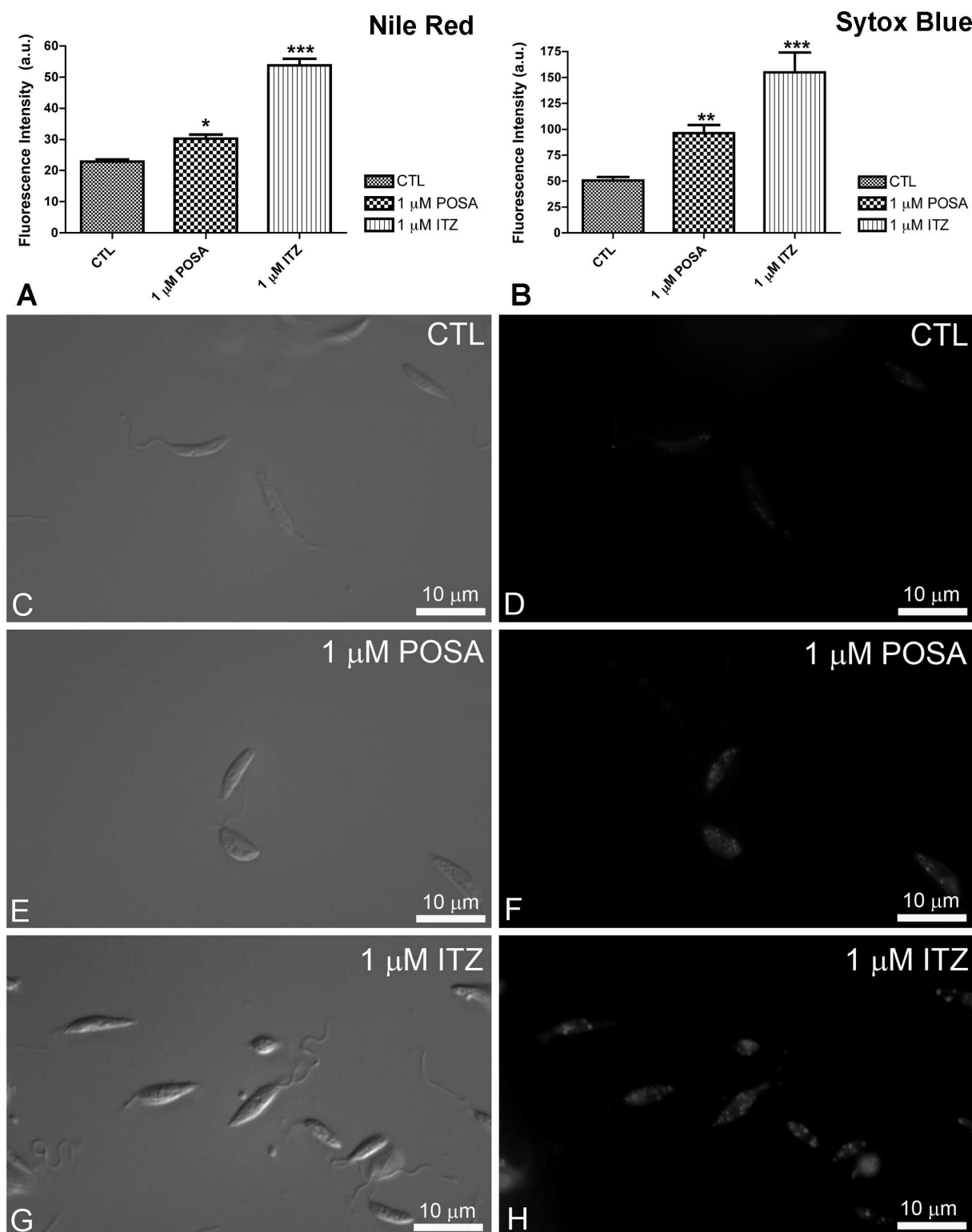


**Figure 4. Analysis of lipid body accumulation and plasma membrane integrity in *L. amazonensis* promastigotes.** (A–B) Quantitative fluorimetric analysis using Nile Red (A) and Sytox Blue (B). Fluorescence intensity is expressed as arbitrary units (A.U.). The results were plotted as mean of three independent experiments and the bars represent the standard deviation. \* $p<0.01$ ; \*\* $p<0.05$ ; \*\*\* $p<0.0001$ . (C–H) Differential interference contrast (DIC) microscopy (C, E, G) and fluorescence microscopy using Nile Red (D, F, H) of control *L. amazonensis* promastigotes and promastigotes treated with 1 μM POSA or ITZ for 48 h. The images demonstrate an accumulation of lipid bodies that are randomly distributed throughout the cytoplasm, confirming the increase in the fluorescence intensity observed in Fig. 4A.

doi:10.1371/journal.pone.0083247.g004

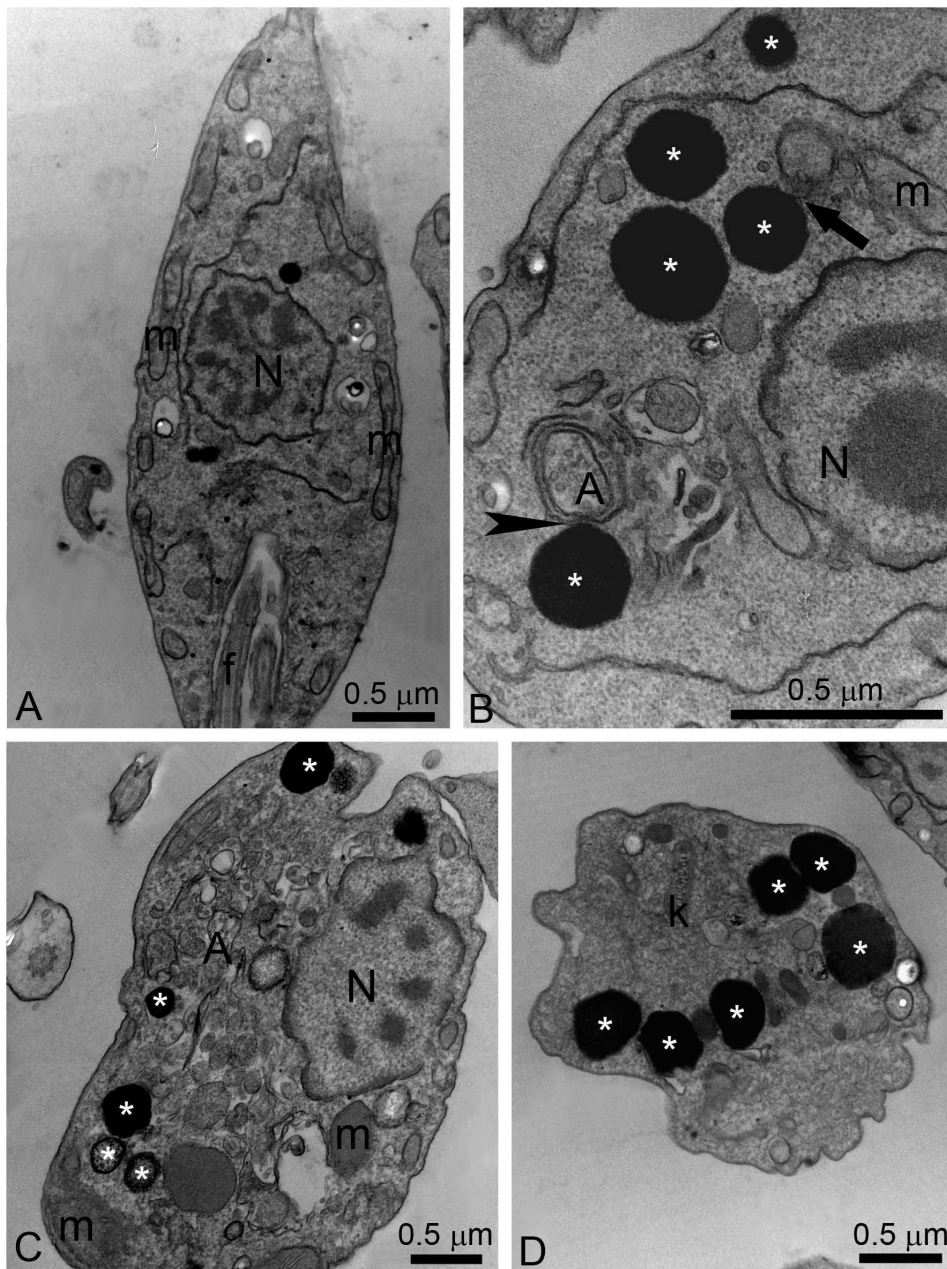


**Figure 5. Ultrathin sections of control *L. amazonensis* promastigotes (A) and promastigotes treated with ITZ (B–D).** (A) Control promastigotes; (B–C) 5  $\mu$ M ITZ; (D) 1  $\mu$ M ITZ. The images show the presence of several electron-dense lipid bodies (asterisks), which sometimes appear near the plasma membrane, the endoplasmic reticulum and mitochondrion profiles (arrow), and autophagosomes (arrowhead). A, autophagosome; f, flagellum; k, kinetoplast; m, mitochondrion; N, nucleus.

doi:10.1371/journal.pone.0083247.g005

observation under a Zeiss Axioplan epifluorescence microscope using an optical filter set with 450–490 nm for excitation and 528 nm for emission.

#### Statistical Analysis

All the graphics were made using the mean of three independent experiments and the bars represent the standard deviation of those. The statistical significance of differences among the groups was assessed using the one-way analysis of variance (ANOVA) test followed by Bonferroni's multiple comparison test in the GraphPad Prism 4 Software. Results were considered statistically significant when  $p < 0.01$ .

## Results

### Susceptibility of *Leishmania amazonensis* to POSA and ITZ

Figure 1 shows the effects of POSA and ITZ on the proliferation of *L. amazonensis* promastigotes and intracellular amastigotes *in vitro*. Both drugs were effective against promastigotes, causing concentration- and time-dependent inhibition of growth. IC<sub>50</sub> values of 3.94  $\mu$ M and 0.88  $\mu$ M were observed for POSA and ITZ, respectively, after 48 h of treatment. After 72 h of treatment, the IC<sub>50</sub> values were 2.74  $\mu$ M and 0.44  $\mu$ M for POSA and ITZ, respectively. When incubated with intracellular amastigotes, the

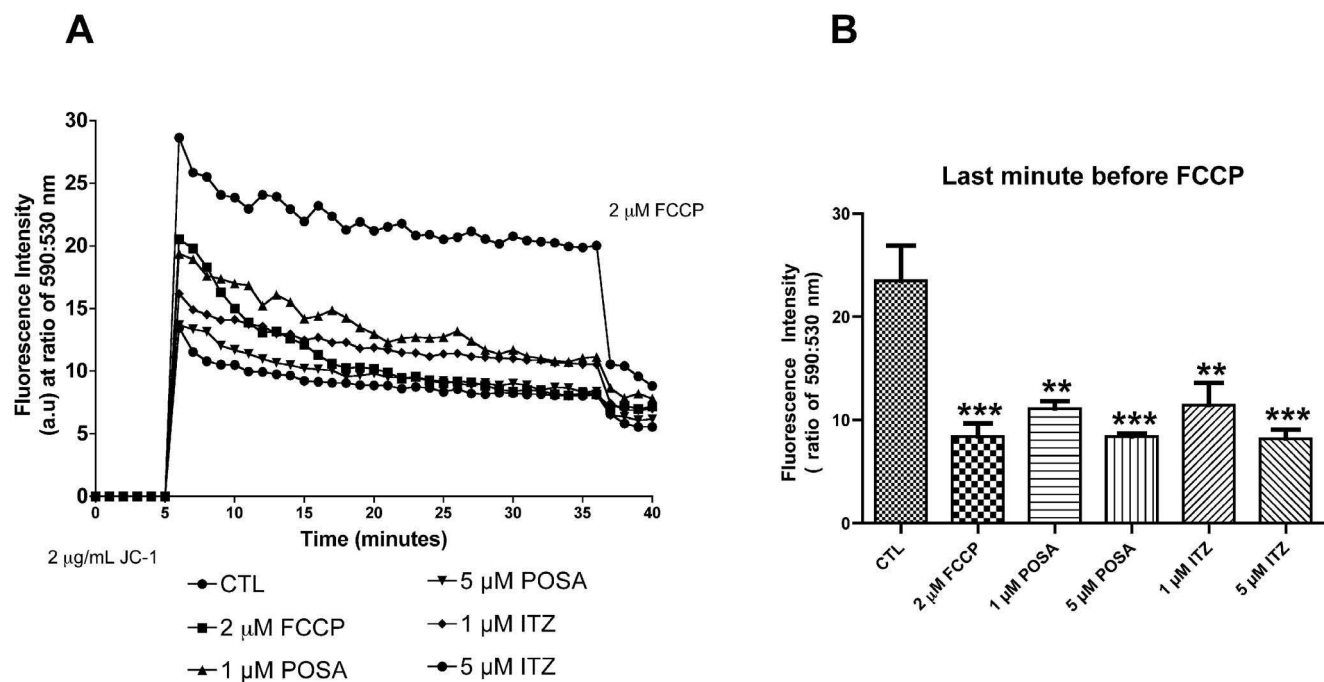


**Figure 6. Evaluation of mitochondrial transmembrane electric potential ( $\Delta\Psi_m$ ) in *L. amazonensis* promastigotes using the JC-1 fluorochrome.** (A) Values of  $\Delta\Psi_m$  were evaluated over 36 min, before the addition of 2  $\mu\text{M}$  FCCP to abolish the mitochondrial potential. Two concentrations of POSA and ITZ were used (1 and 5  $\mu\text{M}$ ) for 48 h of treatment. The  $\Delta\Psi_m$  values are expressed as the ratio of the reading at 590 nm (aggregate) to the reading at 530 nm (monomer). (B) Analysis of  $\Delta\Psi_m$  at the last minute before the addition of 2  $\mu\text{M}$  FCCP. The data suggest that similar alterations in  $\Delta\Psi_m$  are induced by POSA, ITZ, and FCCP. The experiments were performed three times, each time in triplicate, and the figures shown are representative of these experiments. \*\* $p < 0.05$ ; \*\*\* $p < 0.0001$ .

doi:10.1371/journal.pone.0083247.g006

clinically relevant form of the parasite, the effect of the drugs on parasite growth was more potent, with  $\text{IC}_{50}$  values of 1.95  $\mu\text{M}$  and 0.64  $\mu\text{M}$  for POSA and ITZ after 48 h of treatment, respectively, and 1.63  $\mu\text{M}$  for POSA and 0.08  $\mu\text{M}$  for ITZ after 72 h of treatment. All the  $\text{IC}_{50}$  values are summarized in Table 1. Figure 2 shows several images from bright field optical microscopy of the infections during the treatment. Parasites were not observed after 72 h of treatment with concentrations of POSA  $> 4 \mu\text{M}$  and concentrations of ITZ  $> 1 \mu\text{M}$  (Figs. 2C–H). The cytotoxic effects of POSA and ITZ were evaluated against murine macrophages using the MTS assay, and the  $\text{CC}_{50}$  values are summarized in Table 1. POSA was less toxic than ITZ, with  $\text{CC}_{50}$  values of 20  $\mu\text{M}$  and 15  $\mu\text{M}$ , respectively. Selectivity indexes were calculated using the  $\text{IC}_{50}$  values obtained after 72 h of treatment, and ITZ was more selective than POSA *in vitro* (Table 1).

Scanning electron microscopy revealed a dramatic alteration in the shape of promastigotes after treatment with POSA or ITZ for just 48 h (Figs. 3B–I). Promastigotes appeared rounded (Figs. 3D, G, H, and I), swollen (Figs. 3B, C, and E) or with cytoplasmic shrinkage (Fig. 3F). In addition, cells with more than one flagellum (Fig. 3E) and changes in the cell surface (Figs. 3B, C, and I) were also observed.

#### Effects of ITZ and POSA on Plasma Membrane Integrity and Nile Red Accumulation

To evaluate the effects of EBIs on plasma membrane integrity and Nile Red accumulation, control and treated promastigotes were incubated with Sytox Blue and Nile Red, respectively. Nile Red is a fluorescence marker with special affinity for neutral lipids that become concentrated in the lipid bodies. Sytox Blue is a vital dye with high affinity for nucleic acid that easily penetrates cells

with a compromised plasma membrane; thus, it is an efficient dead-cell indicator. Quantitative fluorimetric analysis indicated that treatment with 1  $\mu\text{M}$  POSA and ITZ for 48 h induced significant effects in the accumulation of lipid bodies (Fig. 4A) and in plasma membrane integrity (Fig. 4B). For both analyses, the effects induced by ITZ were greater than those induced by POSA (Figs. 4A, B), congruent with the relative effects of the drugs on promastigote proliferation. Fluorescence images indicated that Nile Red accumulated inside lipid bodies that were randomly distributed throughout the cytoplasm and that the number of lipid bodies markedly increased in drug-treated promastigotes (Figs. 4F, H). Transmission electron microscopy confirmed the presence of lipid bodies after treatment with ITZ and POSA. Lipid bodies were observed in control parasites (Fig. 5A), but in treated promastigotes, several osmophilic lipid-storage bodies appeared close to the plasma membrane (Fig. 5B–D, asterisks), the endoplasmic reticulum, autophagosomes (Fig. 5B–C, asterisks and arrowhead), and the mitochondrion (Fig. 5B, arrow).

#### Effects of POSA and ITZ on Mitochondrial Physiology and Ultrastructure in *L. amazonensis*

The effects of POSA and ITZ on mitochondrial function and ultrastructure were analyzed using two criteria: mitochondrial transmembrane electric potential ( $\Delta\Psi_m$ ), indicated by the JC-1 fluorochrome, and transmission electron microscopy.

Promastigotes were treated with 1 and 5  $\mu\text{M}$  POSA and ITZ, respectively, for 48 h prior to the analysis of  $\Delta\Psi_m$  with JC-1, a cell-permeant cationic, lipophilic fluorochrome. The classic protonophore uncoupler FCCP was used as a positive control to dissipate the mitochondrial electrochemical  $\text{H}^+$  gradient. Simultaneous measurements of J-aggregates (red fluorescence), which

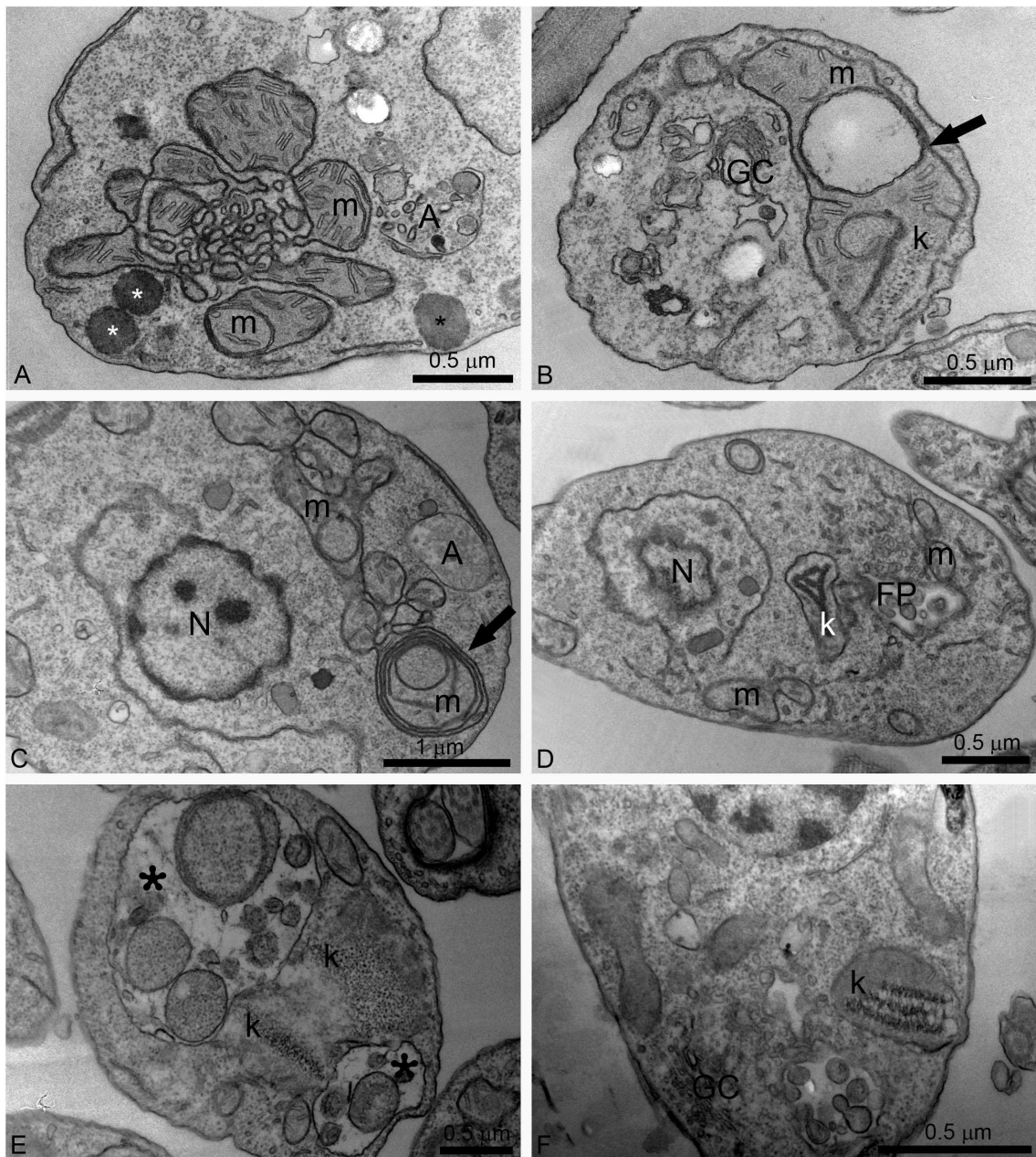


**Figure 7. Ultrathin sections of *L. amazonensis* promastigotes treated with different concentrations of ITZ and POSA.** (A, B) 1  $\mu\text{M}$  ITZ; (C) 1  $\mu\text{M}$  POSA; (E) 3  $\mu\text{M}$  POSA for 48 h; (F) 5  $\mu\text{M}$  POSA for 72 h. Several alterations were observed in the mitochondrion-kinetoplast complex such as: intense disorganization and swelling (A, B, D); alterations in the mitochondrion membranes and the appearance of circular cristae (B, C, arrows); changes in the structure of the kinetoplast (B, D, E, F); and the presence of autophagosomes (A, C, D). In Fig. 7E, two large vacuoles containing membranes and portions of the cytoplasm were observed (asterisks). FP, flagellar pocket; GC, Golgi complex; k, kinetoplast; m, mitochondrion; N: nucleus; A: autophagosome.

doi:10.1371/journal.pone.0083247.g007

accumulate in intact and energized mitochondria, and of J-monomers (green fluorescence) that are a marker for de-energized mitochondria, were used to calculate the  $\Delta\Psi_m$ , expressed as a ratio of fluorescence intensity obtained at 590 and 530 nm. A decrease in the red:green fluorescence intensity ratio indicates a collapse in the mitochondrial transmembrane potential [36]. Pre-treatment of promastigotes for 48 h with POSA and ITZ at the indicated concentrations led to a marked reduction in the  $\Delta\Psi_m$  (Figs. 6A, B), which was concentration-dependent (Fig. 6B). To compare the effects of EBIs on the  $\Delta\Psi_m$  with the effects of a

classical inhibitor of mitochondrial metabolism, control (untreated) promastigotes were incubated with 2  $\mu\text{M}$  FCCP during the evaluation of  $\Delta\Psi_m$  (Fig. 6B), and the observed alteration in the mitochondrial electrochemical  $\text{H}^+$  gradient was similar to that observed in cells pre-treated with 5  $\mu\text{M}$  EBIs.

Alterations in mitochondrial ultrastructure were also investigated by transmission electron microscopy. Figure 5A shows a control promastigote presenting a normal ramified mitochondrion near the plasma membrane. Treatment with POSA and ITZ induced dramatic alterations of the mitochondrion ultrastructure (Figs. 7A–

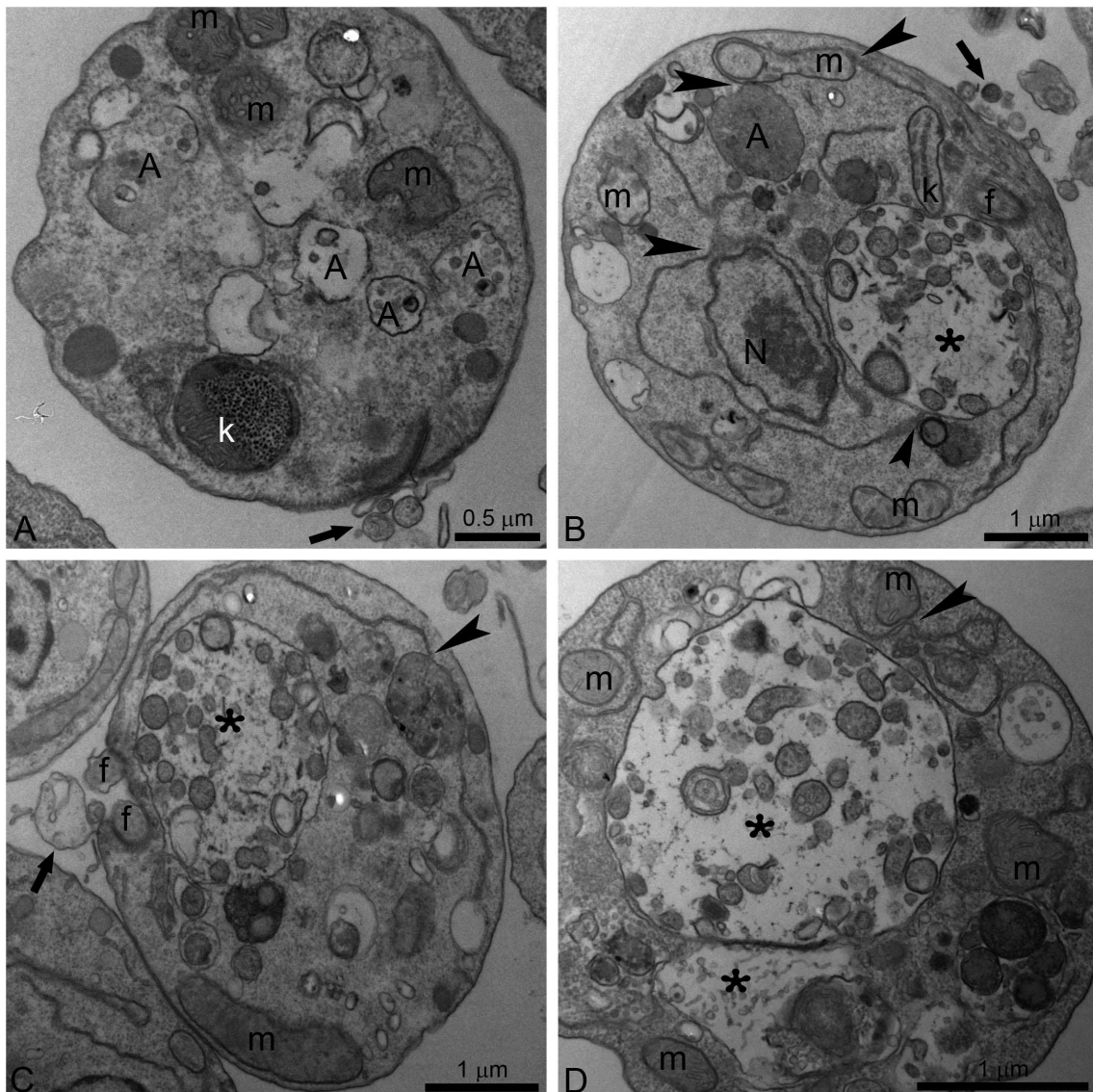


**Figure 8. Ultrathin sections of *L. amazonensis* promastigotes.** Promastigotes were treated with 1  $\mu$ M POSA (A, B), and 3  $\mu$ M POSA (C, D) for 48 h. All images show the presence of small and large vacuoles containing several vesicles, membrane profiles and portions of the cytoplasm (asterisks). The endoplasmic reticulum appears in close association with the nucleus, the mitochondrion and autophagosomes (B–D, arrowheads). In Fig. 8A, changes in kinetoplast structure and vesiculation of the inner mitochondrial membrane were observed. N: nucleus; k: kinetoplast; m: mitochondrion; f: flagellum; A: autophagosome; FP: flagellar pocket.

doi:10.1371/journal.pone.0083247.g008

F). The main alteration observed was a profound mitochondrial swelling, which was followed by remarkable changes in the mitochondrion morphology (Fig. 7A) and its membranes, leading to the appearance of several circular cristae (Figs. 7B–C, arrows). Significant alterations in kinetoplast structure, suggesting a decompaction of the kDNA, were also observed after treatment with both EBIs (Figs. 7B, D–F). In addition, structures similar to autophagosomes (represented by letter A and asterisks in the images) sometimes appeared near the mitochondrion (Figs. 7A, C, E).

#### Effects of POSA and ITZ on the General Ultrastructure of *L. amazonensis* Promastigotes and Intracellular Amastigotes

Alterations in the Golgi complex of promastigotes were observed after treatment with 1  $\mu$ M ITZ for 48 h (Fig. 7B). In addition, autophagosomes were observed after treatment with different concentrations of POSA for 48 h (Figs. 8A–D). These promastigotes presented a total disorganization of the cytoplasm, with the endoplasmic reticulum appearing in close association with the nucleus, the mitochondrion and autophagosomes (Figs. 8B–D, arrowheads). Several large vacuoles containing many small vesicles and membrane profiles were found in treated promastigotes (Figs. 8B–D, asterisks). In addition, some treated parasites also presented with vesicles leaving the flagellar pocket (Figs. 8A, C, arrows).

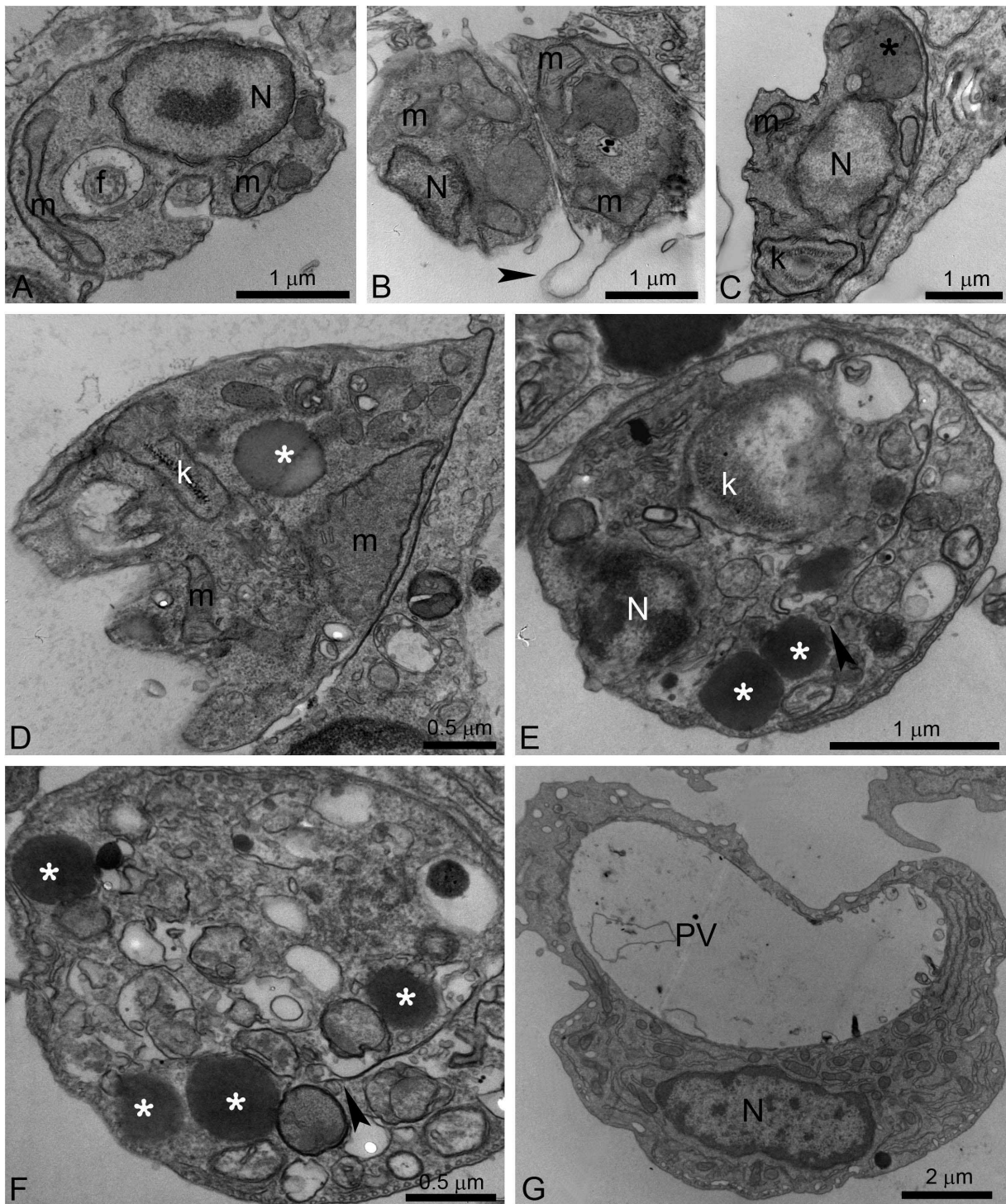


**Figure 9. Ultrathin sections of *L. amazonensis* intracellular amastigotes.** Control intracellular amastigotes (A) and treated amastigotes with ITZ and POSA (B–G) were observed. (B, C) 500 nM ITZ; (D) 1 μM ITZ; (E–G) 6 μM POSA. Different ultrastructural alterations were observed: mitochondrial swelling (B, D); detachment of the plasma membrane (B, arrowhead); presence of a large megasome (C, black asterisk), lipid bodies (D, E, G, white asterisks) and many vacuoles in the cytoplasm (D, E, G); changes in kinetoplast structure (C, E); and a cell with an empty parasitophorous vacuole (PV) (G). f, flagellum; m, mitochondrion; N: nucleus; PV: parasitophorous vacuole, A: autophagosome, k: kinetoplast.

doi:10.1371/journal.pone.0083247.g009

Ultrastructural alterations were also observed in *L. amazonensis* intracellular amastigotes after treatment with both EBIs (Figs. 9B–G). Figure 9A shows a control amastigote displaying normal ultrastructure of the plasma membrane, the nucleus, the

mitochondrion, and the flagellum. Figure 9B shows changes in the plasma membrane that suggest the membrane is detached from the cytoplasm (arrowhead). Different alterations in the mitochondrion were also observed, such as mitochondrial swelling

(Fig. 9D) and changes in the kDNA structure (Figs. 9C, E). Megasomes containing membrane profiles (Fig. 9C, asterisk), lipid bodies randomly distributed throughout the cytoplasm (Figs. 9D–F, asterisks) and parasites with abnormal chromatin condensation (Fig. 9E) were also observed. In Figures 9E–F, a close association of lipid bodies with the endoplasmic reticulum (arrowheads) and the mitochondrion can be observed. Finally, macrophages also presented with many empty vacuoles (Fig. 9G).

## Discussion

POSA and ITZ are known azole antifungals that inhibit ergosterol biosynthesis at the level of sterol C14 $\alpha$ -demethylase (CYP51). Previous studies demonstrated that POSA has potent antiparasitic activity in a murine model of cutaneous leishmaniasis caused by *Leishmania amazonensis*, although it was less active against visceral leishmaniasis caused by *Leishmania donovani* [18]. In addition, POSA was also effective in the treatment of a patient with cutaneous leishmaniasis caused by *L. infantum* [30], and ITZ was effective in the treatment of cutaneous leishmaniasis [32–33]. POSA is currently undergoing phase II clinical trials for the treatment of chronic Chagas disease. Thus, it is important to better understand the effects of these azoles against *L. amazonensis*, which causes infections that respond poorly to standard therapies.

In this study, we confirmed the antiproliferative effects of POSA and ITZ against *L. amazonensis* promastigotes and intracellular amastigotes. Our results are similar to those previously obtained after *in vitro* treatment of *L. amazonensis* promastigotes with POSA [18]. The observed antiproliferative effects indicated that POSA and ITZ were more potent against intracellular amastigotes than promastigotes, and ITZ was more active than POSA against both developmental stages. However, it is important to point out that the experimental condition for each stage is different, which could contribute to the differences in susceptibility observed between them. Against pathogenic fungi, POSA was more efficient than ITZ, with IC<sub>50</sub> values varying from one to eight times lower than those found for ITZ, depending on the species [37]. The concentrations of POSA and ITZ required to inhibit *L. amazonensis* growth were similar to those required for antifungal activity in previous studies [22–26]. Compared with its anti-*Trypanosoma cruzi* activity, POSA was less active against *L. amazonensis*, with IC<sub>50</sub> values significantly higher than those previously published (14 nM and 0.25 nM for *Trypanosoma cruzi* epimastigotes and amastigotes, respectively) [17].

In the present study, different techniques, such as fluorimetry, fluorescence microscopy and electron microscopy were used to investigate the cellular and subcellular structures and to identify organelles affected by drug treatments. Scanning electron microscopy (SEM) revealed profound alterations in the shape of *L. amazonensis* promastigotes, which became rounded and swollen, as well as changes in the cell surface. In addition, fluorimetric analysis with Nile Red and Sytox Blue revealed an accumulation of lipid bodies and important alterations in plasma membrane integrity, respectively. The presence of many lipid bodies randomly distributed throughout the cytoplasm of promastigotes and intracellular amastigotes was confirmed by transmission electron microscopy. These lipid bodies sometimes appeared in close association with the mitochondrion and the endoplasmic reticulum, which could be related to their biogenesis or to lipid mobilization and utilization, as described for other eukaryotic cells [38]. In addition, lipid bodies also appeared near autophagosomes, suggesting that these organelles could be acting to remove abnormal lipids, likely precursors of sterol biosynthesis, which accumulate in the cytoplasm during treatment with EBIs.

Alterations in the plasma membrane of intracellular amastigotes were also observed by transmission electron microscopy. These effects have been described after treatment of *L. amazonensis* and *T. cruzi* with different EBIs [15,19,36,39,40], including POSA [41], and may be associated with alterations in the lipid composition of treated parasites [42]. SEM also revealed a possible alteration in the cell cycle; some cells presented with more than two flagella, which indicates aberrant cytokinesis. As shown in a previous study [19], other EBIs had the same effect on the cell division, which could be related to alterations in the composition of certain lipids that regulate the cell cycle, or to alterations in cytoskeletal components involved in this cellular process.

We also observed important alterations in the mitochondrion, such as a significant reduction in the mitochondrial membrane potential ( $\Delta\Psi_m$ ) after 48 h of treatment at concentrations near the IC<sub>50</sub>. This reduction was very similar to that observed after incubation of parasites with FCCP, a classical protonophore that dissipates the mitochondrial electrochemical H<sup>+</sup> gradient. Transmission electron microscopy confirmed the mitochondrial alterations after treatment with different concentrations of either ITZ or POSA. The images suggest an intense remodeling of the mitochondrial membranes, which could be related to depletion of the parasite's endogenous sterols, as demonstrated for other trypanosomatids after treatment with EBIs [43]. These membranes, in contrast with mammalian mitochondrial membranes, contain high levels of endogenous sterols [44]. These alterations are similar to those observed after treatment with amiodarone, an antiarrhythmic drug that also interferes with ergosterol biosynthesis [17,36,40], and other EBIs [20–21]. In addition, an interesting alteration in kinetoplast structure was also observed (Fig. 7). In trypanosomatids, the kinetoplast appears physically associated with the mitochondrial membrane and the basal body by thin filaments, which form a complex structure known as the tripartite attachment zone (TAC) that is essential for the positioning of the mitochondrial genome and its correct segregation during cell division [45]. This type of alteration in kinetoplast structure has not been previously described during treatment with EBIs and could result from the fragility of the surrounding mitochondrial membranes. Thus, alterations in the mitochondrial membranes could indirectly explain the changes observed in the kinetoplast.

Treatment with POSA and ITZ also induced an intense accumulation of autophagosomes in promastigotes and amastigotes (Fig. 8). These subcellular structures appear to be engulfing parts of the cytoplasm and are located near important organelles, such as the mitochondrion and the endoplasmic reticulum. The autophagosomes were frequently observed as large structures containing many small vesicles and cellular debris, indicating an intense recycling of abnormal membrane structures, organelles and lipid intermediates that accumulated after drug treatment. Autophagy has been described in different protozoan parasites as an important survival mechanism; however, it is also associated with treatment with several classes of compounds [39,46]. In *T. cruzi*, it was demonstrated that naphthoimidazoles induce an overexpression of the ATG8 genes, which promotes the induction of autophagy in these parasites [47]. Naphthoimidazoles also induced these effects in *Leishmania*; however, treatment with 3-methyladenine, a classic autophagic inhibitor, indicated that autophagy serves as a survival mechanism and that its inhibition causes an increase in apoptotic cell death in the early hours of treatment [48]. The remodeling of damaged cellular structures could be related to the presence of several megasomes, which are lysosome-like organelles of intracellular amastigotes.

In summary, our results show that ITZ and POSA have a strong antiproliferative effect on *L. amazonensis* promastigotes and

intracellular amastigotes. These drugs alter the general ultrastructure and the mitochondrial physiology of *L. amazonensis* and likely trigger the three known phenotypes of cell death: apoptosis, necrosis, and autophagy. Our observations suggest that ITZ and POSA, either alone or in combination, may be effective in the treatment of leishmaniasis.

## Acknowledgments

We thank Joseane Lima Prado Godinho for helpful discussions.

## References

- Alvar J, Vélez ID, Bern C, Herrero M, Desjeux P, et al. (2012) Leishmaniasis worldwide and global estimates of its incidence. *PLoS One* 7: e35671.
- Herwaldt BL. (1999) Leishmaniasis. *Lancet* 354: 1191–1199.
- Grimaldi G Jr, McMahan-Pratt D. (1991) Leishmaniasis and its etiologic agents in the New World: an overview. *Prog Clin Parasitol* 2: 73–118.
- Liew FY, O'Donnell CA. (1993) Immunology of leishmaniasis. *Adv Parasitol* 32: 161–259.
- Barral A, Pedral-Sampaio D, Grimaldi Jr G, Momen H, McMahon-Pratt D, et al. (1991). Leishmaniasis in Bahia, Brazil: evidence that *Leishmania amazonensis* produces a wide spectrum of clinical disease. *Am J Trop Med Hyg* 44: 536–546.
- Lainson R, Shaw JJ, Silveira FT, de Souza AAA, Braga RR, et al. (1994). The dermal leishmaniasis of Brazil, with special reference to the eco-epidemiology of the disease in Amazonia. *Mem Inst Oswaldo Cruz* 89: 435–443.
- Singh S, Sivakumar R. (2004) Challenges and new discoveries in the treatment of leishmaniasis. *J Infect Chemother* 10: 307–315.
- Goto H, Lindoso JAL. (2010) Current diagnosis and treatment of cutaneous and mucocutaneous leishmaniasis. *Expert Rev Anti Infect Ther* 8: 419–433.
- Croft SL, Sundar S, Fairlamb AH. (2006) Drug resistance in leishmaniasis. *Clin Microbiol Rev* 19: 111–126.
- Alvar JC, Cañavate C, Gutierrez-Solar B, Jimenez M, Laguna F, et al. (1997) *Leishmania* and human immunodeficiency virus coinfection: the first 10 years. *Clin Microbiol Rev* 10: 298–319.
- Rosenthal E, Marty P, Poizot-Martin I, Reynes J, Pratlong F, et al. (1995) Visceral leishmaniasis and HIV-1 co-infection in southern France. *Trans R Soc Trop Med Hyg* 89: 159–162.
- Murray HW, Berman JD, Davies CR, Saravia NG (2005) Advances in leishmaniasis. *Lancet* 366: 1561–1577.
- van Griensven J, Balasegaram M, Meheus F, Alvar J, Lynen L, et al. (2010) Combination therapy for visceral leishmaniasis. *Lancet Infect Dis* 10: 184–194.
- Godinho JLP, Simas-Rodrigues C, Silva R, Ürményi TP, de Souza W, et al. (2012) Efficacy of miltefosine treatment in *Leishmania amazonensis*-infected Balb/C mice. *Int J Antimicrob Ag* 39: 326–331.
- de Souza W, Rodrigues JCF. (2009) Sterol biosynthesis pathway as target for anti-trypansomatid drugs. *Interdiscip Perspect Infect Dis* 2009: 642502.
- Urbina JA, Docampo R. (2003) Specific chemotherapy of Chagas disease: controversies and advances. *Trends Parasitol* 19: 495–501.
- Benaim G, Sanders JM, García-Marchán Y, Colina C, Lira R, et al. (2006) Amiodarone has intrinsic anti-*Trypanosoma cruzi* activity and acts synergistically with posaconazole. *J Med Chem* 49: 892–899.
- Al-Abdely HM, Graybill JR, Loebenberg D, Melby PC. (1999) Efficacy of the triazole SCH 56592 against *Leishmania amazonensis* and *Leishmania donovani* in experimental murine cutaneous and visceral leishmaniasis. *Antimicrob Agents Chemother* 43: 2910–2914.
- Rodrigues JCF, Conception JL, Rodrigues C, Caldera A, Urbina JA, et al. (2008) *In vitro* activities of ER-119884 and E5700, two potent squalene synthase inhibitors, against *Leishmania amazonensis*: antiproliferative, biochemical, and ultrastructural effects. *Antimicrob Agents Chemother* 52: 4098–4114.
- Rodrigues JCF, Bernardes CF, Visbal G, Urbina JA, Vercesi AE, et al. (2007) Sterol methenyl transferase inhibitors alter the ultrastructure and function of the *Leishmania amazonensis* mitochondrion leading to potent growth inhibition. *Protist* 158: 447–456.
- Rodrigues JCF, Attias M, Rodrigues C, Urbina JA, de Souza W. (2002) Ultrastructural and biochemical alterations induced by 22,26-azasterol, a  $\Delta^{24(25)}$ -sterol methyltransferase inhibitor, on promastigote and amastigote forms of *Leishmania amazonensis*. *Antimicrob Agents Chemother* 46: 487–499.
- Perfect JR, Cox GM, Dodge RK, Schell WA. (1996) *In vitro* and *in vivo* efficacies of the azole SCH56592 against *Cryptococcus neoformans*. *Antimicrob Agents Chemother* 40: 1910–1913.
- Faergemann J. (1984) *In vitro* and *in vivo* activities of ketoconazole and itraconazole against *Pityrosporum orbiculare*. *Antimicrob Agents Chemother* 26: 773–774.
- Van Cutsem J, Van Gerven F, Van de Ven MA, Borgers M, Janssen PA. (1984) Itraconazole, a new triazole that is orally active in aspergillosis. *Antimicrob Agents Chemother* 26: 527–534.
- Espinel-Ingroff A, Shadomy S, Gebhart RJ. (1984) *In vitro* studies with R 51,211 (itraconazole). *Antimicrob Agents Chemother* 26: 5–9.
- Uchida K, Yokota N, Yamaguchi H. (2001) *In vitro* antifungal activity of posaconazole against various pathogenic fungi. *Int J Antimicrob Agents* 18: 167–172.
- Saag MS, Dismukes WE. (1988) Azole antifungal agents: emphasis on new triazoles. *Antimicrob Agents Chemother* 32: 1–8.
- Alsip SA, Stamm AM, Dismukes WE. (1986) Ketoconazole, miconazole, and other imidazoles. In: *Fungal Diseases of the Lung*, Sarosi GA, Davies SF, editors. Orlando: Grune & Stratton. 335–376.
- Urbina JA, Payares G, Contreras LM, Liendo A, Sanjoa C, et al. (1998) Antiproliferative effects and mechanism of action of SCH 56592 against *Trypanosoma (Schizotrypanum) cruzi*: *in vitro* and *in vivo* studies. *Antimicrob Agents Chemother* 42: 1771–1777.
- Paniz-Mondolfi AE, Stavropoulos C, Gelanew T, Loucas E, Alvarez AMP, et al. (2011) Successful treatment of Old World cutaneous leishmaniasis caused by *Leishmania amazonensis* with posaconazole. *Antimicrob Agents Chemother* 55: 1774–1776.
- Nassiri-Kashani M, Firooz A, Khamesipour A, Mojtabah F, Nilforoushzadeh M, et al. (2005) A randomized, double-blind, placebo-controlled clinical trial of itraconazole in the treatment of cutaneous leishmaniasis. *Eur Acad Dermatol Venereol* 19: 80–83.
- Consigni J, Danielo C, Gallerano V, Papa M, Guidi A (2006). Cutaneous leishmaniasis: successful treatment with itraconazole. *Int J Dermatol* 45: 46–49.
- Baroni A, Aiello FS, Vozza A, Vozza G, Faccenda F, et al. (2009) Cutaneous leishmaniasis treated with itraconazole. *Dermatol Ther* 22: S27–S29.
- Warren LG. (1960) Metabolism of *Schizotrypanum cruzi* Chagas. I. Effect of culture age and substrate concentration on respiratory rate. *J Parasitol* 46: 529–539.
- Henriques C, Moreira TLB, Maia-Brigagão C, Henriques-Pons A, Carvalho TMU, et al. (2011) Tetrazolium salt based methods for high-throughput evaluation of anti-parasite chemotherapy. *Anal Methods* 3: 2148–2155.
- de Macedo-Silva ST, de Oliveira Silva TL, Urbina JA, de Souza W, Rodrigues JC. (2011) Antiproliferative, Ultrastructural, and Physiological Effects of Amiodarone on Promastigote and Amastigote Forms of *Leishmania amazonensis*. *Mol Biol Int* 2011: 876021.
- Galgiani JN, Lewis ML. (1997) *In vitro* studies of activities of the antifungal triazoles SCH56592 and Itraconazole against *Candida albicans*, *Cryptococcus neoformans*, and other pathogenic yeasts. *Antimicrob Agents Chemother* 41: 180–183.
- Walther TC, Farese RV Jr. (2009) The life of lipid droplets. *Biochim Biophys Acta* 1791: 459–466.
- Rodrigues JCF, de Souza W. (2008) Ultrastructural alterations in organelles of parasitic protozoa induced by different classes of metabolic inhibitors. *Curr Pharm Des* 14: 925–938.
- Serrano-Martín X, García-Marchán Y, Fernandez A, Rodriguez N, Rojas H, et al. (2009) Amiodarone destabilizes intracellular  $\text{Ca}^{2+}$  homeostasis and biosynthesis of sterols in *Leishmania mexicana*. *Antimicrob Agents Chemother* 53: 1403–1410.
- Veiga-Santos P, Barrias ES, Santos JF, de Barros Moreira TL, de Carvalho TM. (2012) Effects of amiodarone and posaconazole on the growth and ultrastructure of *Trypanosoma cruzi*. *Int J Antimicrob Agents* 40: 61–71.
- Urbina JA, Vivas J, Visbal G, Contreras LM. (1995) Modification of the sterol composition of *Trypanosoma (Schizotrypanum) cruzi* epimastigotes by  $\Delta^{24(25)}$ -sterol methyltransferase inhibitors and their combinations with ketoconazole. *Mol Biochem Parasitol* 73: 199–210.
- Palmié-Peixoto IV, Rocha MR, Urbina JA, de Souza W, Einicker-Lamas M, et al. (2006) Effects of sterol biosynthesis inhibitors on endosymbiont-bearing trypansomatids. *FEMS Microbiol Lett* 255: 33–42.
- Rodrigues CO, Catisti R, Uyemura SA, Vercesi AE, Lira R, et al. (2001) The sterol composition of *Trypanosoma cruzi* changes after growth in different culture media and results in different sensitivity to digitonin-permeabilization. *J Eukaryot Microbiol* 48: 588–594.
- Ogbadoyi EO, Robinson DR, Gull K. (2003) A high-order trans-membrane structural linkage is responsible for mitochondrial genome positioning and segregation by flagellar basal bodies in trypanosomes. *Mol Biol Cell* 14: 1769–1779.
- Klionsky DJ, Abdalla FC, Abieliovich H, Abraham RT, Acevedo-Arozena A, et al. (2012) Guidelines for the use and interpretation of assays for monitoring autophagy. *Autophagy* 8: 445–544.

47. Menna-Barreto RF, Corrêa JR, Cascabulho CM, Fernandes MC, Pinto AV, et al. (2009) Naphthoimidazoles promote different death phenotypes in *Trypanosoma cruzi*. *Parasitology* 136: 499–510.
48. Sengupta S, Chowdhury S, Bosedasgupta S, Wright CW, Majumder HK. (2011) Cryptolepine-induced cell death of *Leishmania donovani* promastigotes is augmented by inhibition of autophagy. *Mol Biol Int* 2011: 187850.